UNIVERSIDADE D
COIMBRA

Mariana Simões Marques

Functional brain connectivity underlying decision making in social cognition: an fMRI study in ASD

Thesis submitted to the Faculty of Sciences and Technology of the University of Coimbra for the Master degree in Biomedical Engineering with specialization in Medical Imaging and Radiation, supervised by Prof. Doctor Miguel de Sá e Sousa de Castelo and Dr. Teresa Sousa

September 2023

FACULDADE DE CIÊNCIAS E TECNOLOGIA
UNIVERSIDADE D COIMBRA

Functional brain connectivity underlying decision making in social cognition: an fMRI study in ASD

Mariana Simões Marques

Thesis submitted to the Faculty of Sciences and Technology of the University of Coimbra for Master's degree in Biomedical Engineering with specialization in Medical Image and Radiation.

Supervisors:
Miguel Castelo Branco (MD, PhD)
Teresa Sousa (PhD)

Coimbra, 2023

This work was developed in collaboration with:

Department of Physics, University of Coimbra, Portugal

FCTUC DEPARTAMENTO DE FÍSICA
FACULDADE DE CIÊNCIAS E TECNOLOGIA
UNIVERSIDADE DE COIMBRA

Coimbra Institute for Biomedical Imaging and Translational Research (CIBIT), University of Coimbra, Portugal

Institute of Nuclear Sciences Applied to Health (ICNAS), University of Coimbra, Portugal

Agradecimentos

Durante a realização deste projeto, muitos foram aqueles que me acompanharam e apoiaram. Obrigada, a todos vocês do fundo do coração.

Primeiramente, dirijo um agradecimento aos meus orientadores, ao Professor Doutor Miguel Castelo Branco, por quem expresso uma grande admiração e agradeço toda a ajuda dada e à Doutora Teresa Sousa, que foi incansável em toda a sua orientação, que sempre me esclareceu em tudo e preocupou-se sempre em fazer com que eu mostrasse o melhor trabalho possível.

Ao meu Departamento de Física, eterna casa, que me acolheu durante 5 anos e que me proporcionou as melhores memórias com as melhores pessoas, o meu eterno obrigada.

Aos cruzados, por serem os meus confidentes e ouvirem-me sempre, foi ótimo fazer esta jornada ao vosso lado, teria custado muito mais sem vocês.

Ao Costini, sem dúvida o meu melhor amigo, e aquele que fez com que os meus cinco anos fossem os melhores, o maior obrigada. És o irmão que nunca tive e o melhor apoio que tive na faculdade, mesmo com as nossas chatices, que (sendo honesta) eu tanto gosto, és daqueles que qualquer pessoa quereria ter na sua vida.

À Eva, por ser a minha go to everytime. Por ter passado os melhores cinco anos comigo, por ter feito parte de tudo desde o início, obrigada. Levo-te para sempre comigo.

À minha família de praxe, por se preocuparem sempre comigo e por todo o companheirismo, em especial às minhas colegas de casa, Laura e Carolina, por me dizerem sempre que sou capaz.

À Filipa, à Jacinta e à Sofia, por terem sido um grande apoio mesmo à distância, obrigada por estarem sempre comigo.

À Joana, à Bule e à Fipas por todo o companheirismo e por todo o apoio.

À Margarida por estar sempre comigo e me fazer rir quando estava nos momentos de mais desespero, e por seres a melhor vizinha, amiga e afilhada. É importante ter alguém como tu na vida.

Às minhas OG de Seia, um dos meus maiores apoios, a vida é mais fácil com vocês, obrigada por serem as minhas fãs número um. Prometo que serei sempre vossa também. Obrigada por toda a força que sempre me deram.

Por último, o mais importante agradecimento, à minha família, aos meus pais e em especial à minha mãe, por ser a melhor do mundo em tudo. Obrigada por serem o meu apoio incondicional, e por saberem sempre o que dizer. Obrigada por me permitirem alcançar os meus objetivos. Por vocês, tudo, sempre.

Resumo

A perturbação do espectro do autismo é conhecida por afetar a forma como um indivíduo perceciona e age num ambiente social, o que pode levar a dificuldades de interação e comunicação. As suas características e os seus padrões comportamentais podem ser identificados logo no início da infância de um indivíduo, apesar das dificuldades de diagnóstico frequentemente presentes. No entanto, a etiologia e a patogénese desta perturbação são ainda objeto de investigação.

O objetivo deste estudo é, através da utilização da técnica de Ressonância Magnética Funcional (*fMRI*, do inglês, functional magnetic resonance imaging), avaliar as diferenças de conectividade funcional do cérebro entre indivíduos com autismo e indivíduos saudáveis. Em primeiro lugar, foi efetuada uma análise da resposta cerebral para verificar se existem potenciais regiões-chave que apresentem hipoactivação ou hiperactivação no grupo clínico, e para verificar se existem potenciais biomarcadores que possam permitir um diagnóstico mais precoce. A segunda parte deste trabalho centra-se principalmente no conceito de conectividade funcional e na possibilidade de encontrar redes cerebrais afetadas em indivíduos com autismo.

Neste projeto, foram utilizados dados de *fMRI* adquiridos durante uma tarefa visual baseada em animações geométricas simples. Ambos os grupos tinham de visualizar quatro tipos diferentes de interação entre duas esferas, uma positiva (interação afliativa), uma negativa (interação antagonista), uma indiferente (interação neutra) e uma linear (sem interação).

Os resultados mostraram que sujeitos com autismo apresentam uma menor conectividade funcional entre as redes da saliência e da teoria da mente (ToM), bem como entre regiões-chave conhecidas como as mais importantes quando se estuda o "cérebro emocional". Tanto sulco temporal superior (*STS*, do inglês, superior temporal sulcus) como a junção temporo-parietal (*TPJ*, do inglês, temporoparietal junction) mostram hipoconectividade com o giro inferior frontal (*IFG, do inglês inferior frontal gyrus*) no grupo clínico. Estes correlatos podem estar relacionados com o facto de indivíduos afetados por esta condição poderem nem sempre compreender o ambiente que os rodeia e terem dificuldades em integrar e compreender as regras de uma simples interação social.

Ao comparar a conectividade funcional entre grupos durante cada interação, os resultados mostram ser durante a visualização das interações positiva e negativa que ocorrem as diferenças mais notórias. Os sujeitos do grupo de controlo revelam maior conectividade entre o giro supramarginal/ *TPJ* com o giro medial temporal(*MTG*, do inglês, middle temporal gyrus) e com o

IFG, duas regiões importantes do sistema de neurónios espelho (*MNS*, do inglês, mirror neuron system), com um papel importante na compreensão das ações dos outros.

Em suma, os nossos resultados sugerem que várias regiões da rede de saliência apresentam um fraco nível de conectividade com regiões da rede ToM e sugerem também que as funções desempenhadas pelo *SMG* (importantes na interpretação do contexto social) podem estar comprometidas, devido à sua pior comunicação com o *TPJ* e com o *IFG*. O nosso estudo está, portanto, de acordo com estudos anteriores que sugerem padrões de hipoconectividade no autismo entre redes neuronais relacionados com a cognição social.

Abstract

Autism Spectrum Disorder (ASD) is a condition known for affecting how an individual perceives and acts in a social environment, which can lead to difficulties in interacting and communicating. The hallmarks of this condition and its consistent behavioral patterns can be detected in early childhood, despite the diagnostic difficulties that are often present. ASD prevalence is estimated at approximately 1/100 children around the world and has been following a rapid increase. However, the etiology and pathogenesis of this disorder are still a matter of investigation.

This study aimed to use the functional resonance imaging technique (fMRI) to evaluate the functional brain connectivity in ASD when compared to healthy individuals. Firstly, potential key regions showing hypoactivation or hyperactivation in the autism group were analyzed, to ascertain for novel and simple brain response biomarkers, which might contribute to improve diagnosis. Then, functional brain connectivity analysis was performed to investigate brain networks potentially affected in individuals with this condition.

It has been suggested that ASD individuals show lower functional connectivity between salience and theory of the mind networks, as well as between key regions known as being the most important when studying the "emotional brain". Here, to test this hypothesis, fMRI data acquired during a simple geometric animation visual task were analyzed. Both ASD and healthy individuals visualized four different types of interactions, a positive, a negative, an indifferent, and a linear one during the acquisition.

Our results suggested that both the temporoparietal junction (TPJ) and the superior temporal sulcus (STS) show task-related hypoconnectivity with the inferior frontal gyrus (IFG) in the clinical group, which might be linked with ASD difficulties in comprehending the surrounding environment and integrating simple social cues.

When comparing how each group processes the visualized interactions, our results showed that the positive and negative interactions are where the differences are notorious. ASD subjects revealed lower connectivity patterns between the supramarginal gyrus (SMG)/TPJ and the medial temporal gyrus (MTG) and also with the IFG, two important regions in the mirror neuron system, responsible for understanding other people's actions.

In sum, our results suggest that in autism several regions of the salience network show a poor level of connectivity with regions from the ToM network and that functions performed by the SMG (important in interpreting social context) might be compromised, due to its poorer

connectivity with the TPJ and IFG. Our study thus supports previous literature suggesting autism hypoconnectivity in neural networks relevant for social cogniton.

Contents

List of Figures

List of Tables

List of Abbreviations

AC anterior cingulate. 18, 19
ACC anterior cingulate cortex. xv, 16, 22, 55, 69
AI anterior insula. xvi, 18, 19
ASD Autism Spectrum Disorder. xix, 16, 17, 18, 19, 22, 23, 24, 30, 33, 34, 35, 36, 38, 40, 42, 44, 48, 49, 55, 56
ATP adenosine triphosphate. 6

BOLD blood-oxygen-level-dependent. 5, 6, 7, 8, 24, 56

CBF local blood flow. 6, 7
CBV local blood volume. 6
CDC Centers for Disease Control and Prevention. 1
CNT control. xix, 35, 48, 49, 50, 51, 53

DAN dorsal attention network. 33
DMN default mode network. xvi, 19, 33

ECN executive network. xvi, 19
EEG Electroencephalogram. 24

fMRI functional magnetic resonance imaging. 1, 9, 10, 16, 20, 21, 22, 24

GLM general linear model. 2

HRF hemodynamic response function. 7, 8

IFG inferior frontal gyrus. xv, xix, 16, 18, 20, 23, 34, 49, 50, 57
IPL inferior parietal lobe. xvi, 20, 21
IPS intraparietal sulcus. 69

LEAS Levels of Emotional Awareness Scale. 1
lpSTG left-posterior superior temporal gyrus. xvii, 30, 38, 39

MEG Magnetoencephalography. 24
MNS mirror neuron system. 20
mPFC medial prefrontal cortex. xv, xvi, xviii, xxi, 16, 20, 21, 22, 23, 30, 44, 45, 56, 57, 69
MRI Magnetic Resonance Imaging. 6, 7, 22

MTG middle temporal gyrus. 57

PCC posterior cingulate cortex. 69
PFC prefrontal cortex. 21
PMC premotor cortex. xvi, 20, 21
pSTS posterior superior temporal sulcus. xviii, 40

ROIs regions of interest. 30, 50
RPFC right prefrontal cortex. 69
rs-fMRI Resting-state functional magnetic resonance imaging. 8, 12, 31

SFG superior frontal gyrus. 49
SMG supramarginal gyrus. xvii, xix, xxi, 36, 37, 38, 48, 49, 55, 56, 57, 69
SPM stastical parametric map. 9, 29, 31
STG superior temporal Gyrus. xix, 18, 22, 47, 55, 56
STS superior temporal sulcus. xvi, xviii, xxi, 18, 20, 21, 22, 30, 34, 40, 41, 50, 56, 57

ToM Theory of the mind. xvi, 15, 16, 21, 22, 23, 30, 33, 50, 57, 58
TPJ temporo parietal junction. xv, xvi, xviii, 16, 20, 21, 22, 23, 29, 30, 34, 42, 43, 50, 55, 56, 57

VAN ventral attention network. 33

1

Introduction

1.1 Motivation

According to the Centers for Disease Control and Prevention (CDC), about 1% of the world's population is diagnosed with Autism Spectrum Disorder (ASD), that is over 75 million people and four men to one woman correspondence [Mouga et al., 2015]. Despite the high prevalence, ASD features a wide range of symptoms and levels of severity. This leads to the difficulty in diagnosing ASD, and in defining parameters to take under consideration when performing it [Thomas et al., 2020].

ASD is defined by a set of conditions that implicate symptoms such as communication deficits, lack of attention in daily activities, increased difficulties in interpretation of others' intentions and their actions, and a low level of social cognition, as described by the Levels of Emotional Awareness Scale (LEAS) [Genovese and Butler, 2020, Tavares et al., 2011].

This developmental disorder becomes apparent around the age of three and lasts for the rest of an individual's life. Since no precise biological markers are known, it is characterized in terms of behavior. Moreover during development, the profile and severity may change and it may be accompanied by other co-morbidities and influenced by outside variables (such as education and environment) [Ward, 2006].

The causal factors for this condition remain uncertain, with no universally validated intervention. Nonetheless, there are several attenuation mechanisms, with the most effective one being an early diagnosis and control of this disorder from the beginning and not in an advanced stage [Tavares et al., 2011].

Behavioral investigations of patients with brain injuries and functional imaging studies of healthy volunteers have been the two main sources of evidence for the neurological underpinnings of the theory of mind (ToM). It describes the mechanisms related to the ability to understand and infer the mental states of other people and has been consistently hypothesized to be altered in autism [Ward, 2006].

Our main motivation, considering this, is to investigate such mechanisms in autism using functional magnetic resonance imaging (fMRI) to map its underlying dynamics. By analyzing the functional brain connectivity we want test for altered brain mechanisms adding to the

understanding of social behavioral challenges in ASD.

1.2 Main Goals

Functional brain connectivity during a particular task has been suggested to highlight key aspects of brain function, such as how easily information can be transferred between various regions [Schurz et al., 2020]. It has been hypothesized to be affected in ASD and other associated pathologies, which might raise the potential for novel biomarkers of the condition.

The main goals of this project were thus focused on:

- Map the principal brain regions recruited during social cognition and investigate how they are modulated depending on the social meaning of dynamic visual stimuli representing different social interactions. A stimulus using basic actions with simple objects was used to avoid bias from other cues;
- Analyze which brain regions are affected by each socioemotional interpretation, and evaluate their connections, considering the type of social interaction present or not;
- Investigate, through the clinical and control groups comparison, if ASD patients show particular changes in defined brain circuits;

The activation maps would be evaluated using general linear model (GLM) while the connectivity maps would be evaluated using roi-to-roi correlation analysis on the network of interest.

The targeted clinical group of this study is ASD patients whose illnesses have been present for a long period (adult subjects). Moreover, it was aimed a matched healthy group (also adult subjects) for control proposes.

1.3 Hypothesis and Contributions

Functional brain connectivity underlying decision-making in social cognition is still a matter of research, in particular, regarding its dependence on the emotional content/valence. In this project, we followed the hypothesis that ASD subjects, which are believed to have impaired social and emotional cognition, show altered functional brain connectivity, as revealed by task-based fMRI analysis, during social cues interpretation. Given the spatial resolution allowed by the fMRI technique, we expect to contribute to reveal which are the key nodes (regions) of the ToM network for social interactions' identification. We also contribute to uncovering more about the brain circuits related to altered social abilities in ASD.

2

Background Concepts

This chapter introduces the main concepts related to the work developed on this project.

2.1 Autism Spectrum Disorder (ASD)

ASD is the term used for a severe, lifelong neurodevelopmental condition. Characterized by its early manifestations, ASD patients present symptoms such as early communication deficits and repetitive sensory-motor responses, with mostly genetic causes [Mouga et al., 2015].

"Autism" was initially used as a diagnostic name by Leo Kanner in 1943, to describe a particular syndrome seen in young children and characterized by early onset, and recognizable symptomatology regarding impaired social and emotional interactions. Nowadays, although, ASD patients reflect the condition in different ways, depending on the severity of it, they usually present difficulties identifying emotional, verbal, or non-verbal social interactions, and they also commonly show difficulties in initiating or keeping conversations with people (as well as answering accordingly) [Genovese and Butler, 2020].

In addition, motor problems are also present, such as repetitive and stereotyped behaviors. This includes strict routines, intense focus on one or more particular hobbies, and repetitive body gestures (such as hand or body waving) [Deng et al., 2022].

The ASD condition is now largely acknowledged as a complex disorder with a strong social impact. Health, education, social services, housing, employment, welfare benefits, and labor markets are just a few of the many areas where ASD has significant direct and indirect consequences. These effects often last into adulthood and place a heavy financial burden on families. It is thus critical, a better understanding of the neurobiological mechanisms behind this disorder to allow for more effective intervention and support [Masi et al., 2017].

2.1.1 Pathogenesis

Although many factors have been linked to the etiology of autistic disorders, its precise pathogenesis is still unknown [Kana et al., 2014].

Genetic studies have identified two types of mutations that contribute to ASD: "de novo copy number" mutations and rare variant mutations. These mutations can result in abnormal versions of genes in the affected person or their close relatives. These genetic changes are linked to differences in the brain structure and behavior that are observed in individuals with ASD. The affected genes are often involved in the functioning of synapses, which are the connections

between nerve cells in the brain. When these genes are not functioning properly, a disruption of the normal development of the brain can occur, leading to neurodevelopmental issues commonly seen in ASD [Samsam et al., 2014].

Thus, several clinical phenotypes and related multiple medical conditions have turned into the defining characteristics of ASD, as a result of the discovery of numerous genes as well as interactions of multiple genes in one person, epigenetic factors, and effects of environmental modifiers on these genes. Autism risk may also be correlated with exposure to specific environmental factors during pregnancy or in the early stages of development. According to some research, exposure to pesticides, environmental chemicals, certain drugs, infections, and air pollutants during pregnancy may all contribute to the development of autism. These relationships, however, are currently being studied and are not yet conclusively understood [Miani et al., 2021].

Therefore, no trustworthy model of causation, or biomarker of autism has been identified [Kana et al., 2014, Samsam et al., 2014].

The diagnosis is thus still made primarily on the observation of unusual behaviors, together with criteria for chronic social communication deficiencies and repetitive behavior patterns [Masi et al., 2017].

2.1.2 Clinical Features of ASD and Diagnosis

The Diagnostic and Statistical Manual of Mental Disorders, Fifth Edition (DSM-5) states that children with ASD have restricted or repetitive patterns of behavior, interests, or activities, in addition to a tendency to respond inappropriately in a conversation and a lack of relationship-building skills [Fakhoury, 2015].

ASD individuals are often not diagnosed until they reach the age of three [Mouga et al., 2015]. This condition is mostly recognizable by the presence of two broad symptom categories. One of the categories, the core one, is characterized by reduced social interaction and language abilities, as well as the existence of stereotypical and repetitive behaviors. The other one is known as the secondary symptoms, which might include amongst other side effects, self-harm, hyperactivity, and aggressiveness as well as co-occurring mental health conditions like anxiety and concerned states of depression [Fakhoury, 2015].

Although, ASD presents a complex amount of symptoms, the level of severity might be different from one patient to another. It mostly depends on the subject age. ASD affects 20 out of every 10,000 children, and the first signs can be seen in youngsters as young as 1 to 3 years old [Mouga et al., 2015, Newschaffer et al., 2007].

The tests used to diagnose autism usually involve a combination of behavioral observation, interviews with parents or caregivers, questionnaires, and standardized tests [Randall et al., 2011, Rujeedawa and Zaman, 2022]. Some common tests and assessments used to diagnose autism are the ADI-R (Autism Diagnostic Interview-Revised), the ADI-R (Autism Diagnostic Interview-Revised), CARS (Childhood Autism Rating Scale), and the GARS (Gilliam Autism Rating Scale). All of them take into consideration direct observations of the social behavior and communication of children.

According to the DSM-5, the level attribution is based on the necessary degrees of support

to help ASD individuals (figure: 2.1) [Masi et al., 2017].

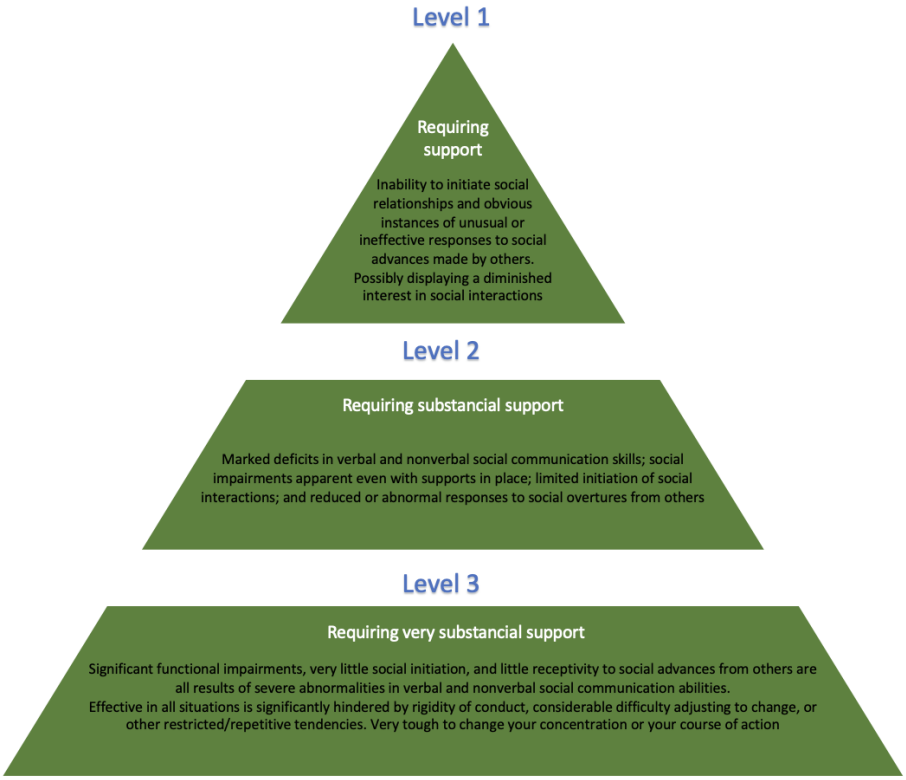

Figure 2.1: Current severity specifiers/levels for ASD. Adapted from [Weitlauf et al., 2014].

The range of support and service needs can be wide, and the ability to operate throughout all life stages and in all skill areas necessary for everyday living is frequently unrelated to the degree of autism symptoms. The International Classification of Functioning, Disability, and Health core sets for ASD are now being developed to address the challenges related to the proper evaluation of functioning, a crucial component in understanding the influence of severity on outcomes [Weitlauf et al., 2014].

Although not used for diagnostic purposes, several functional neuroimaging techniques such as functional magnetic resonance imaging (fMRI), functional near-infrared spectroscopy (fNIRS), and electroencephalogram (EEG) are used to investigate the neurobiological underpinnings of ASD. Due to its superior spatial resolution, fMRI has been frequently utilized to study ASD functional brain patterns associated with characteristics of the condition [Deng et al., 2022].

It is important to remember that the diagnosis of autism must be made by a healthcare professional trained and qualified in assessing and treating autism [Randall et al., 2011].

2.2 Functional magnetic resonance imaging (fMRI)

fMRI is a neuroimaging technique developed in the early nineties. Characterized for being a variant of magnetic resonance imaging, it is used to measure the blood-oxygen-level-dependent (BOLD) signal, related to brain activity. This signal allows us to map and detect human brain

activity.

There are neurovascular changes that can be consequent to task-induced brain state changes or the result of unregulated processes in the resting brain [Soares et al., 2016, Glover, 2011].

Properties that make fMRI one of the greatest functional neuroimaging techniques, are the fact that it is fundamentally not invasive, does not require injection of a radioisotope or other pharmacologic agent, and can access images with high spatial resolution, signal reliability, robustness, and reproducibility [Soares et al., 2016, Glover, 2011].

2.2.1 Bold Signal Contrast

The level of activity of nerve cells in each region of the brain can be traced in fMRI images, given the versatility of Magnetic Resonance Imaging (MRI) technique. Thus, there are two primary consequences of increased neuronal activity and both can be detected by MRI: increased local cerebral blood flow (CBF) and the respective changes in oxygenation concentration (BOLD contrast or Bold Oxygen Level Dependent) [Glover, 2011, Ogawa and Lee, 1990].

The second mechanism and the one used in most studies, BOLD contrast, was firstly tested in rats [Glover, 2011, Kwong et al., 1992] and later in humans [Ogawa and Lee, 1990, Glover, 2011].

Changes in the magnetic field surrounding blood cells depend on the oxygenation of the present hemoglobin. Oxygenated hemoglobin (HbO2) is diamagnetic and practically cannot be distinguished, magnetically, from brain tissue. In the opposite case, if hemoglobin is not oxygenated, it has four unpaired electrons and it becomes paramagnetic. These changes in the magnetic field originate the BOLD contrast, using the two forms of deoxygenated hemoglobin (Hb) to indirectly calculate brain activity [Lindquist and Wager, 2016].

2.2.2 Bold Signal Mechanism

Several neuronal brain processes require energy, including the formation and propagation of action potentials, the binding of vesicles to the presynaptic junction, and the release of neurotransmitters across the synaptic gap. The energy used for these mechanisms comes in the form of adenosine triphosphate (ATP) [Glover, 2011]. When neuronal activity increases after neuronal activation, resulting in a locally increased energy requirement, this provokes an up-regulated cerebral metabolic rate of oxygen (CMRO2) in the brain region being recruited [Buxton and Frank, 1997].

As the local storage of oxygen in tissues adjacent to capillaries is consumed by glycolysis and waste products enlarge, the increased blood flow and blood volume (local blood flow (CBF) and local blood volume (CBV)), respectively) acts to restore the local O2 level required to overcome the transient deficit and stabilize the process. As a result, neural up-regulation results initially in a build-up of Hb and a decrease in HbO2 in the intra and extravascular spaces, followed by a vasodilatory response that reverses the situation. This results in an increase of HbO2 and a decrease of Hb [Glover, 2011, Buxton and Frank, 1997].

Given the fact that the paramagnetic Hb disrupts the homogeneity of the magnetic field,

the MRI signal ought to decrease. However, the rise in CBF overcompensates the drop in O2 since it makes a greater contribution. As a result, even with an increase in CMRO2, more oxygen is given than is consumed [Glover, 2011, Lindquist and Wager, 2016].

The resulting neural excitation demonstrates local increases in the T2* signal strength due to reduced deoxyhemoglobin concentration and provides the BOLD signal/contrast mechanism [Glover, 2011].

2.2.3 Hemodynamic Response to a Stimulus

Via a mechanism known as neurovascular coupling, elevated neuronal activity affects changes in local blood flow, blood volume, and oxygen absorption [Gong et al., 2014].

So far, extracellular local field potentials are believed to be more closely correlated with the BOLD signal than the quantity of "active" nerve cells. Compared to depolarization peaks, local field potentials have a significantly longer time course and are gradually shifting voltages recorded from large populations of brain cells. The sum of the positive and negative postsynaptic potentials at various dendritic connections, as well as neuronal discharges, are included in the overall activity of regional neural networks that it reflects [Gong et al., 2014].

The hemodynamic response function (HRF) denotes the regional BOLD response produced by a short external stimulus. It is the mathematical transfer model that relates the BOLD of neurovascular connections with regional brain activity. The HRF has a common, known shape (figure: 2.2). However, several studies have proved that variations in HRF shape occur between individuals and brain regions [Rangaprakash et al., 2020]. Such differences can be associated with vascular size and density, alcohol, caffeine, and fat consumption, global magnetic susceptibilities, slice timing variations, and pulse/respiration variations [Rangaprakash et al., 2020].

Three primary factors, including response height, time-to-peak, and full-width at half-max, are usually used to describe HRF shapes (FWHM). The HRF amplitude is measured by response height. While FWHM pertains to the length of the BOLD response, and time to peak assesses delay. The HRF typically shows an initial small dip, followed by a peak (overshoot), and then a post-stimulus undershoot (figure: 2.2).

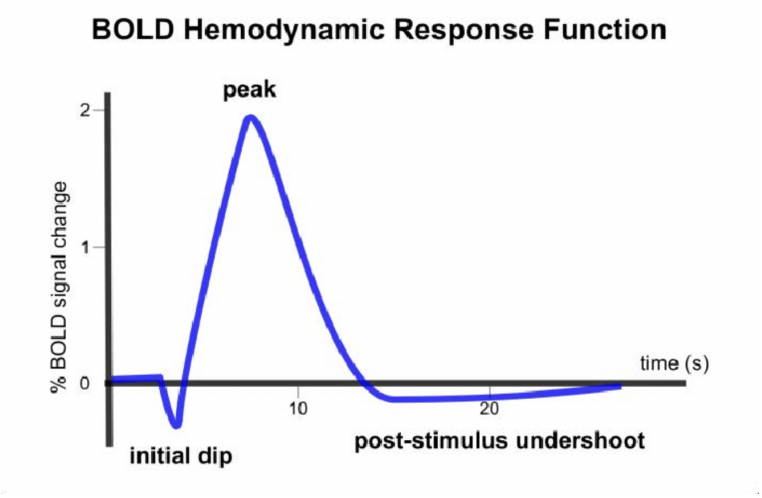

Figure 2.2: Hemodynamic response function following a brief stimulation (at 0 seconds), used under the terms of the Creative Commons Attribution License (CC BY) from [Georgiopoulos, 2019].

The initial dip is variable and inconsistent, characterized by the quick consumption of oxygen by the cells, a response to increased neuronal activity, without altering the blood flow.

After two seconds, approximately, followed by a hyperoxic phase (vasodilation of arterioles, increased cerebral blood flow), an over-compensatory response occurs quickly surpassing the initial dip. In contrast to the current metabolic demands, regional cerebral blood flow increases out of proportion. As a result, the ratio of oxyhemoglobin to deoxyhemoglobin briefly rises.

After 12–14 seconds, a sustained response is kept and followed by the undershoot phase, most commonly observed in longer stimulus experiments (lower magnetic resonance signal) [Rangaprakash et al., 2020, Georgiopoulos, 2019].

The HRF shape can be used to infer a determined neuronal activity condition by interpreting the BOLD signal response to the stimulus [Park et al., 2020].

2.2.4 fMRI Data Processing and Analysis

Normally, we can define two approaches when performing fMRI:

Resting-state functional magnetic resonance imaging (rs-fMRI)

This approach is commonly used to determine, without any task intrinsic brain architectures, and spontaneous connections between brain areas. Other than attempting to keep their head still while being scanned, patients just need to stay relaxed. Thus, the behavioral protocol is rather basic ("hold still and try to stay awake") [Park et al., 2020, Logothetis, 2008].

Task-based experiments

Task-based experiments are one of the most effective means of determining brain connectivity and functions. They can be used to describe better the differences between the group of control participants and the clinical. This is conceivable because doing a certain activity will demand the modulation of specific areas and networks [Park et al., 2020, Logothetis, 2008].

Moreover, combining data from task runs and resting runs can provide a more complete

and integrated view of brain connectivity in different states and conditions, allowing a better understanding of the brain's functional organization. In addition, using both approaches allows verification of whether observed changes in connectivity during tasks are due to differences in task performance and reflect in fact changes in underlying functional connectivity.

In functional magnetic resonance imaging (fMRI) acquisitions, both anatomical and functional runs are performed. The anatomical runs provide a better spatial resolution, allowing for the identification of different structures situated closely. A time series of 3D functional volume data, or a four-dimensional volume, makes up functional runs in a task or resting state (4D, space, and time dimensions). A 3D image of the brain is created by stacking all the 2D slices that make up each functional volume and that were recorded at various moments throughout the chosen TR (repetition time) [Molloy et al., 2014].

The first step is to preprocess data. Data must be preprocessed to eliminate undesirable artifacts and prepare the data for analysis. Several tools are freely available for processing neuroimaging data, including stastical parametric map (SPM), AFNI, FSL, FreeSurfer, Workbench, and fMRIPrep [yong Park et al., 2019].

- **fMRI Preprocessing (general steps)**

Due to the presence of non-neuronal components in BOLD signals (fluctuations of no interest in the data), artifacts may emerge from physiological noise (respiration, sleepiness, patient mobility), or temperature noise, making fMRI results challenging to interpret. In addition, the choice of image acquisition parameters has a significant impact on the quality of fMRI data. Thus, preprocessing steps are necessary to handle these issues. Listed below are the usual preprocess steps, however, depending on the equipment used, some can be optional [Campos et al., 2016, Di and Biswal, 2023].

Slice Timing Correction

An interpolation-based method to adjust the time disparities at which each slice was obtained [Smith and Beckmann, 2017].

Realignment, Head Motion Correction and Volume Scrubbing

During fMRI acquisitions, participants tend to move their heads, and while some of these movements can be controlled, others are involuntary and unavoidable, causing artifacts and data corruption. The solution is to perform motion correction on the data. All volumes are registered to a reference volume using a rigid-body transformation to complete the operation. Any volume can serve as the reference volume, but most often the first or middle volume of the entire data set is chosen. The removal of volumes with extreme head motion is the next phase. Volume scrubbing is the term used to describe this method [Power et al., 2012].

Field homogeneity correction

Each tissue has a distinct intensity that changes in response to changes in the magnetic field. This step is optional because older neuroimaging studies may not have acquired field map data which is necessary to perform this correction. However, if the field map-corrected EPI (echo planar imaging) data is collected, the images are standardized and corrected, making the intensity of each tissue more homogeneous and uniform [yong Park et al., 2019].

Coregistration

fMRI data has low spatial resolution and low inter-visual contrast when compared to structural images. To coregister the fMRI data onto the standard space, two transformation matrices are combined and then applied to the data. The first one involves using a rigid-body transformation to coregister fMRI data onto a high-resolution, previously processed T1-weighted structural MRI data of the same individual. The T1-weighted structural MRI data is then registered into the reference space via an affine transformation. [Jenkinson et al., 2012].

Normalization

This next step consists of modifying the brain so that it closely resembles the brain of other subjects or templates so that their sizes, orientations, shapes, and gyroscopic anatomies are equal.

Data Segmentation

The segmentation of fMRI allows the visualization and separation of different important structures as well as parts of the brain, such as grey matter, white matter, cerebrospinal fluid, bone, soft tissue, and air. With this specific process, we can collect information and estimate noise contributions to the signal (only in the tissues of interest).

Noise Variable Removal

Noise variable removal in fMRI data is not always used, but it is a common and important step in the preprocessing and analysis of data. Physiological noise correction is necessary to eliminate components of head motion, White Matter, Cerebrospinal Fluid, cardiac pulsations, and arterial and large vein-related inputs. Usually, respiration or cardiac pulsations generate time-varying signals that are multiple times mistaken with neural brain activity [Chen et al., 2019].

Spatial Smoothing

The goal is to blur the measured signal in close-by voxels, noise will average out and the signal of interest will not be greatly impacted, increasing the signal-to-noise ratio (SNR). Although smoothing fMRI data has the benefit of lowering noise, it can also weaken the signal's strength. Consequently, while using spatial smoothing, researchers must proceed cautiously [Worsley and Friston, 1995].

Temporal Filtering

The signals of relevance in fMRI data lie in the low-frequency region. Very low-frequency signals, however, are regarded as slow drifts. As a result, high-pass filters are frequently utilized to obtain the desired signals [Biswal et al., 1995].

Estimating brain response amplitude- GLM analysis

The General Linear Model (GLM) has emerged as the central tool for fMRI data analysis within the neuroimaging community following its introduction by Friston and colleagues [Friston et al. 1994, 1995]. This popularity is primarily due to its ability to accommodate a wide range of quantitative and qualitative independent variables.

From the perspective of multiple regression analysis, the GLM aims to elucidate the variation in a dependent variable by means of a linear combination (weighted sum) of several reference functions. The dependent variable is represented by the observed fMRI time course of a voxel, while the reference functions are time courses that mirror the anticipated (idealized)

fMRI responses for various conditions within the experimental paradigm. The reference functions are also called predictors, regressors, explanatory variables, covariates, or basis functions [BrainVoyager, nd]. A set of designated predictors collectively forms what is known as the design matrix, often referred to simply as the model. A predictor time course is typically obtained by convolution of a block condition protocol time course with a standard hemodynamic response function. Each predictor time course X gets an associated coefficient or beta weight b, quantifying its potential contribution in explaining the voxel time course y. The voxel time course y is modeled as the sum of the defined predictors, each multiplied by the associated beta weight b. Because this linear combination cannot perfectly account for the data due to the presence of noise fluctuations, an error term e is incorporated into the GLM matrix of equations with n data points and p predictors [Doan, 2015].

$$y = \beta_0 + \beta_1 X1 + \beta_2 X2 + \beta_3 X3 + \epsilon \tag{2.1}$$

Given the data y and the design matrix X, the GLM fitting procedure has to find a set of beta values explaining the data as well as possible. Comparisons between conditions can then be formulated as contrasts, which are linear combinations of beta values corresponding to null hypotheses.

2.3 Brain Connectivity

Brain connectivity analysis is used to investigate how the brain's networks are set up and how information is transmitted. It can be used to examine how the brain changes in response to various stimuli and how these changes connect to psychological states.

The principal goal is to define neuropsychological events that are happening at the same time but spatially apart [Faber et al., 2019]. When two or more brain regions' responses are specifically related in time, they are considered to show functional connectivity. If one region's behavior is regularly connected with another, it is thought that they are linked or that they are elements of the same network.

Nevertheless, brain connectivity can also be analyzed in structural terms using techniques such as Diffusion Tensor Imaging (DTI). Moreover, when based on brain function, it can be considered functional connectivity or effective connectivity. The former does not make any assumptions about the causes of the relationships between the regions, and the latter model's causal influences between different brain regions [Faber et al., 2019, Bullmore and Sporns, 2009].

2.3.1 Functional Connectivity

Brain functional connectivity measures provide information on which brain regions are functionally connected to form brain networks that subserve either behavioral/cognitive task performance or the brain's resting/default state [Mohammad-Rezazadeh and Frohlich, 2016].

Moreover, these approaches study the interdependency among different brain regions. Such interdependency can be measured by using statistical methods such as covariance, phase coher-

ence, phase locking, and correlation [Mohammad-Rezazadeh and Frohlich, 2016].

Furthermore, functional connectivity can be studied at different levels, from correlations between specific brain areas to the analysis of entire networks and their properties. Sophisticated methods, such as rs-fMRI analysis and dynamic connectivity analysis, allow us to investigate the temporal dynamics of brain networks and how they reorganize in response to stimuli or changes in cognitive demands, respectively [Pamplona, 2014].

Thus, fMRI-based functional connectivity attempts to quantify the level of functional integration across different brain areas by measuring the temporal correlations among the BOLD signal fluctuations in these areas. Despite the relative simplicity of its definition, there are easily hundreds of different functional connectivity metrics approaches [Nieto-Castanon, 2020]. One of the most used and simplest approaches to estimate functional connectivity is following a ROI-to-ROI connectivity analysis. It allows for characterizing the connectivity between pairs of regions of interest *ROIs* among a pre-defined set of brain regions. The resulting matrix represents the level of functional connectivity between each pair of *ROIs*, where each element is usually defined as the Fisher-transformed bivariate correlation coefficient between a pair of ROIs BOLD time series [Nieto-Castanon, 2020]:

$$r(i,j) = \frac{\int R_i(t)R_j(t)dt}{\left(\int R_i^2(t)dt \int R_j^2(t)dt\right)^{1/2}}$$

$$Z(i,j) = tanh^{-1}\big(r(i,j)\big)$$

Figure 2.3: Fisher-transformed bivariate correlation coefficient between a pair of ROIs BOLD time series, where R is the BOLD time series within each ROI, r is a matrix of correlation coefficients, and Z is the symmetric matrix of Fisher-transformed correlation coefficients.

2.3.2 Brain Networks

Over the years, brain connectivity has been investigated in several studies. The advance of computational methods, like machine learning and non-invasive functional neuroimaging, has allowed the definition of different brain networks. Some of the most known brain networks include the default mode network, the executive network, the visual network, the auditory network, and the salience network. Besides, there are other specific networks, which are involved in different cognitive functions such as attention, memory, emotion, and decision-making [Salmón and Leoni, 2019]. Overall, brain networks spatially define areas with related functions. That is, regions similarly modulated by the stimulus, although anatomically not adjacent, exhibit spontaneously correlated fluctuations arising from hemodynamic activity

Multiple brain networks depend on how a network is defined, at the most fundamental level, the brain can be viewed as having seven major ones: the dorsal attention network, the default mode network, the salience network, the sensorimotor network, the visual network, the limbic network, and the central executive network, listed in table: 2.1 and in figure: 2.4 [brain networks, nd, Thomas Yeo et al., 2011].

Table 2.1: Table with the seven major brain functional networks and the associated brain regions/nodes [brain networks, nd].

Brain Network	**Functional Areas**
Sensorimotor Network	primary motor cortex, cingulate cortex, premotor cortex, the supplementary motor area and the primary and sensory cortices in the parietal lobe
Visual Network	visual area 1(V1) , the dorsal visual network area is adjacent to the parietal lobe in the dorsal stream, which stretches from V1 into the parietal lobe
Limbic Network	amygdala, thalamus, hypothalamus, hippocampus, ACC, medial temporal network, parahippocampal gyrus, olfactory lobe, and the ventral tegmental area
Central Executive Network	anterior cingulate cortex, the inferior parietal lobe, and the posterior-most portions of the middle and inferior temporal gyrus
Default Mode Network	mPFC, PCC, inferior parietal lobe, lateral temporal cortex and hippocampal formation
Salience and Ventral Network	anterior cingulate, the anterior insula, the pre-supplementary motor areas, it also includes nodes in the amygdala, hypothalamus, ventral striatum, thalamus, and ACC, medial temporal network and parahippocampal gyrus
Dorsal Attention Network	areas in the lateral occipital lobe, the pre-central sulcus, the dorsal-most portion of the superior frontal sulcus, the ventral premotor cortex, superior parietal lobule, intraparietal sulcus, and motion-sensitive middle temporal area

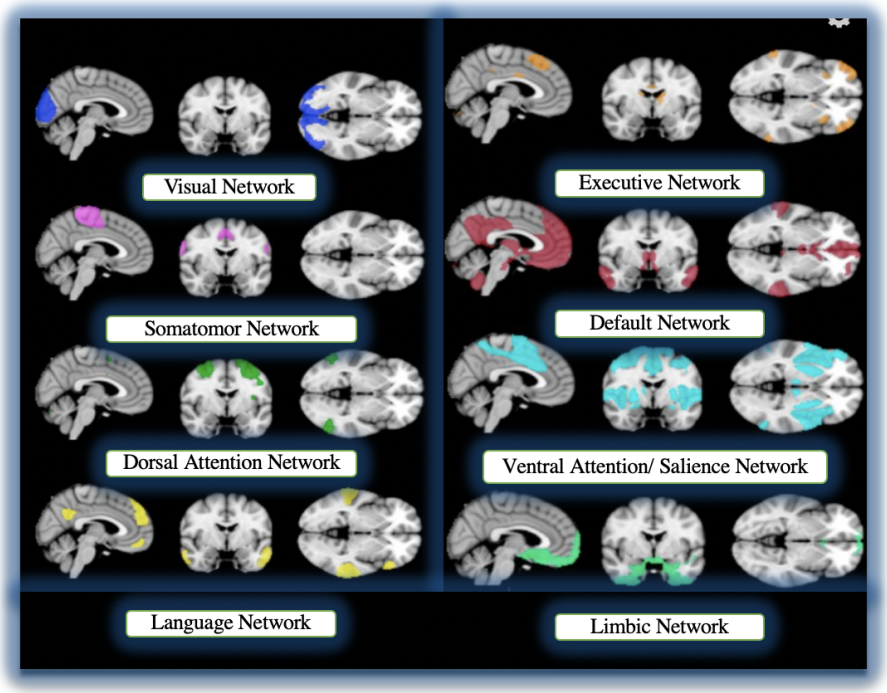

Figure 2.4: Representation of the main known brain networks, from [intrinsic networks, nd]. Copyrights authorization pendent.

3

The neural underpinnings of social cognition- state of the art

Emotions play a crucial role in our everyday life behaviors, they guide us in what to do, what to avoid, and what to search for. They translate how we feel when something is happening around us and are often provoked by external factors. They arise from interactions with people, with the surrounding environment, or from any kind of stimulus, simple or complex that a person can feel. Thus, emotions are what people call, the principal resource of decision-making [Ward, 2006].

Social cognition is the term used concerning the cognitive processes involved in comprehending and remembering details about other people, including oneself, as well as interpersonal conventions or procedures [Baron-Cohen et al., 2000].

3.1 Neural correlates of social cognition: from brain activation to connectivity

3.1.1 Theory of the Mind

Several theories of emotion have been developed over the years. Recent studies and meta-analyses have been done particularly in the mentalizing one, or Theory of the mind (ToM) [Karoğlu et al., 2022, Szamburska-Lewandowska et al., 2021]. This theory infers about how we can attribute mental states to others and share emotions and mental states with them (mirroring) [Ward, 2015].

Different social and emotional related stimuli such as facial expressions and eye gazes, have been applied to investigate the neural mechanisms of ToM in social cognition [Schurz et al., 2020, Ward, 2015].

To illustrate, a ToM task is for example: interacting with socials or even observing them will make us predict their actions or their feelings, and we instantaneously put their actions on ourselves and in how we would react if we were them (mirroring). The ability of social cognition in others and ourselves activates on average most frequently the bilateral temporal-parietal and anterior temporal cortex, the medial prefrontal cortex, and posterior and anterior cingulate (figure: 3.1). These areas overlap with a known brain network, Default Mode Network (DMN), which is characterized by the mediation of self-generated cognition [Schurz et al., 2020].

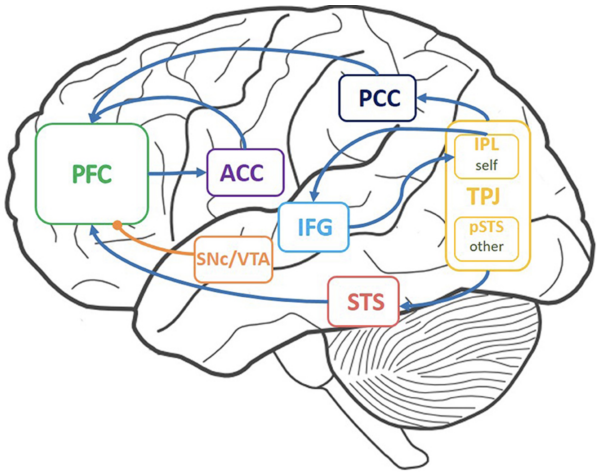

Figure 3.1: Brain regions in Theory of Mind: temporo parietal junction (TPJ), medial prefrontal cortex (mPFC), anterior cingulate cortex (ACC), and inferior frontal gyrus (IFG) interconnected. Source: [Zhao et al., 2022], used under the terms of the Creative Commons Attribution License (CC BY).

Along the next subsections, we describe previous fMRI results regarding different brain regions involved in social cognition, and their connections, particularly, in the ToM theory. We also describe previous findings regarding brain activity and connectivity alterations in Autism Spectrum Disorder (ASD) patients, which have been linked to the lack of social-emotional complexity in the subjects.

3.1.2 Brains regions recruited in emotion processing

When someone is presented with a stimulus such as a social interaction, the emotional brain circuit is recruited. Inferring transient states, such as objectives, intents, and aspirations of others, even when they are erroneous and unfair from our perspective, can be beneficial [Genovese and Butler, 2020, Tavares et al., 2011]. Several theoretical hypotheses, for example, the "Circuit theory anatomy" (figure: 3.2), try to explain how various brain areas process information crucial for social cognition. Nevertheless, some brain networks are used to process both social stimuli (our perceptions and interactions with others) as well as nonsocial stimuli with affective properties (such as spiders, food, and electric shocks) [Ward, 2006].

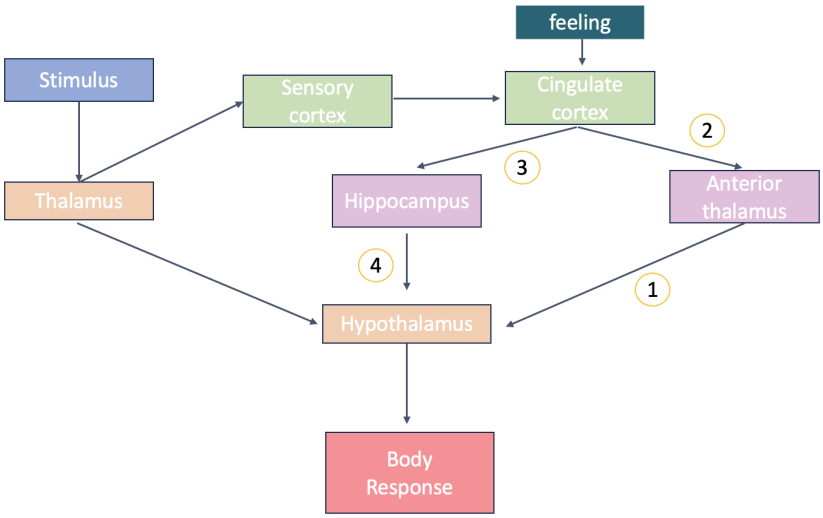

Figure 3.2: The Emotion Circuit Theory in Neuroanatomy. Connection from the hypothalamus to the anterior thalamus (1) and onto the cingulate cortex (2). Emotional feelings happen when the cingulate cortex integrates these signals from the hypothalamus with information from the sensory cortex. Output from the cingulate cortex to the hippocampus (3) and then to the hypothalamus (4) allows the control of emotional responses. Adapted from [Dalgleish, 2004].

Among the variety of theories regarding emotional brain processes, some researchers, using fMRI, studied mentalist inferences about another person's thoughts or feelings based on facial expressions. Their conclusions showed that patients with generalized autism spectrum disorder (ASD) did not exhibit amygdala activation, while people without autism did. Therefore, it is suggested that the amygdala is one of the numerous brain areas that are dysfunctional in autism [Baron-Cohen et al., 2000].

The amygdala is a region believed to play an important role in memory formation and in learning whether a response to a situation should be associated with a reward or a punishment. It's closely linked to the processing of emotions, especially fear. In an initial study conducted with mice [Phillips and LeDoux, 1992], an auditory tone is used as a neutral stimulus (CS-). This means that the tone, by itself, does not naturally elicit a fear response in them. Secondly, an electric shock is introduced, and it naturally triggers a specific response, in this case, fear, without any prior learning. When the electric shock is paired with the auditory tone (CS-), the mice start to associate the tone with the shock. As a result, the auditory tone eventually begins to elicit a fear response from the mice on its own, even when the electric shock is not present. The once-neutral auditory tone (CS-) has now become a conditioned stimulus (CS+) (fig: 3.3). Explanations suggest that the amygdala is likely involved in this process. It is known to be associated with fear responses and emotional learning [Ward, 2015].

However, if the amygdala is dysfunctional in mice, they will not learn this association. The result thrives from the fact that this region is important for both storing and learning responses.

Although this experience was performed in mice, the amygdala is also essential for pro-

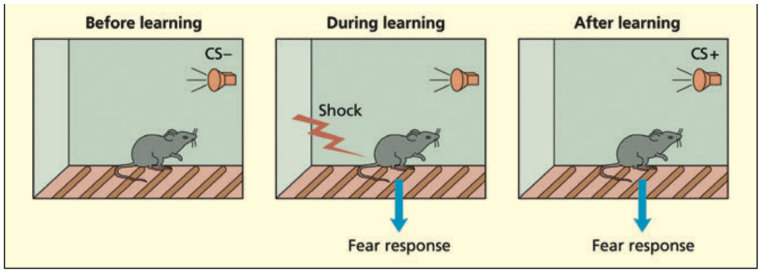

Figure 3.3: Example of the paradigm used to test emotions, particularly, fear. The fundamental step in fear conditioning entails shocking an initially neutral stimulus (the CS-, for example, a tone). The stimulus will eventually cause a fear reaction without also causing a shock (it will then become a CS+) [Ward, 2015]. Copyright authorization pendent.

cessing socially significant information, such as facial expressions of fear, body movements, and eye contact in humans. Amygdala lesions can lead to an inability to demonstrate conditioned emotional responses and can affect the verbal learning of associations [Ward, 2015].

In another study [Baron-Cohen et al., 2000], to understand how the people's brains with autism (the clinical group) are different from those without these conditions (the control group), they used two tasks:

A: Showed both groups pictures of eyes and asked them to decide whether the eyes belonged to a man or a woman. **B**: Showed the same eye pictures but asked both groups to choose which words best described the person's thoughts and feelings in the picture.

They concluded that the clinical group's brain did not activate much in certain areas, like the front part of their brains (specifically the left dorsolateral prefrontal cortex and the left medial frontal cortex). They also noticed that the clinical group's brain did not show any activity in the amygdala.

In contrast, the control group's brains were more active in areas like the right insula, left IFG, and left amygdala. They also found that a part of the brain called the superior temporal Gyrus (STG) was more active in the clinical group. So, in simple terms, this study showed that the brains of people with autism might work differently when it comes to understanding emotions and thoughts through people's eyes, and they might rely on different brain areas to do this [Baron-Cohen et al., 2000, Ward, 2015].

Another "emotion area" is the insular cortex. It is located deep within the lateral sulcus of the brain, the "limbic integration cortex". This description is mostly based on the anatomical connection patterns of this area, which gets input from the orbitofrontal, olfactory cortex, anterior cingulate (AC), and superior temporal sulcus (STS) and projects to the amygdala, lateral orbital cortex, olfactory cortex, and to the AC. [Uddin and Menon, 2009].

The anterior insula (AI) plays a crucial role in how we understand and interact with others. This region was often overlooked in earlier research on ASD, which used to focus on other brain areas like the fusiform gyrus, STS, or the amygdala. Recent research has found that people with ASD show less activity in the right AI when compared to others [Uddin and Menon, 2009]. This might be because the AI is not communicating properly with other brain parts responsible for emotions and sensory information, affecting their ability to notice important things and

behave appropriately in social situations. The AI acts as a central hub of the salience network, connecting different brain networks that are involved in focusing our attention and our self-directed thoughts. This makes the insula essential for handling and understanding important information. It mediates interactions between systems that deal with our internal thoughts, default mode network (DMN), and those that handle our attention to the outside world, executive network (fig: 3.4) [Uddin and Menon, 2009, Gasquoine, 2014].

Given these network interactions, some considerations have been made inferring that the hypoactivity observed in ASD patients may be due to a breakdown in communication between the insula and the limbic (emotional) and sensory parts of the brain that send signals to it. This could lead to problems in detecting what is important in a given situation and in mobilizing the attention needed for appropriate social behavior. [Uddin and Menon, 2009, Gasquoine, 2014].

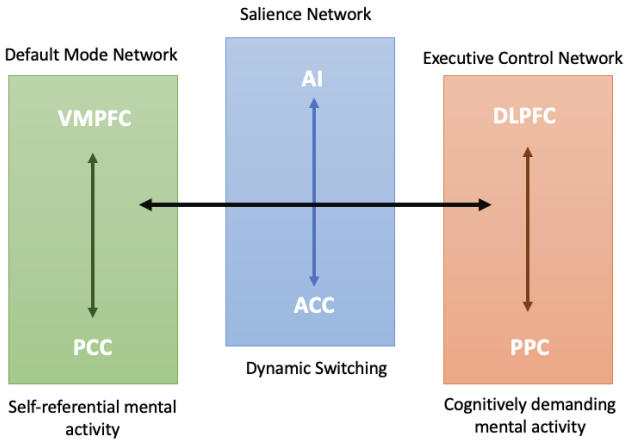

Figure 3.4: Model of AI function: the AI as a part of the salience network responsible for facilitating dynamic switches between the DMN and the executive network (ECN). The AI dysfunction in autism impairs the AI's typical role in coordinating these large-scale brain networks. Adapted from: [Gasquoine, 2014]. Copyrights authorized by the author.

In addition to the aforementioned, there are other brain regions like the orbitofrontal cortex, anterior cingulate, and the ventral striatum that also play a big part in social cognition. Normally, the first one is associated with rewarding emotions, based on "prediction error" signals. For example, *"The chocolate was rated as pleasant and participants were motivated to eat it, but the more they ate the less pleasant it became"* [Ward, 2015]. When actions like this one take place, the orbitofrontal cortex is mobilized.

The AC is often associated with the value of responses if the action is likely to provoke a reward or a punishment. It can differ from the orbital frontal cortex function [Ward, 2015].

These brain areas associated with emotions play a vital role in evaluating and understanding social signals in both animals and humans. The AC isn't just activated by physical pain, it also responds to emotional pain caused by social experiences (isolation, for example). Also, the AC is mobilized when we make choices to cooperate with someone else, and not only in response to rewards [Ward, 2015]. Likewise, the amygdala is engaged in assessing not only whether a

sound might lead to a painful shock, but also whether another person is experiencing fear or other emotions. In conclusion, the right function of these brain regions is very important to the social and emotional environment around us and has a substantial effect when interacting with people. [Ward, 2015, Baron-Cohen et al., 2000, Uddin and Menon, 2009].

3.2 Altered brain network interactions underlying social cognition in ASD

3.2.1 The two main social brain areas: temporoparietal junction and medial prefrontal cortex

Although multiple brain areas activate with a determined emotion or feeling, and we immediately associate the stimulus with that specific activation, we have concluded that these brain areas connect particularly with the temporal poles and the prefrontal cortex.

According to several fMRI studies [Ward, 2015, Baron-Cohen et al., 2000], the two main principal brain areas in human social cognition are the TPJ and the mPFC, which are connected with functions with the amygdala, insula, anterior cingulate, orbitofrontal cortex and ventral stratium (mentioned before) [Overwalle, 2009].

Some investigators claim that mentalizing is a high-level mental function that is primarily supported by the mPFC and other cortical midline structures [Sommer et al., 2007]. However, a growing number of authors contend that the TPJ performs unique social roles, particularly for determining the purposes or intentions underlying actions, in conjunction with "mirror neurons". [Overwalle, 2009].

3.2.2 Mirror Neuron System

The mirror neuron system (MNS) englobes a group of specific neurons that are able "to mirror" the behavior and actions of others [Rizzolatti and Craighero, 2004, Overwalle, 2009].

The mirror neuron system (MNS) is a very interesting proposal because, through it, one can analyze simple explanations for self and other's intentions. Some fMRI studies with monkeys [Matsumoto and Tanaka, 2004], highlighted that cortical structures involving the STS, inferior parietal lobe (IPL), and the premotor cortex (PMC) including the IFG, are involved in the mirror system [Overwalle, 2009].

The visual information in the STS is passed to the IPL and then propagated for the PMC, responsible for action execution. The action is identified by resemblance with our actions and passed for the IPL (fig: 3.5). The shared representation of self and others is related to inferences about what is not sure but will most likely occur next [Overwalle, 2009].

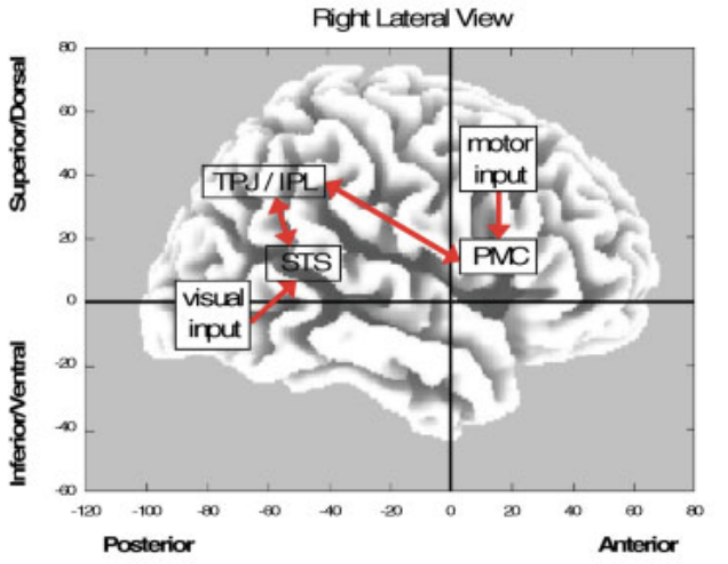

Figure 3.5: The mirror neuron system. Visual input in the STS is propagated to the TPJ/IPL, and further to the PMC where it is compared with our action schemas and associated goals. The correspondent goal behind the action detected at the PMC is sent back to the TPJ/IPL (for goal identification) [Overwalle, 2009]. Copyright authorization pendent.

The TPJ extends from the STS to the IPL and it is believed to be responsible for inferring the intention of a social movement or behavior, identifying the agent of the social action and distinguishing the actions of others from the self [Overwalle, 2009].

3.2.3 How the mPFC relates to social beliefs and traits

The ability to remember the behavior of people over a long period under various circumstances and recognize the common goal in these behaviors is a necessary component of long-lasting social dispositions and interpersonal knowledge, such as personality traits and social rules [Overwalle, 2009].

There is increasing evidence that the mPFC is involved in assigning traits, through connections with the anterior STS, the TPJ, the prefrontal cortex (PFC), and other brain areas.

This region is also implicated in the pragmatics of irony and metaphor and people with autism seem to have difficulties with this [Ward, 2015]. fMRI studies suggest that mPFC is related both to the ToM and with establishing the pragmatic coherence between sentences [Stuss et al., 2001, Roca et al., 2011]. It can bind different kinds of information, like actions, goals, and beliefs to create a social interaction. Some sub-regions respond more when the participants make judgments about themselves, and also about others, which they consider to be similar to their own. Thus, this region does not attribute mental states but thinks of the other as the self [Ward, 2015].

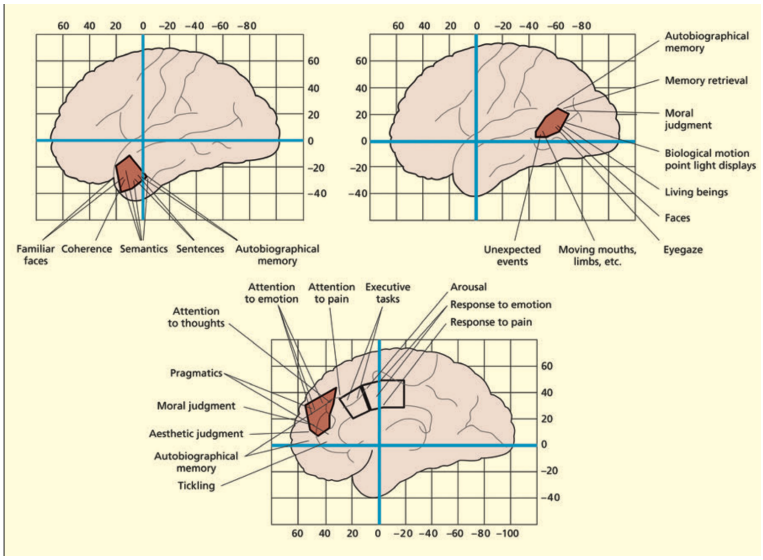

Figure 3.6: The brain location of the three important regions in ToM (shaded). The temporal poles (top left), TPJ, and medial frontal lobes (bottom). From [Ward, 2015]. Copyright authorization pendent.

3.2.4 The mPFC and TPJ in ASD patients

In an fMRI study, participants with and without ASD, were asked to watch a set of black and white comic strip stories while inside an MRI scanner [Murdaugh et al., 2014]. Their task was to choose the ending that made the most sense for each story. These stories depicted non-verbal social situations where events could be explained by either physical causes or intentional actions. The study aimed to understand how individuals with ASD differed from controls in the processing of these social scenarios.

The analysis was conducted considering three components, A, B, and C [Murdaugh et al., 2014]. The component A encompassed the following brain areas: ToM network, including bilateral pSTS at the TPJ, right-mPFC, and ACC. Component B was constituted by the posterior cingulate cortex and the middle temporal gyrus while, component C was made of up STG, postcentral gyrus, middle cingulate gyrus, and posterior cingulate gyrus [Murdaugh et al., 2014].

Underlying intentional causality, component A was the network that showed the highest level of correlation with the task time course and revealed a network consisting of ToM regions identified before, such as the TPJ and the mPFC.

Given the fact that both TPJ and mPFC were part of the same component (A), further evaluation was made to observe the correlation of each region with the overall component A network. This step was considered to identify differences in functional connectivity between both regions separately and the rest of the brain areas of the component.

The results showed that TPJ had considerably higher functional connectivity within the ToM network (regions involved in mentalizing, mentioned in section one) connectivity than the mPFC (fig: 3.7 and fig: 3.8). This suggests that the TPJ appeared to be more active in terms of exchanging information with other parts of the brain.

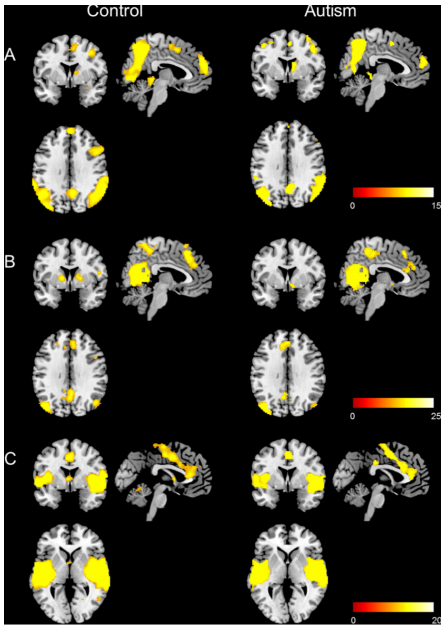

Figure 3.7: The three components representation with the highest temporal correlation with the intentional causality task condition. Component A with higher correlation within ToM regions. Maps are thresholded at $p<0.05$, FDR corrected. The color bar represents Z-scores. [Murdaugh et al., 2014]

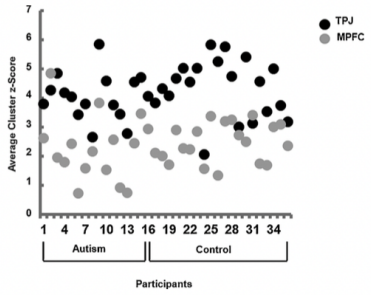

Figure 3.8: Scatter plot showing average cluster z-scores for each subject for the TPJ and mPFC in Component A. It showed higher within-network connectivity in the TPJ compared to mPFC during intentional causal attribution; *(t(35) p<0.0001)*) [Murdaugh et al., 2014].

Research suggests that as a person ages, the mPFC loses its mentalizing specialization and becomes more active in the general meta-representation of social and non-social information, whereas the TPJ becomes more activated and specialized in mentalizing processes [Kana et al., 2014]. The authors defended that the TPJ and IFG, rather than the mPFC, are primarily involved in deliberate causality.

The study also compared these two regions' functional connectivity between individuals with autism and a control group (people without autism). In individuals with autism, they observed reduced connectivity related to the TPJ within the ToM network. These findings suggest that there is a clear difference in the functioning of the TPJ in individuals with ASD, but this difference is not noticed in the mPFC.

TPJ and mPFC thus seem to play distinct roles in the mentalizing process, which is the ability to understand and interpret the emotions and feelings of others. Moreover, the social problems associated with ToM may be caused by TPJ dysfunction, which is seen in people with ASD. To put it another way, the changes in how the TPJ works may be a factor in the difficulties that people with autism have comprehending and engaging with others in social contexts.

3.2.5 Brain systems interactions in ASD Patients

Articles and published papers have reported throughout the years that ASD individuals when compared with typically developed individuals, show lower brain connectivity patterns. However,

results from recent studies have proven that the typical notion of decreased connectivity between distal regions and increased connectivity between close brain regions depends on the method used to measure brain connectivity and its metrics [Mohammad-Rezazadeh and Frohlich, 2016].

The type of functional technique used, Electroencephalogram (EEG), Magnetoencephalography (MEG) or fMRI, the patient's age, the regions to be observed, the connectivity's frequency band and interval, and the cognitive and behavioral components of the experience can be some reasons in the discrepancies between studies.

A few fMRI papers have concluded that ASD individuals have decreased connectivity (or hypo-connectivity) between distant brain regions like the frontal and parietal lobes

[Mohammad-Rezazadeh and Frohlich, 2016].

DMN is proven to be one of the most known brain networks showing hypoconnectivity in ASD patients, as well as its lack of communication with regions like the amygdala (medial temporal lobe network, limbic system) and the insula (salience network) [Hull et al., 2017a]. This finding suggests that the limbic and salience systems may be implicated as dysfunctional networks when the condition is present.

Even though considerable investigation has been made on the topic, brain connectivity in ASD patients is still a complex issue for researchers when studying connectivity patterns in individuals, as they need to consider several factors such as the experimental task used (simple and short to avoid artifacts and provide a clean analysis), the time it takes for certain sensory or cognitive processes to occur, the frequency range of interest, and the specific brain regions or networks being studied. These factors are important to consider to accurately interpret and classify different patterns of brain connectivity in ASD and to identify subgroups within the condition that may have different biological mechanisms or outcomes [Fishman et al., 2019].

Nowadays, brain connectivity is being studied as an ASD risk marker in early development stages. It's believed that fMRI task-based functional connectivity analysis is useful to investigate intrinsic connectivity in individuals with ASD compared to non-ASD individuals, as it can identify brain networks that are involved in specific cognitive and emotional functions. This can add, to the understanding of how these networks may be altered in different clinical or psychiatric conditions. Researchers can also identify task-specific networks or brain regions that are particularly active or synchronized during the task when using a fMRI task-based data.

The concept of under-connectivity/ hypoconnectivity is thus still a matter of investigation and discussion. In the context of functional neuroimaging, it has been used to refer to a reduction in the strength or synchronization of neural activity between brain regions or within specific networks, as compared to a normative or standard value observed in unaffected/ healthy individuals. When discussing whether ASD patients have higher or lower levels of functional connectivity between regions, we are examining the correlation between the strength and timing of BOLD signal fluctuations in different voxels to determine how well these regions are synchronized. If patients show a decrease in the correlation of these signals compared to control individuals, it is hypothesized that their brain regions are not functioning in harmony, and show under connectivity [Hull et al., 2017b]. Through it, altered brain networks are related to specific conditions and in the future might provide earlier diagnosis and improved interventions.

4

Methodology

The data analyzed in the thesis were collected in the context of a clinical research project of the host institution, approved by the ethics committee of the University of Coimbra. All participants filled out informed consent forms before the experiment was performed.

4.1 Dataset

The dataset used in this study includes 11 male healthy participants (mean age= 23, s.d=±3) and 11 male ASD (mean age= 22,s.d± 7) as summarized in table 4.1. The included individuals were diagnosed with high-functioning autism spectrum disorder (ASD), defined by a full-scale intelligence quotient (FSIQ) greater than 70. Participants with ASD were recruited from both the Neurodevelopment and Autism Unit at our local hospital and the national association for autism spectrum developmental disorders. An experienced neurodevelopmental clinician confirmed a clinical diagnosis for all patients, following the criteria outlined in the Diagnostic and Statistical Manual of Mental Disorders, 5th edition (DSM-5). It is important to note that all cases of ASD in this study were categorized as idiopathic.

Control participants underwent screening for ASD using the Social Communication Questionnaire, with a cutoff score bigger than 15 to identify potential ASD cases. None of the control participants scored above this threshold (scores ranged between 1 and 6), ensuring that the control group did not exhibit ASD characteristics.

Furthermore, both the ASD and control groups were assessed for their intellectual abilities using the Wechsler Adult Intelligence Scale – 3rd edition. In the control group, an abbreviated version of this scale was administered, measuring their Full-Scale IQ (FS-IQ), Verbal IQ (assessed through subtests: Information, Similarities, Vocabulary, Arithmetic, and Digit Span), and Nonverbal Performance IQ (evaluated through subtests: Picture Completion, Block Design, Matrix Reasoning, and Digit Symbol-Coding).

All research procedures received approval from our local Ethics Committees and adhered to the principles outlined in the Declaration of Helsinki.

Table 4.1: Dataset details, presenting the number of participants, as well as the mean age, QI verbal, and QI realization for each group.

	CNT	ASD
N	11	11
Age (mean ± std, in years)	23 ± 3	22 ± 7
Gender (male)	11	11
QI Verbal	109 ± 18	97 ± 16
QI Realization	104 ± 13	96 ±17

4.1.1 Imaging acquisition

The MR scans were acquired at the Portuguese Brain Imaging Network facilities, on a 3 T research scanner (Magnetom TIM Trio, phased array 12-channel birdcage head coil—Siemens, Munich, Germany). We acquired a 3D anatomical MPRAGE (magnetization-prepared rapid gradient echo) scan using a standard T1w gradient echo (GE) pulse sequence (repetition time (TR) = 2,300 milliseconds; echo time (TE) = 2.98 milliseconds; TI (inversion time) = 900 milliseconds; flip angle 9°; 160 slices with voxel size = 1 × 1 × 1 mm3; field of view (FOV)= 256 mm). A functional imaging series consisted of: 4 runs of 190 GE, echo-planar imaging (EPI) brain scans (TR = 2,000 milliseconds; TE = 39 milliseconds; flip angle 90°; 29 interleaved slices with voxel size 3 × 3 × 4 mm3; FOV = 256 mm) in a block design stimulation paradigm for measurement of BOLD signal.

4.1.2 Geometric animation stimulus

In this study, participants observed a series of brief animated movies with two "sprites" wandering around in a two-dimensional world while undergoing fMRI. The sprites were created to display socially neutral, aggressive, or friendly behavior. Participants were asked to concentrate on the social behavior being displayed by the sprites and on the spatial characteristics of their movements. The objective was to evaluate the neuronal mechanisms behind the identification of each interaction presented [Tavares et al., 2011, Madeira et al., 2021].

The experimental sessions were projected by means of an LCD projector (Avotec Real Eye Silent Vision 6011, resolution 1024×768, 60 Hz refresh rate - Avotec Incorporated, Stuart, FL, USA) onto a screen pad positioned in the bore at a distance of 163 cm from the projector (image size in the screen pad $22.62^{o} \times 17.06^{o}$; mirror distance from the screen, 50 cm).

Participants viewed the screen through a mirror placed above their eyes. The animations were divided into four categories: (1) Positive (affiliative interaction), (2) Negative (aggressive interaction), (3) Indifferent (neutral interaction) and (4) Linear (no interaction). These categories, which were created to generate the sensation of various interpersonal situations, served as stimuli to trigger social interpretations and the respective brain-related responses. An example of such animations can be found in the following link: https://doi. org/10.1016/j.nicl.2021.102836.

The experiment consisted of 4 functional runs. Each block began with 2 seconds of fixation. The film was then displayed for 14 seconds, followed by a jittering period of 1 second. The

question appeared for 8.5 seconds and lastly the baseline for 10 seconds (figure: 4.1).

After, participants were asked to indicate whether each motion pattern was associated with positive (affiliative), negative (antagonistic), indifferent, or no mood patterns. The answers were given via button press with a Cedrus Lumina LP-400, LU400 PAIR response box (Cedrus Corporation, San Pedro, CA, USA).

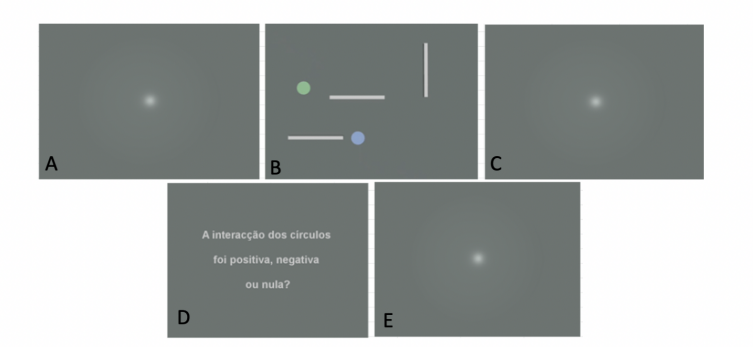

Figure 4.1: Schematic representation of the geometric animation stimulus. Experimental paradigm: A: Fixation point (baseline); B: interaction; C: Jittering period; D: Question; E: Fixation point (baseline).

4.2 Identification of Regional Brain Activation

To study the brain regions significantly responding during the task, and the differences between the two groups being analyzed, the Statistical Parametric Map (SPM12 version) toolbox was used in MATLAB (R2021b version). SPM refers to the development and evaluation of spatially extended statistical tests applied to functional imaging data. SPM, a free open-source software, is an implementation of these concepts [Friston et al., 2011].

4.2.1 Data preprocessing

In this thesis, the pre-processing of data in SPM was done following the guidelines proposed by Andy Jahn [Andybrainbook, nd] and SPM uses the MNI (Montreal Neurological Institute) coordinate space as the standard space for analyzing neuroimaging data. It starts with realignment and slice-timing correction, which corrects misalignment and timing errors in the functional images (quality 0.9; separation between sampled points 4 mm; smoothing 5 mm kernel), before moving on to coregistration and normalization.

4.2.2 Data analysis

We used the General Linear Model (GLM) to analyze which brain regions were significantly responding during our task [Friston, 2011, Worsley and Friston, 1995].

Brain regions that exhibit a modulation in activity in relation to a particular task can be identified by using the GLM in SPM, in order to model the relationship between the hemodynamic response detected in fMRI data and the underlying neural activity. The GLM is defined

by a number of regressors that describe brain activity in response to different experimental conditions and tasks, so we defined four regressors, one for every interaction/ condition, positive, negative, indifferent, and linear.

A model describing the expected appearance of the BOLD response is first built (figure: 4.2-A), and then it is fitted to the time series at each voxel (figure: 4.2-B). Statistical maps can then be used to visualize how well the model fits. Once thresholded, these statistical maps will only display the voxels that have statistically significant model fits (figure: 4.2-C) (figure: 4.2) [Andybrainbook, nd].

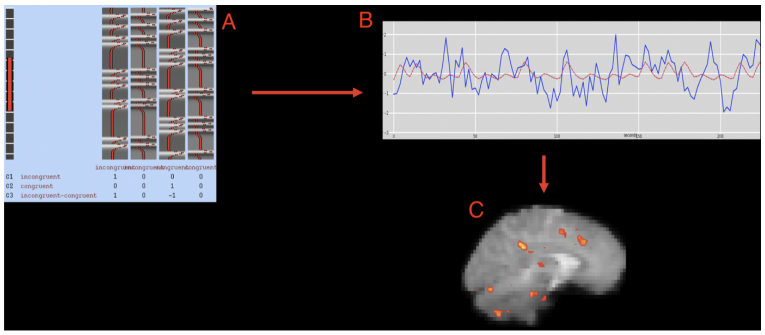

Figure 4.2: Representation of how to fit a model to the data. (A): Created model predicting the BOLD response; (B): Time-series of the signal at each voxel; (C): Statistical map thresholded to show only the voxels with a statistically significant model fit; Copyrights authorized by the author [Andybrainbook, nd].

When the model has been fully estimated, the program is ready to draw contrasts. The difference between the estimated beta weights for each condition was used to determine the contrast estimate at each brain voxel. By doing this for each voxel, a contrast map will be produced.

To evaluate the brain response to our task, contrasts were created to analyze the differences between the perception of each valence/condition for both control and clinical groups.

The first one was social interaction Vs. non-social interaction. It was respective to the contrast estimate between conditions positive, negative, and indifferent when compared to the linear one (no interaction), for both clinical and control groups. The other contrasts created, compared the effect of each condition separately versus the ones remaining (the linear one was not considered since it was a "no interaction"). To contrast the different conditions, a positive weight was given to the one of interest and a negative one to the ones it was being compared with. We created three contrasts of this type, considering the positive, negative, and indifferent interactions individually.

When we perform an analysis considering the whole brain, we are making an exploratory analysis. We thus make use of hypothesis-driven analysis to investigate regions of interest (*ROIs*) specifically related to our research question. Considering this, we performed a restricted analysis, considering only data from the voxels of the specific region of interest.

To perform simply the restriction of the whole brain to these specific structures, a MATLAB toolbox was used, the MarsBar.

Mark Brett Harwell developed MarsBaR to assist in analyzing neuroimaging data and defining *ROIs* using SPM software.

Within the interface, it was possible to create spherical masks of the *ROIs* and overlay them with the whole brain. The MNI *ROIs* were created with 5 mm (radius) each and were then applied to the contrast being visualized. An example is provided in fig: 4.3, the contrast between the social interaction and non-social interaction in the control group. The whole brain map is then overlaid with the spherical specific *ROI*, right-TPJ. This process was done for the two groups using the contrasts mentioned before.

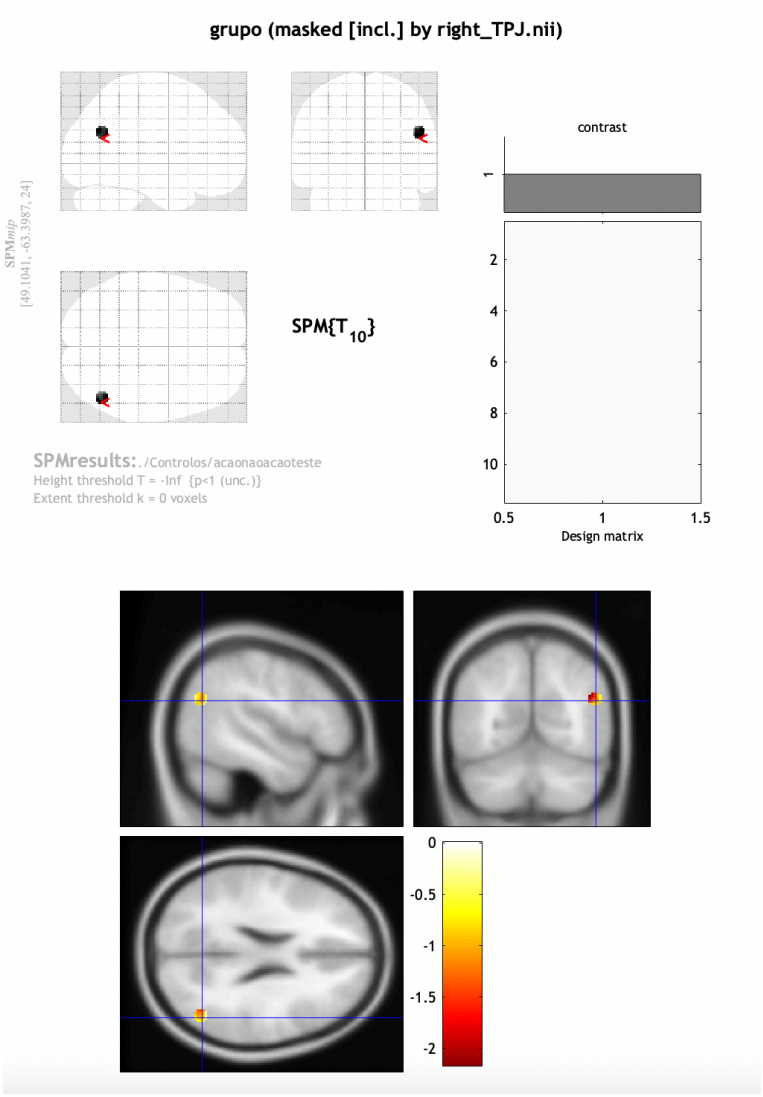

Figure 4.3: Interface of the MarsBar GUI with a chosen ROI to restrict the analyses. The contrast used is the social interaction vs. non-social interaction one for the control group, overlaid with the right- TPJ mask. The color map represents statistical values for the contrast.

To perform a brain region activation analysis we chose five specific *ROIs* based on literature [Hyatt et al., 2020, Direito et al., 2019, Madeira et al., 2021]. The five areas are believed to be crucial in emotion perception, and social cognition, and seem, also, to be implicated in autism (table: 4.2).

Table 4.2: Table with the ROIs chosen for the brain region activation analysis, considering previous literature, as well as its MNI coordinates and number of voxels.

Regions Of Interest	MNI Coordinates	Number of Voxels
right Superior Temperoparietal Junction	48 -64 26	81
medial Prefrontal Cortex	0 36 46	81
right Supramarginal Gyrys	64 -48 24	56
posterior Superior Temporal Sulcus	56 -39 4	70
left posterior Superior Temporal Gyrus	-62 -42 14	81

The TPJ and the mPFC are crucial regions in autism pathophysiology. TPJ and mPFC usually show activity deficits in people with ASD and are both implicated in the ToM network which means that autistic individuals have, probably, less capabilities of interpreting emotions due to the less activation or connectivity in these two regions [Hyatt et al., 2020].

In social perception and cognition, the posterior STS, is believed to have a role in interpreting other people's behavior or mental states as well as perceiving and picturing facial emotions. According to this hypothesis, this region might have implications in understanding and potentially influencing social perception and cognition processes [Direito et al., 2019].

Two other regions of interest (ROIs), the SMG and the left-posterior superior temporal gyrus (lpSTG) were also identified because of their relevance in a social cognition and emotion perception study, using the same stimulus as this one [Madeira et al., 2021]. However, the clinical group in that study was constituted of bipolar disease and schizophrenia patients instead of ASD ones. The goal was to understand if these regions were also implicated and altered in people with autism.

4.3 Statistical evaluation

To statistically analyze the results of the social interaction vs. non-social interaction between the two groups, we first collected the beta values of the global maximum. To the collected data, a normality test was then applied, the "Jarque-Bera" test. If the data followed a normal distribution, a simple parametric test in MATLAB, t-test, was performed, since we were comparing only one condition between two groups. If the results of the t-test showed a p value inferior to 0.05, the difference was significant. This statistical analysis was performed for each *ROI* chosen.

To analyze the three interactions, individually, between the two groups, we collected the beta values of each interaction in each group. Further, to statistically analyze the results, we performed a two-way ANOVA in SPSS (a software program used by researchers in various disciplines for quantitative analysis of complex data) (version 28). The dependent variable considered was the contrast estimate values, and the fixed factors were the three valences and

the factor group. The results showed if group, valence, or group and valence interactions were significant (p value inferior to 0.05) or not. When a statistically significant interaction was presented, post hoc tests – simple main effects, were applied. These tests are useful to understand where the significant difference is, between which groups, and within which valence in the study.

4.4 Brain functional connectivity analysis

To perform the brain connectivity analysis, the CONN toolbox (version conn21a) was used. The CONN software package is Matlab toolbox with a suite of commands that are designed to be used as an add-on to SPM. CONN is used to analyze resting state data rs-fMRI as well as task-related designs [CONN Toolbox Developers, SD].

4.4.1 Preprocessing and denoising

Just like in SPM, the data has to be pre-processed, and the default steps are the same as the previous analysis using SPM (realignment, slice-timing correction, coregistration, normalization, and smoothing), apart from a very important one performed by the CONN toolbox, the data denoising. Even after these conventional preprocessing steps, the measured BOLD signal often still contains a considerable amount of noise from a combination of physiological effects, outliers, and residual subject-motion factors. If unaccounted for, these factors would introduce very strong and noticeable biases in all functional connectivity measures. The denoising procedures in CONN are used to characterize and remove the effect of these residual non-neural noise sources. CONN's default denoising pipeline combines two steps that were followed: linear regression of potential confounding effects in the BOLD signal, and temporal band-pass filtering.

In the first, confounding effects that could impact the estimated BOLD signal are identified and subsequently eliminated individually for each voxel, subject, and functional run/session. The first step was achieved through the application of ordinary least squares (OLS) regression, which projected each BOLD signal time series onto a subspace orthogonal to all potential confounding effects [Nieto-Castanon, 2020]. The confounding effects included: noise components from white matter and cerebrospinal areas. Within each area, five potential noise components [Nieto-Castanon, 2020] were estimated: the first computed as the average BOLD signal, and the next four computed as the first components in a principal component analysis of the covariance within the subspace orthogonal to the average BOLD signal and all other potential confounding effects. A total of 12 potential noise components were also included, as defined from the estimated subject-motion parameters, in order to minimize motion-related BOLD variability (3 translation and 3 rotation parameters plus their associated first-order derivatives). The influence of the outlier scans on the BOLD signal was also removed, considering a noise component per outlier identified in the preprocessing step. Then, the task-related effects were convolved with a canonical hemodynamic response function, and defined as additional noise components in order to reduce the influence of constant task-induced responses in the BOLD signal.

In the second denoising step, temporal frequencies below 0.008 Hz or above 0.09 Hz were removed from the BOLD signal in order to focus on slow-frequency fluctuations while min-

imizing the influence of physiological, head motion, and other noise sources. Filtering was implemented using a discrete cosine transform windowing operation to minimize border effects [Nieto-Castanon, 2020].

The impact of denoising on functional connectivity measures can be best characterized by examining the distribution of functional connectivity values between randomly selected brain regions before and after denoising. Before denoising, connectivity distributions displayed extensive variability between different sessions and subjects. These distributions often exhibit an asymmetric shape with varying degrees of positive bias. This skewness indicates the presence of global or large-scale physiological effects and subject motion artifacts [Nieto-Castanon, 2020].

However, after the denoising process, they showed a shift toward centralization, revealing the effective removal of noise and artifacts, allowing for a more accurate representation of genuine functional connections in the brain [Nieto-Castanon, 2020].

While some positive bias may still persist, it was notably reduced, as well as the variability across different sessions and subjects. As a result, denoising effectively minimizes the impact of unwanted factors on functional connectivity measures (figure: 4.4).

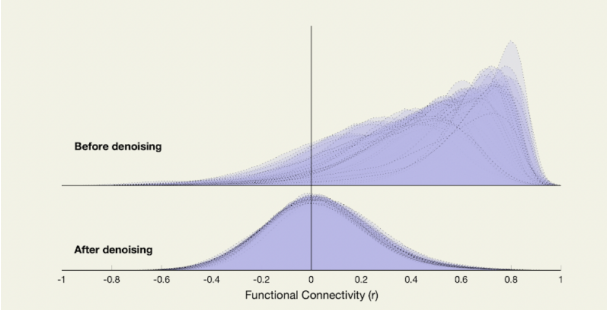

Figure 4.4: Distribution of FC values before (top) and after (bottom) denoising, in a representative sample study from [CONN Toolbox Developers, SD, Nieto-Castanon, 2020]. Copyright authorization pendent.

4.4.2 ROI to ROI functional connectivity mapping

The posterior step was the individual analysis of each subject, followed by the group analysis. We followed a roi-to-roi connectivity approach, considering a pre-defined set of regions.

In the first level analysis, the ROI-to-ROI matrices were estimated as the Fisher-transformed correlation coefficients. In the second level, GLM was applied for statistical inferences following a hypothesis testing framework as implemented in CONN toolbox, which allowed us to test for connectivity differences (as calculated in the first level analysis) between conditions and groups. The GLM defines a multivariate linear association between a set of explanatory/independent measures X, and a set of outcome/dependent measures Y. In the context of functional connectivity MRI analyses, an outcome variable y[n] will typically take the form of a row vector encoding functional connectivity values recorded from the subject in a study across one or multiple experimental conditions, and the explanatory variable x[n] will be a row vector encoding one or several groups, behavioral, or demographic variables for that same subject.

Correlation matrices can be visualized as a network graph, where nodes represent *ROIs*, and

edges represent the strength of connectivity, as can be seen in the example from the "Handbook of functional connectivity Magnetic Resonance Imaging methods in CONN" [Nieto-Castanon, 2020] in the figure: 4.5.

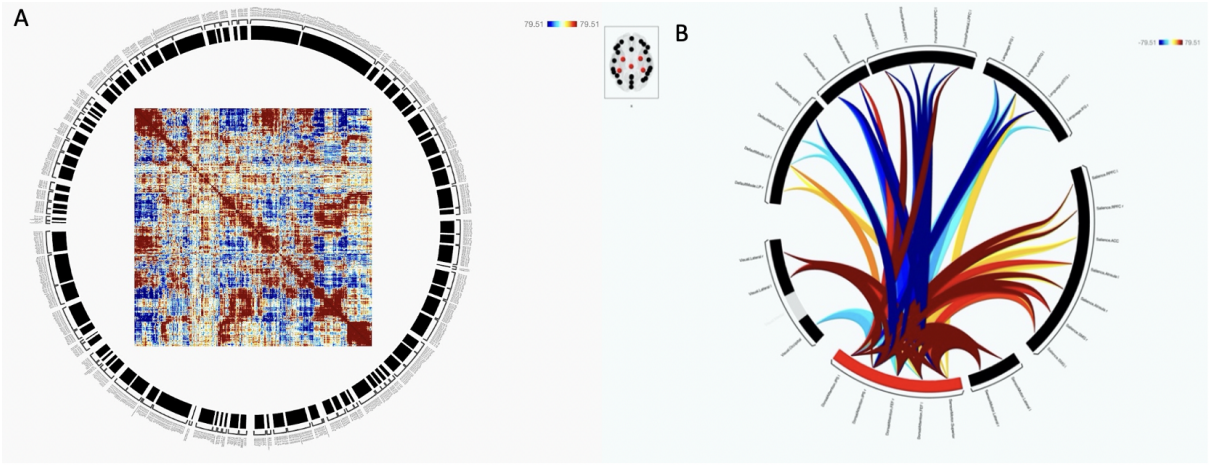

Figure 4.5: A: Example of a RRC matrix composed for 870 ROIs during rest, the average across 198 subjects (color bar representing T-test statistics). B: Example of a functional network connectivity map, ROI-to-ROI group analysis (ring display) with 8 networks, average across 198 subjects (color bar representing one-sample T-test statistics, highlighting the connectivity with the DAN) [Nieto-Castanon, 2020], Copyright authorization pendent.

The *ROIs* chosen for the connectivity analyses were picked based on literature. The DMN has been proved by research studies to be active when an individual is not engaged in specific external tasks and is associated with self-referential thinking, introspection, and mind-wandering, which suggests its association with the ToM [Soares et al., 2023]. Moreover, the DMN may contribute to cognitive processes involved in understanding and attributing mental states to oneself and others [Hughes et al., 2019].

The Salience Network was also of interest, given the critical role of the insula's connectivity, a key component of this network, in the management of unpleasant or emotionally intense stimuli. This is especially relevant when contemplating individuals with neuropsychiatric illnesses, the diminished connectivity in this region may cause them to perceive visceral responses and subjective sensory states differently [Keehn et al., 2021].

The Sensorimotor and Premotor Network has been mentioned as one of the networks associated with social cognition. It is described that the sensorimotor network, along with other networks like the DMN, contributes to social understanding. Regions within the sensorimotor network, such as the supplementary motor area, have been found to exhibit alterations in connectivity in individuals with bipolar disorder. These alterations may be associated with motor and cognitive inhibition difficulties and might be present in individuals with ASD [Jimenez et al., 2019].

Studies have indicated that individuals with ASD exhibit impairments in attention, particularly in the orienting aspect of attention associated with the dorsal attention network (DAN) and the ventral attention network (VAN). During attention-orienting tasks, individuals with

ASD showed reduced activity in brain regions involved in orienting attention, such as the IFG and frontoparietal regions [Farrant and Uddin, 2016].

Lastly, the five regions of interest defined based on the SPM GLM analysis were imported to the CONN toolbox and were also tested to evaluate them in terms of connectivity with other brain regions and not only their own activation. Since the CONN atlas used did not exhibit specific coordinates for two of the five *ROIs* (the TPJ and STS) we created them using 5 mm (radius) spherical ROIs (MNI coordinates).

The tables with the list of ROIs used are presented in the appendix: A.1.1.

After defining the *ROIs*, we created contrasts, starting with one that would be easier to perceive, positive and negative interactions vs. the indifferent one. Positive and negative interactions are frequent social interactions with higher intensity content than indifferent ones. We performed this contrast by attributing a positive weighting to the positive and negative interactions, and a negative one to the indifferent. This was done individually in each group (not comparing them directly).

The other contrasts took into account each direct valence comparison between the two groups. Attributing weighting factors not to the valences but to the groups. Each interaction was individually analyzed by assigning a positive weighting factor to the control group and a negative one to the clinical.

5

Results

5.1 Brain areas recruited during social interactions identification

5.1.1 Whole-brain analysis

We started by comparing the brain regions recruited in ASD and control individuals when an interaction was visualized (positive, negative, or indifferent). For that, the contrast of social interaction versus non-social interaction was performed. The contrast was applied separately for each group to observe if the regions activating in the control group were the same as in the ASD group (figure: 5.1).

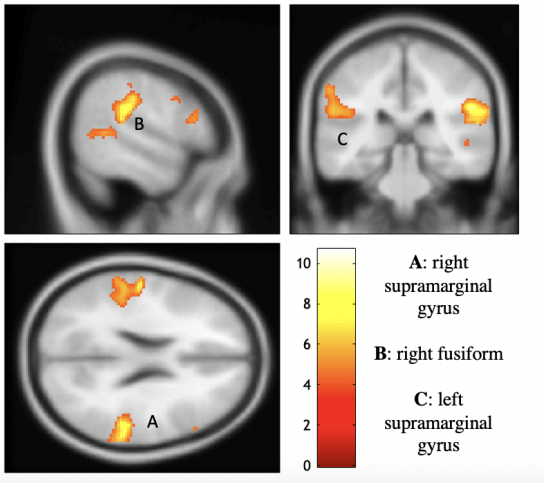

(a) Statistical map representing the clusters with significant activation for the control (CNT) group in the Social Interaction Vs. Non-Social Interaction. Using the threshold, *T= 4.1413 (p <0.01 uncorrected)* and *k=100* voxels. The color map represents statistical values for the contrast.

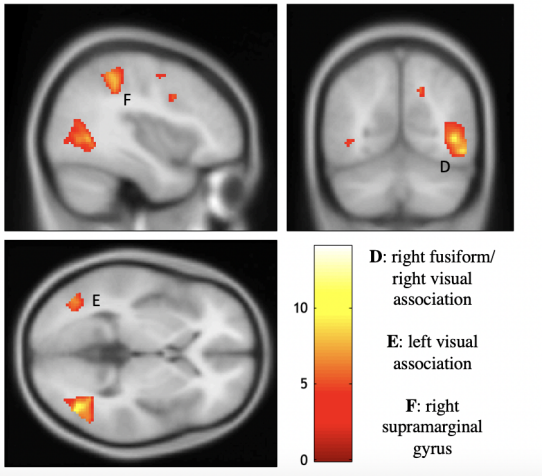

(b) Statistical map representing the clusters with significant activation for the ASD group in the Social Interaction Vs. Non-Social Interaction contrast. Using the threshold, *T= 4.1437 (p <0.01 uncorrected) and k=100 voxels.* The color map represents statistical values for the contrast.

Figure 5.1: Statistical map representing the clusters with significant activation for the CNT and ASD group.

In figure: 5.1a, we can observe the higher activation of the right supramarginal gyrus (57 -31 23), the right fusiform (53 -47 7), and the left supramarginal gyrus (52 -31 24) (MNI coordinates) in the control group. In figure: 5.1b, we can observe that ASD patients showed higher activation in the right visual association/ right fusiform (38 -65 2), in the left- visual association (-39 -67 -2), and in the right- supramarginal gyrus (38 -39 46) (MNI coordinates).

5.1.2 Regions of Interest Analysis

In this subsection, we restricted the analysis to the five ROIs mentioned in chapter 4. The contrast social interaction Vs. non-social interaction was applied to each group with the respective ROI mask. To evaluate which interaction led to higher activation in the respective ROI, we also analyzed each interaction/valence separately. The contrast estimate value of each participant in each contrast can be found in the appendix section: A.2.1.

In figure: 5.2 we can see an apparent higher activation of the right- supramarginal gyrus (SMG) in the CNT group than in the ASD one. However, there were no significant differences between groups ($p = 0.1105$), for the social interaction versus non-social interaction contrast.

Right- SMG

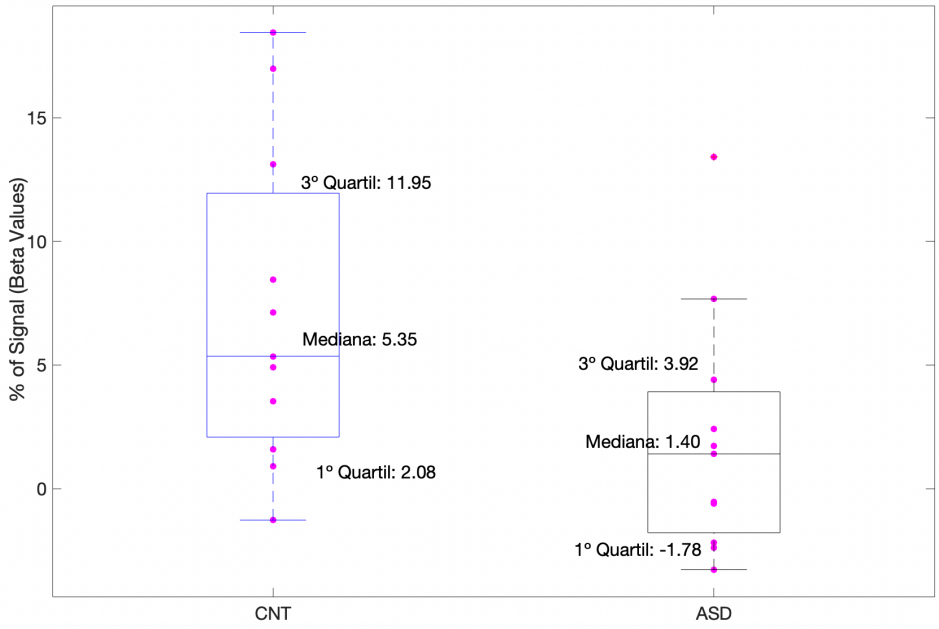

Figure 5.2: Result of the Social Interaction versus Non-Social Interaction contrast overlapped with the spherical ROI mask using the contrast estimate of each patient in the two groups (control (CNT) and clinical (ASD)). (The lower (Q1) and upper (Q3) quartile, represent observations outside the 9 –91 percentile range. The diagram also shows the median and mean. Data falling outside the Q1 – Q3 range are plotted as outliers of the data). The points in each box plot represent the contrast estimate values of each participant (11 controls and 11 clinical). T-test results: *p =0.1105; start: 1.7509; df: 10; sd: 9.8326.* No significant differences between the two groups in this region were found.

In figure: 5.3 we show how much the right- SMG activates when the three interactions are being presented, in both groups. Control group tended to present higher activation than the ASD group when positive and negative interactions, but not when an indifferent one were being visualized. By submitting the data to a two-way ANOVA test, we found (table: 5.1) a statistically significant interaction between group and valence($F(1,64)=5,59,\ p=0.006$). The results of "valence" also show significant results $F(1,64)= 6.41,\ p=0.03$, meaning there are differences in activation between the valences being presented. There were no statistically significant differences between group levels $(p=0.619)$.

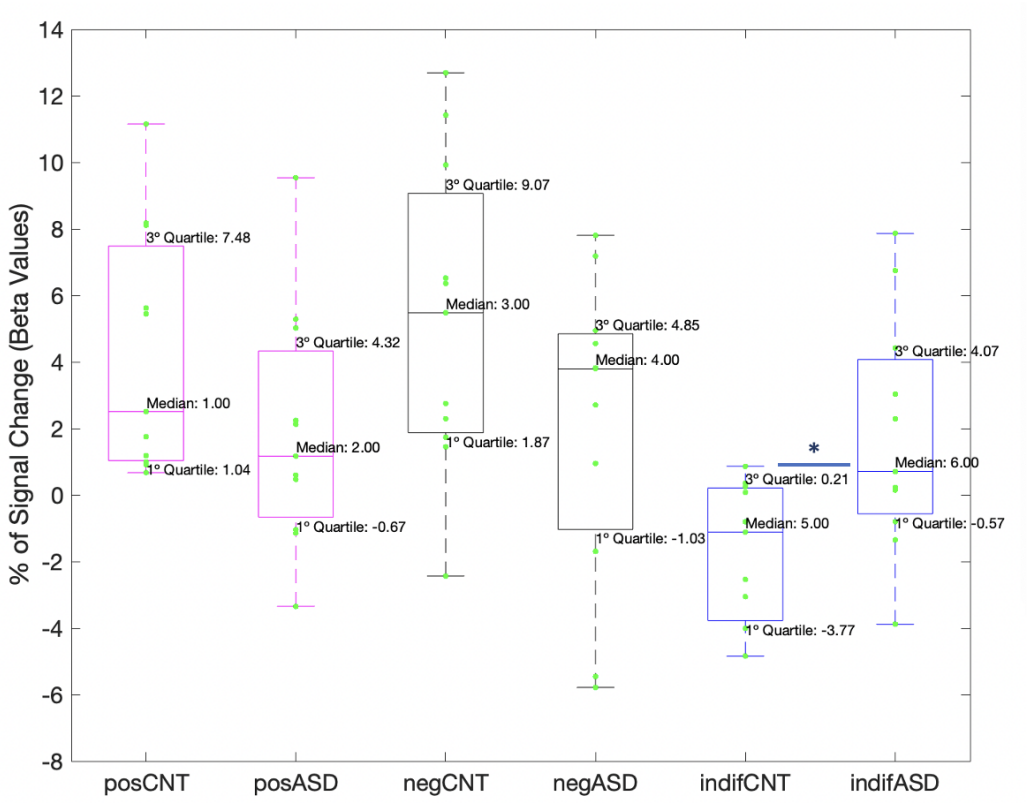

Figure 5.3: Right SMG response during the three interactions (positive, negative, and indifferent) for the autistic (ASD) and control (CNT) groups. The points in each box plot represent the contrast estimate values of each participant (11 controls and 11 clinical). The statistical analysis revealed that there was an interaction between the group and valence (indifferent interaction in the two groups).

Table 5.1: Test of between-subject effects in the SMG.

Origin	Type III Sum of Squares	df	Mean Square	F	Sig.
Group	3.885	1	3.885	0.249	.619
Valence	199.89	2	99.95	6.41	.003
Group*Valence	174.55	2	87.28	5.60	.006

By performing a Tuckey post hoc test (fixating the valence factor) we observed that clinical subjects had significantly more SMG activation during the indifferent animation than control subjects ($p= 0.018$), but there were no differences during positive or negative animations *($p = 0.172$ and $p = 0.061$, respectively).*

The detailed test results can be seen in the appendix: A.3.1.

lpSTG

As shown in figure: 5.4 the lpSTG presented a higher response for the contrast social vs. non-social interaction for the control group than for the ASD one, t-test results proved the existence of a significant difference between them ($p=0.0450$).

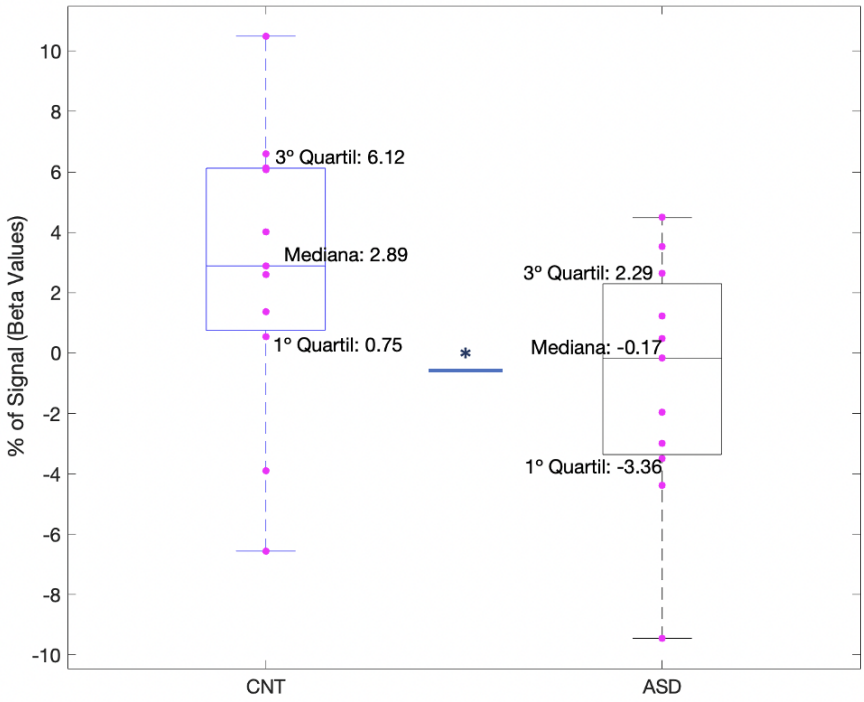

Figure 5.4: Result of the Social Interaction versus Non-Social Interaction contrast overlapped with the spherical ROI mask using the contrast estimate of each patient in the two groups. The points in each box plot represent the contrast estimate values of each participant (11 controls and 11 clinical). T-test results: *p =0.0450 tstat: 2.2899; df: 10; sd: 5.8551*; There is a significant difference between groups in lpSTG activation.

In figure: 5.5 we can observe that there seems to occur a higher activation in the control group than in the ASD when the negative interaction is being presented and the opposite for the positive one. However, the results of the two-way ANOVA test showed no significant main effects.

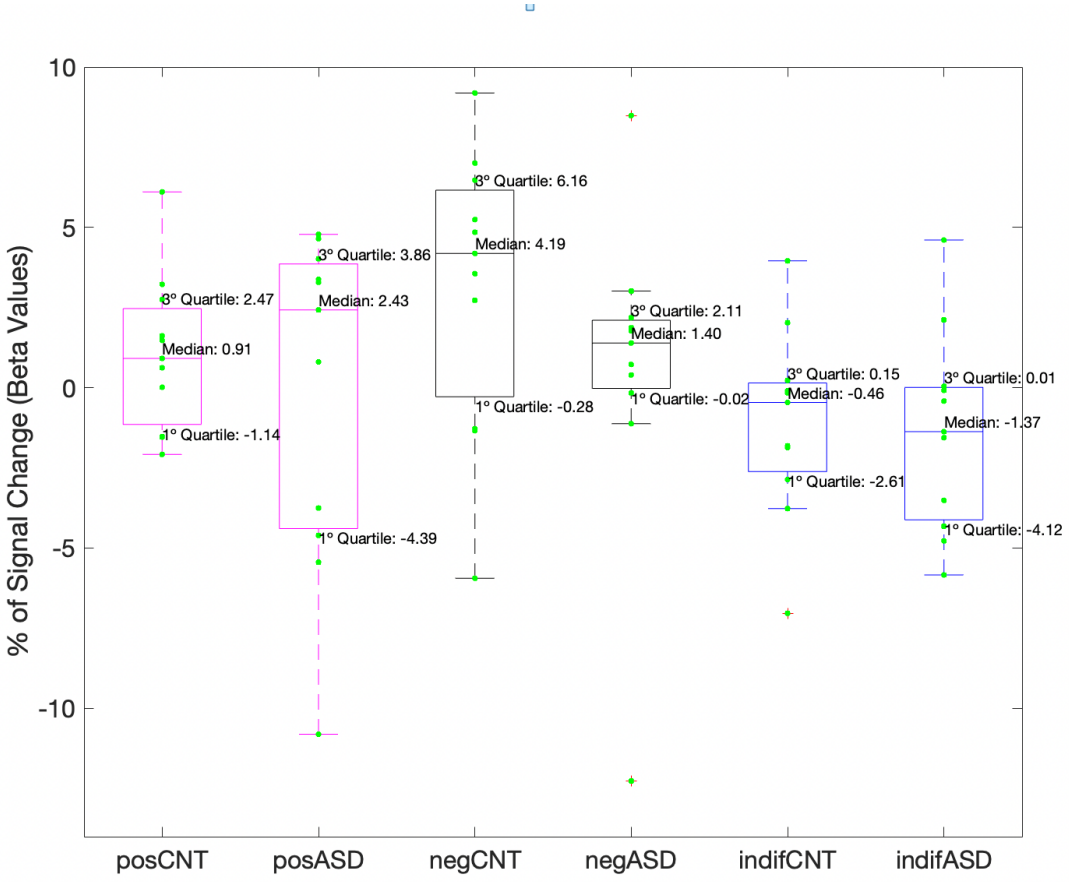

Figure 5.5: Right lpSTG response during the three interactions (positive, negative, and indifferent) for the autistic (ASD) and control (CNT) groups. The points in each box plot represent the contrast estimate values of each participant (11 controls and 11 clinical). No significant differences were found.

pSTS

As illustrated in figure: 5.6, the posterior STS responded significantly more in the control group than in the autistic group during the identification of social interactions (*p=0.0100).*

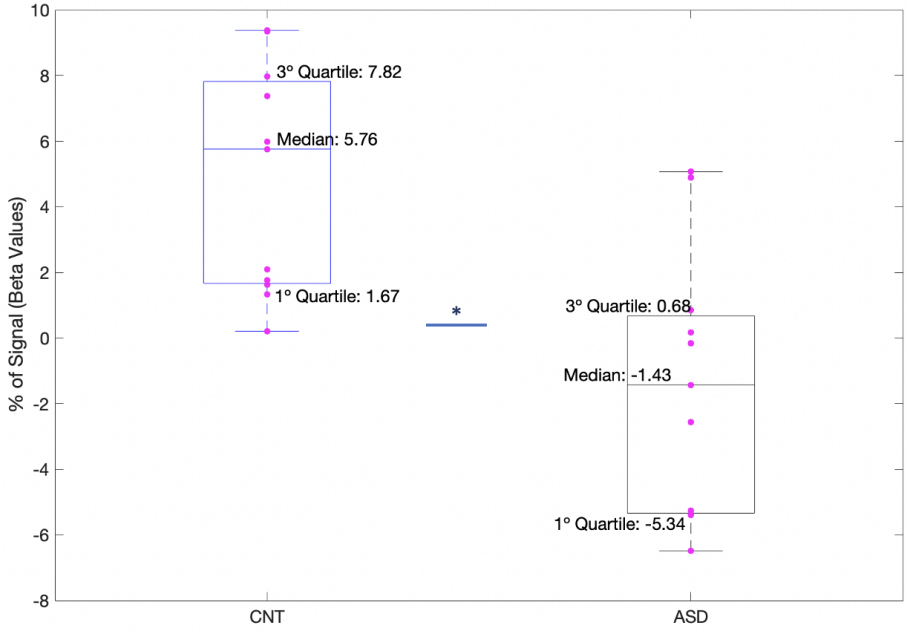

Figure 5.6: Result of the Social Interaction versus Non-Social Interaction contrast overlapped with the spherical ROI mask using the contrast estimate of each patient in the two groups. The points in each box plot represent the contrast estimate values of each participant (11 controls and 11 clinical). T-test results: *p =0.0100; tstat: 3.1702; df: 10; sd: 6.5149*; There is a significant difference between groups in posterior superior temporal sulcus (pSTS) activation.

Figure: 5.7 shows the posterior STS response for each interaction and group. Control group shows higher activation when positive and negative interactions are being visualized, but not when an indifferent one is. By submitting the data to a two-way ANOVA test, we can observe (table: 5.2) that we have a statistically significant interaction between group and valence (*F(1,64)= 4.97, p = .010*). The results of "valence" also show significant results (*F(1,64)= 4.74, p = .012*), meaning there are differences in activation between the valences being presented. There were also statistically significant differences between groups (*F(1,64)= 5.48, p = .023*).

By performing a Tuckey post hoc (fixating the valence factor) test we found that control subjects had significantly more pSTS activation during the positive and negative animation than ASD subjects (*p=0.009 and p=0.013, respectively*), but there were no differences during the indifferent animation (*p =0.227*) (table: 5.2).

The detailed test results can be seen in the appendix: A.3.1.

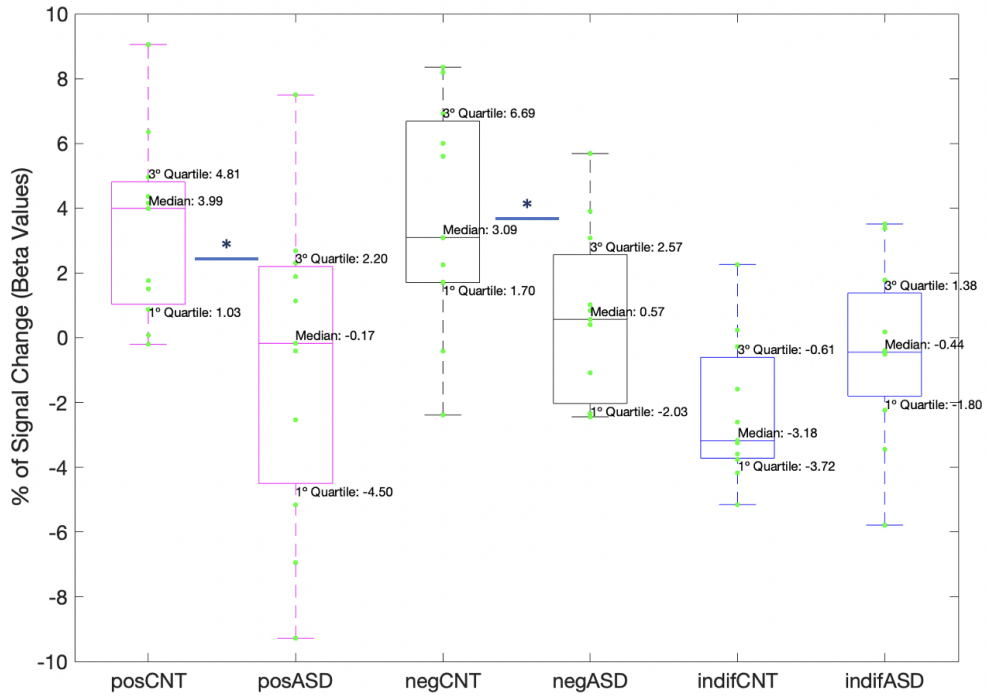

Figure 5.7: Posterior STS response during the three interactions (positive, negative, and indifferent) for the autistic (ASD) and control (CNT) groups. The points in each box plot represent the contrast estimate values of each participant (11 controls and 11 clinical). These results show that there is a significant difference between the positive and negative interactions when comparing the two groups.

Table 5.2: Test of between-subject effects in the STS.

Origin	Type III Sum of Squares	df	Mean Square	F	Sig.
Group	71.032	1	71.032	5.480	.023
Valence	122.77	1	61.389	4.736	.0123
Group*Valence	128.72	1	64.361	4.967	.010

right TPJ

Figure: 5.8 seems to show a higher activation of the TPJ in the clinical group when compared with the control one. However, t-test results showed no significant differences in the activation of this region between the two groups, for the contrast social interaction Vs. non-social interaction (*p=0.9080)*.

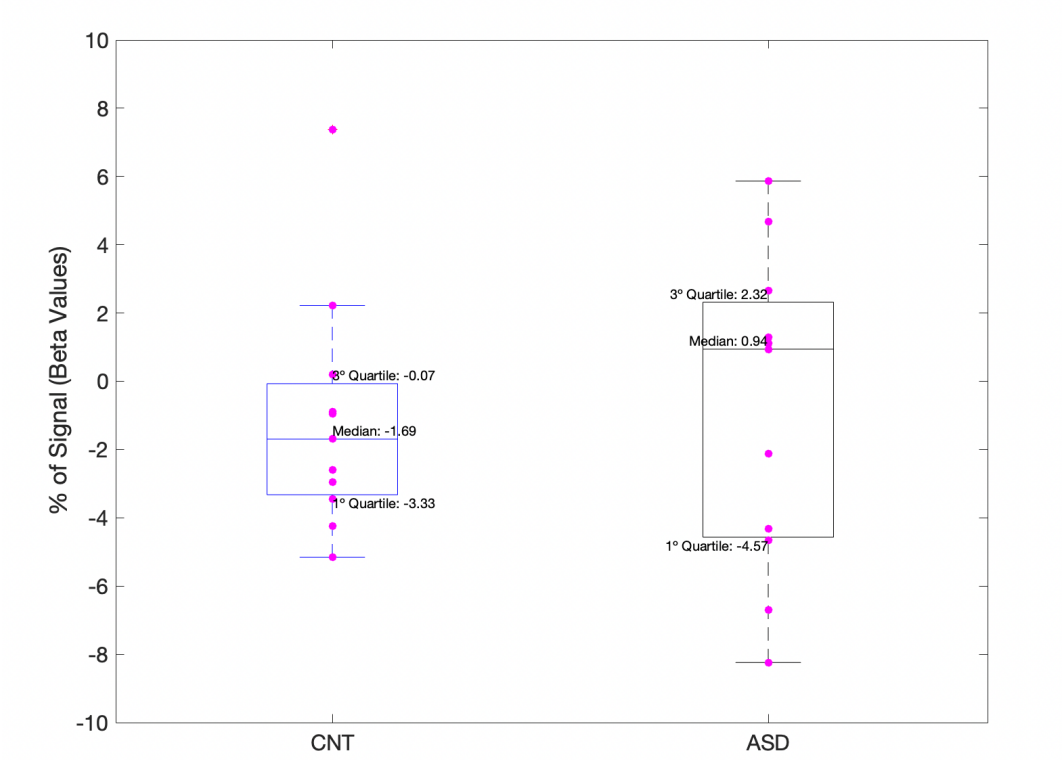

Figure 5.8: Result of the Social Interaction versus Non-Social Interaction contrast overlapped with the spherical ROI mask using the contrast estimate of each patient in the two groups. The points in each box plot represent the contrast estimate values of each participant (11 controls and 11 clinical). T-test results: *p =0.9080; tstat: -0.1185; df: 10; sd: 6.7478*; There is no significant differences between groups in TPJ activation.

In figure: 5.9 we observe how the TPJ activates when the three interactions are being presented, in both groups. ASD group seems to show higher activation when a positive interaction is being visualized but not when an indifferent one is. However, two-way ANOVA test results showed no significant differences.

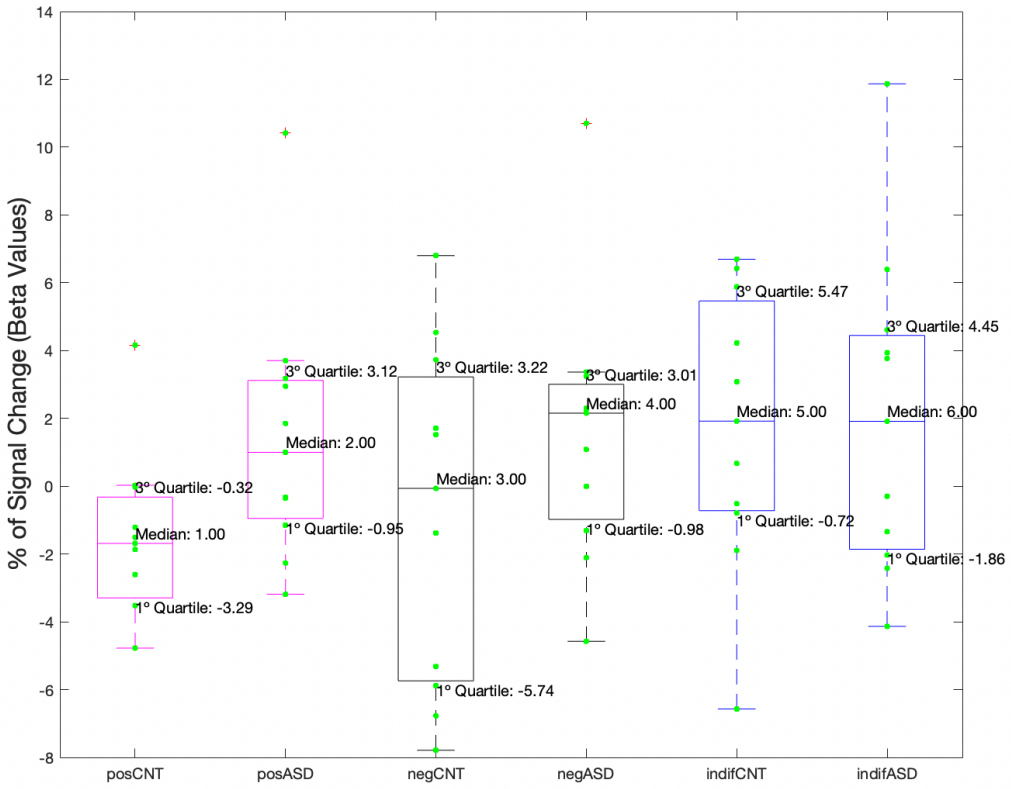

Figure 5.9: Right TPJ response during the three interactions (positive, negative, and indifferent) for the autistic (ASD) and control (CNT) groups. The points in each box plot represent the contrast estimate values of each participant (11 controls and 11 clinical). No significant differences were found.

mPFC

In figure: 5.10 we seem to observe a higher activation of the mPFC in the clinical group when compared with the control one, for the social interaction vs. non-social interaction. However, t-test results showed that there were no significant differences between the two groups in the activation of this region (*p=0.8593*).

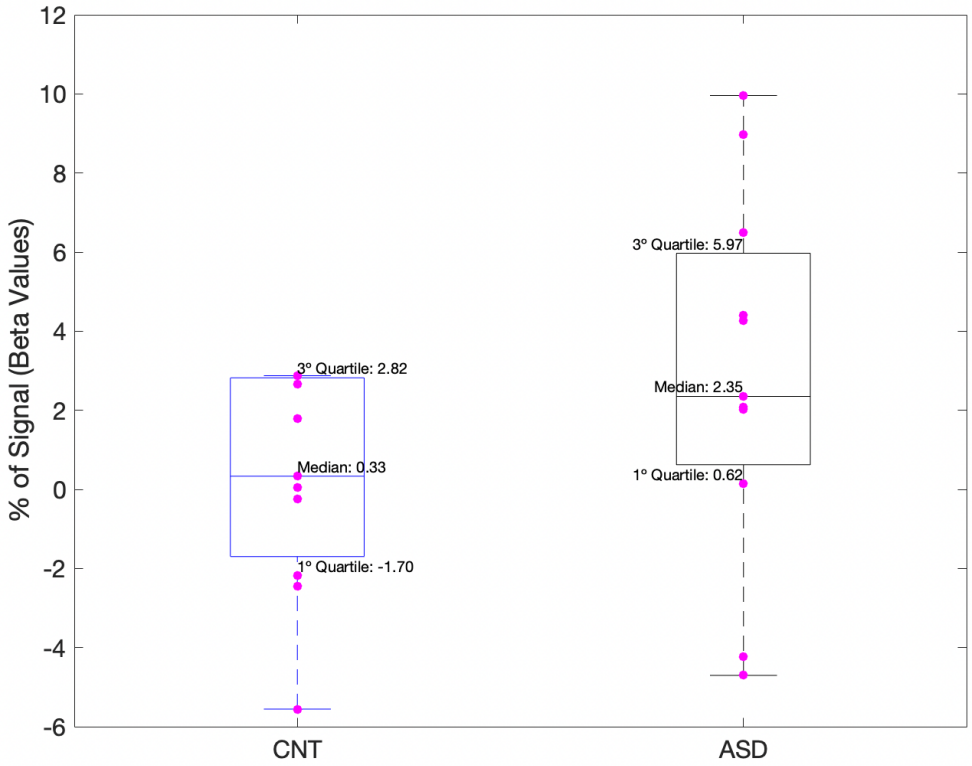

Figure 5.10: Result of the Social Interaction versus Non-Social Interaction contrast overlapped with the spherical ROI mask using the contrast estimate of each patient in the two groups. The points in each box plot represent the contrast estimate values of each participant (11 controls and 11 clinical). T-test results: *p =0.8593; tstat: -0.1819; df: 10; sd: 10.2056*; There is no significant difference between groups in mPFC activation.

In the figure: 5.11 results seem to show that mPFC activates more in the ASD group than in the control one when an indifferent interaction is being visualized. When positive and negative interactions are being visualized, the activation of this region is both groups seems to be equal. By submitting the data to a two-way ANOVA test, we can observe (table: 5.3) that we have a statistically significant interaction between group and valence (*F(1,64)= 4.102, p = 0.021*). Group and valence factors revealed no main effects (*F(1.64)=0.972; F(1,64)=0.874, respectively).*

However, the posthoc tests revealed that autistic subjects had significantly more mPFC activation during the indifferent animation than the control group *(p=0.022)*. There were no differences during the positive and negative animations (*(p =0.125 and p =0.605, respectively)*).

The detailed test results can be consulted in the appendix: A.3.1.

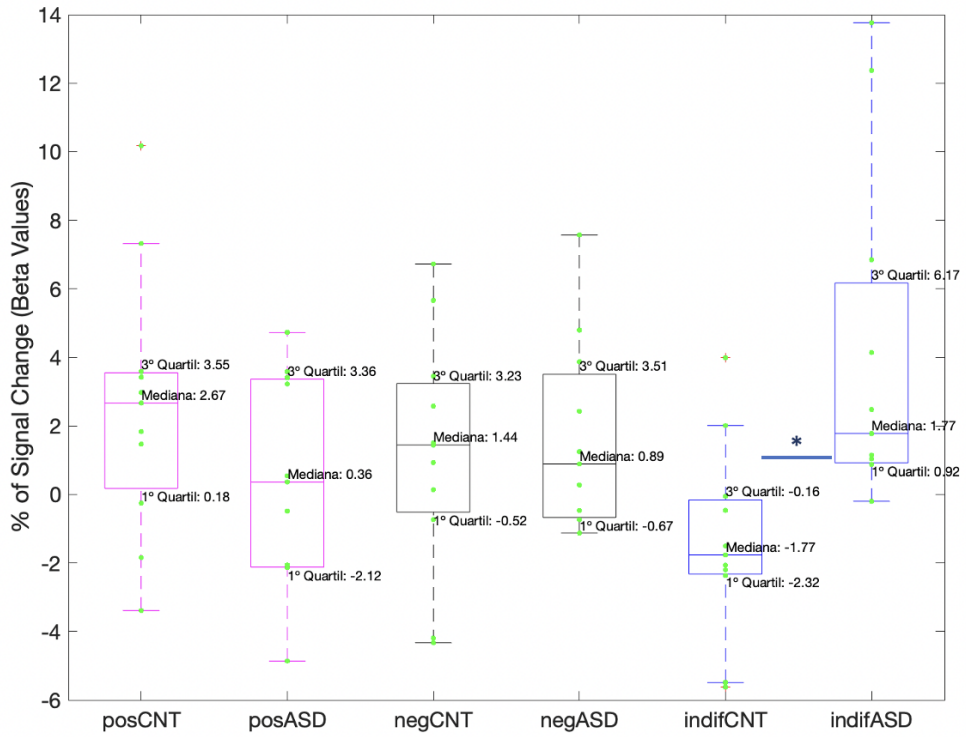

Figure 5.11: mPFC response during the three interactions (positive, negative, and indifferent) for the autistic (ASD) and control (CNT) groups. The points in each box plot represent the contrast estimate values of each participant (11 controls and 11 clinical). These results show that there is a significant difference between the indifferent interaction between the two groups.

Table 5.3: Test of between-subject effects in the mPFC.

Origin	Type III Sum of Squares	df	Mean Square	F	Sig.
Group	0.574	1	0.574	0.025	.874
Valence	1.301	2	0.650	0.029	.972
Group * Valence	184.944	2	92.472	4.102	.021

5.2 Brain Functional Connectivity Analysis

5.2.1 Exploratory Analysis

With the investigation of functional connectivity analysis using the Brain Connectivity toolbox (CONN), implemented in MATLAB, we were able to perform, initially, an exploratory analysis, considering the whole brain (all regions available on the toolbox) to have an overall map of the connectivity differences between the autistic and control groups in the study.

ASD and control group differences during the visualization of the animations

In the statistical map presented in figure: 5.12, we can observe that ASD patients show lower connectivity between ToM regions linked to the salience and ventral attention networks, since, the highest groups' connectivity difference occurs between the right SMG and the right pSTG (*F(4,17)= 8,21 and p-unc= 0.0007*). This connection was stronger in the control group. The same occurred for the connection between the anterior SMG and right pSTG (*F(4,17)=6.74, p-unc= 0.0019).*

In the effect size bars graph presented in figure: 5.13, we can observe that the connectivity values are stronger for both groups in the first cluster (the connection between the right supramarginal gyrus and the posterior superior temporal gyrus) and starts diminishing in the other clusters, especially in the ASD group.

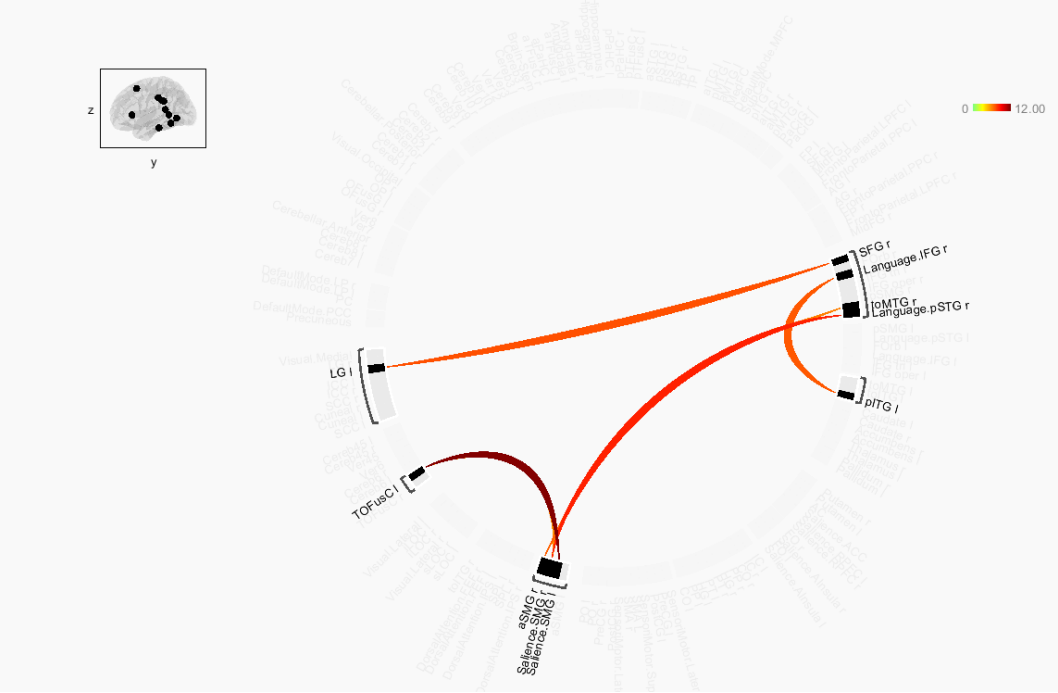

Figure 5.12: ROI to ROI connectivity map showing which connections differ between ASD and control groups (considering the contrast control minus ASD). The presented results are shown with cluster level p-uncorrected (MVPA omnibus test), cluster threshold of $p < 0.005$, and connection threshold of $p < 0.005$). The color bar indicates the statistical parameter F. Lower values (closer to 0) have lower statistical significance, while higher values (closer to 12) (represented in red) indicate higher statistical significance and more substantial differences between groups.

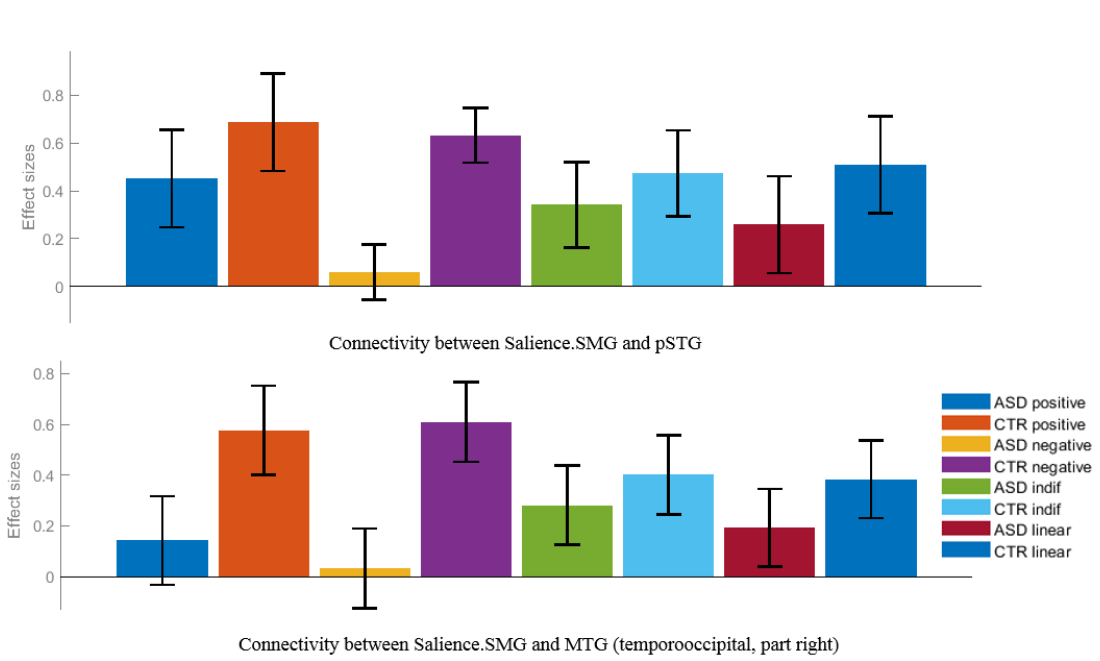

Figure 5.13: Functional connectivity roi-to-roi effect size, representing the ROIs with more connectivity for the control and ASD groups during all tested conditions (social positive, negative and indifferent interaction, and non-social interaction/linear). Cluster 1/406 (the connection between the right supramarginal gyrus and the posterior STG and between the anterior supramarginal gyrus and the MTG) is the cluster with higher levels of connectivity for the control group when compared to the clinical one; (*Cluster threshold: $p < 0.05$ cluster-level p-FDR corrected (MVPA omnibus test); connection threshold $p < 0.005$; $p < 0.05$ p-uncorrected*).

The detailed results' table for the connectivity maps (in the exploratory analysis) can be consulted in the appendix: A.33.

Negative Interaction

During the positive interaction for the whole brain analysis no significant connectivity differences were found. The differences visualized in the entire task connectivity maps arise mainly from the negative interaction recognition (figure: 5.14). The highest groups' connectivity difference occurs between the right SMG and the posterior STG (*T(20) = 6.10; p-FDR: 0.000945*) and between the right SMG and the middle temporal gyrus (*T(20) = 4.47; p-FDR: 0.018927*). These connections were stronger in the control group.

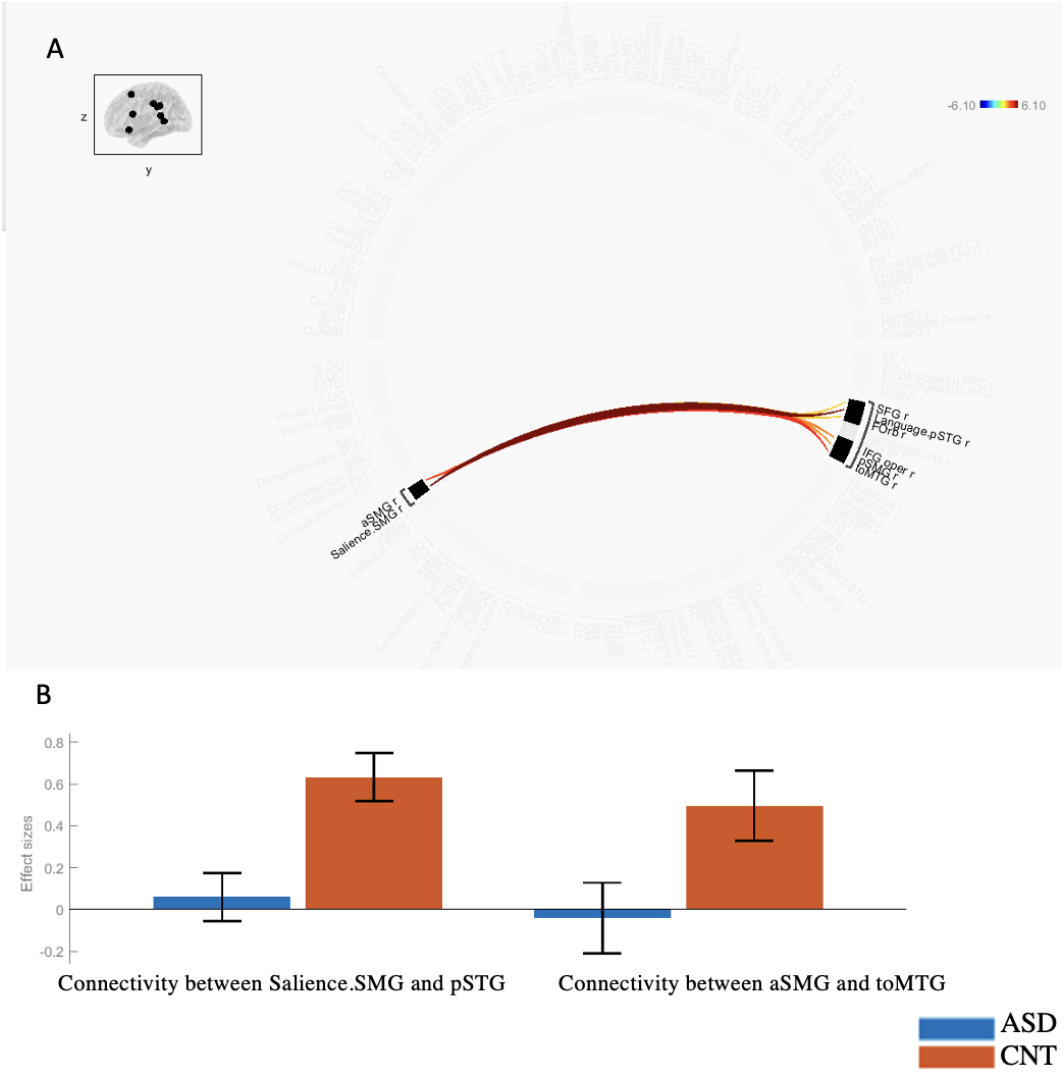

Figure 5.14: Results show a higher level of connectivity between the salience and attention networks and between the anterior and posterior SMG for the control group. A: Connectivity map showing where the average connectivity differs from ASD and CNT subjects (considering the contrast control minus ASD; the color bar represents t statistic parameters that indicate the magnitude of the difference between the means of the conditions compared. B: Functional connectivity roi-to-roi effect size. Connectivity between the right SMG and the posterior STG showing the highest level of connectivity in the control group. (*Cluster threshold: p <0.05 cluster-level p-FDR corrected (MVPA omnibus test); connection threshold p <0.005; p <0.05 p-uncorrected*).

ASD and control group differences during the indifferent interaction

Results presented in figure: 5.15 show significant differences between CNT and ASD groups when presented with an indifferent interaction. Although the posterior SMG and superior frontal gyrus (SFG) have higher connectivity with SCC and ICC in the control group, the results also show that during this interaction the ASD group has a higher level of connectivity than CNT group between the Cuneal I and the posterior SMG and IFG.

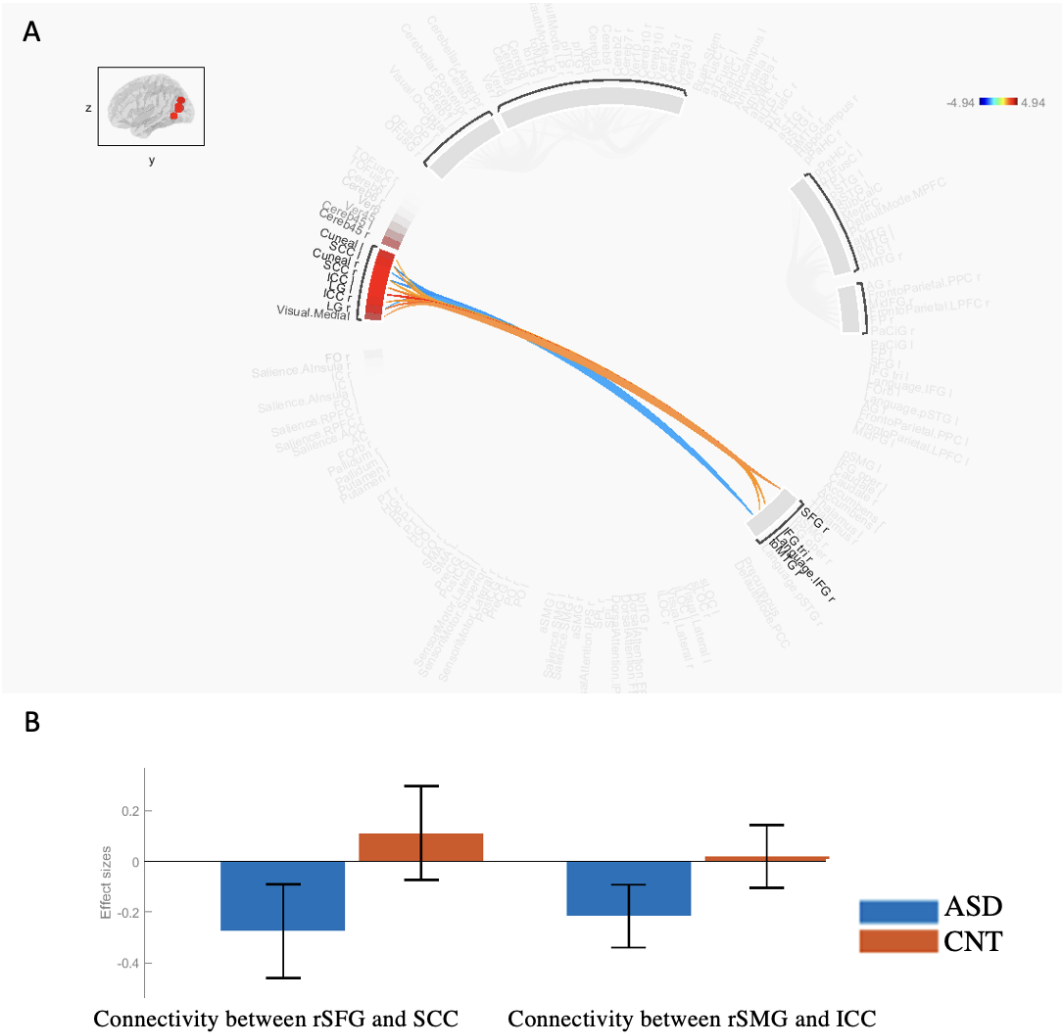

Figure 5.15: A: ROI to ROI connectivity map showing which connections differ between ASD and control groups (considering the contrast control minus ASD). The color bar represents t statistics. Results show that during this interaction the ASD group has a higher level of connectivity than CNT group between the Cuneal I and the posterior SMG and IFG (*Cluster threshold: p <0.05 cluster-level p-FDR uncorrected (MVPA omnibus test); connection threshold p <0.05).* B: Effect size of the ROIs with higher connectivity differences. (*Cluster threshold: p <0.05 cluster-level p-FDR corrected (MVPA omnibus test); connection threshold p <0.005; p <0.05 p-uncorrected*).

5.2.2 Brain connectivity analysis considering within a predefined set of *ROIs* for autism

Exploratory analysis is always a plus in a study. However, a more rigorous hypothesis driven analysis allows us to relate our results with previous studies and with information present in the literature. It also allows us to compare results from theories and hypotheses already tested. To perform a more specific analysis, we use ROIs, mentioned earlier in chapter 4 and listed in the appendix: A.1.1. The analysis with interaction contrasts was performed separately for each group in order to be more easily interpreted. Then, the functional connectivity maps were compared between groups, taking into account each type of interaction.

Positive and Negative Vs. Indifferent

To highlight group connectivity differences, we started by a contrast that would be easier to interpret (positive and negative vs. indifferent). Positive and negative interactions are frequent social interactions with higher intensity/emotional content than indifferent ones.

In figure: 5.16, the control group shows a higher connectivity level between the IFG, which is considered a mirror system region and two ToM areas, the TPJ and the STS (*T(10) = 2.63; p-unc: 0.024992;*). These connections are mainly observed when a positive interaction is presented.

By performing the same process for the ASD group, no differences were found, and so there are no significant differences or connections stronger than others when interpreting a positive or negative interaction.

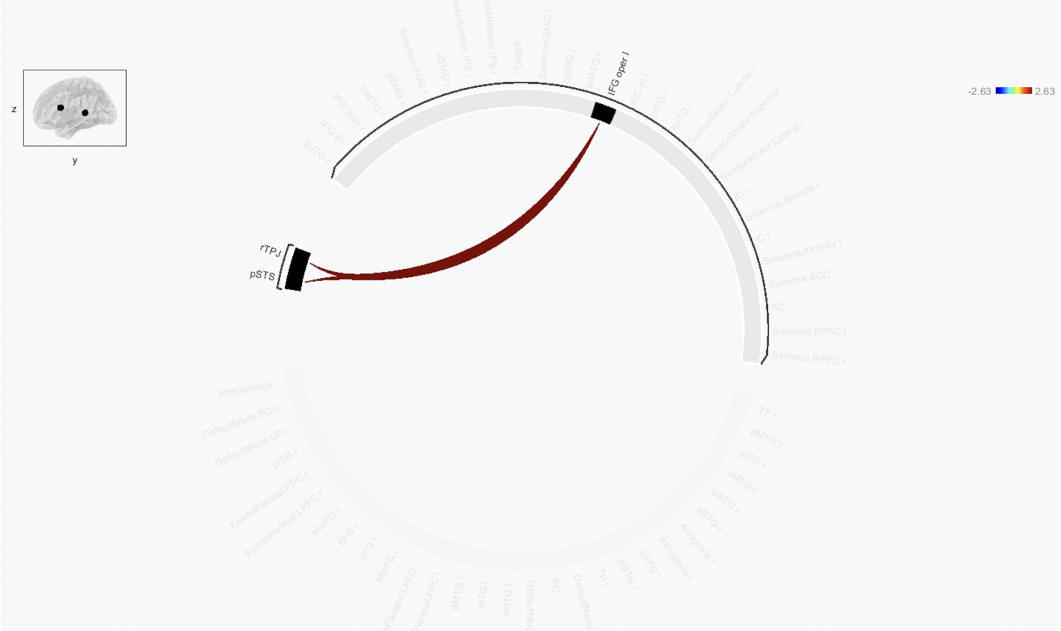

Figure 5.16: Results for the contrast Positive and Negative Interaction Vs. No interaction for the control group. Connectivity map showing where the average combination-connectivity from CNT subjects differs from zero. The color bar represents t statistics. Presented results are shown with a cluster-level *p-uncorrected (MVPA omnibus test); cluster threshold of p<0.05 and connection threshold of p<0.05.*

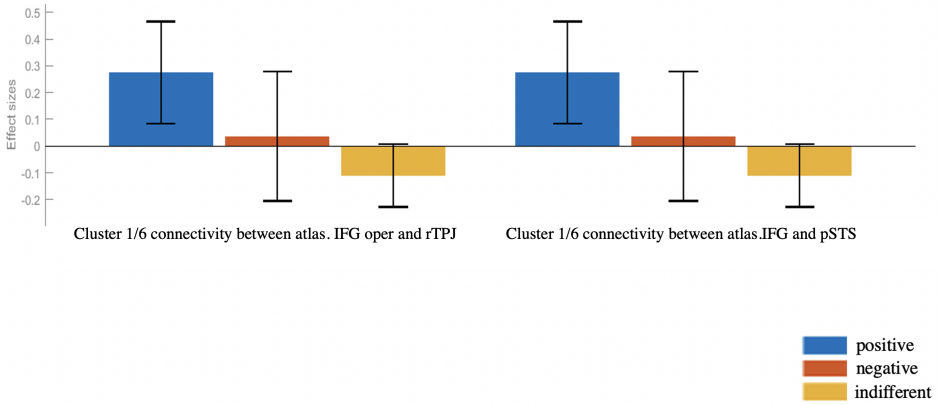

Figure 5.17: Results for the contrast Positive and Negative Interaction Vs. No interaction for the control group. Functional connectivity roi-to-roi effect size. Presented results are shown with a cluster-level *p-uncorrected (MVPA omnibus test); cluster threshold of p<0.05 and connection threshold of p<0.05.*

ASD connectivity alterations during the identification of social positive interaction

This analysis was performed to evaluate if there were regions that would show higher functional connectivity in the CNT group that would not be in the clinical one when a positive interaction was visualized. The results presented in figure: 5.18 show higher connectivity between the posterior division of the left SMG and the IFG (*T(20) = 4.29; p-FDR: 0.010428;*) in the control group. Also in the control group, the posterior division of the left SMG connectivity with the superior frontal gyrus showed higher levels than in the clinical group (*T= 3.13; p-FDR: 0.008323*). However, the connection between the IFG and the MTG is higher in the ASD group when compared to the control one (*T(20) = -2.09; p-unc: 0.049412;*).

The entire results' table can be consulted in the appendix: A.36.

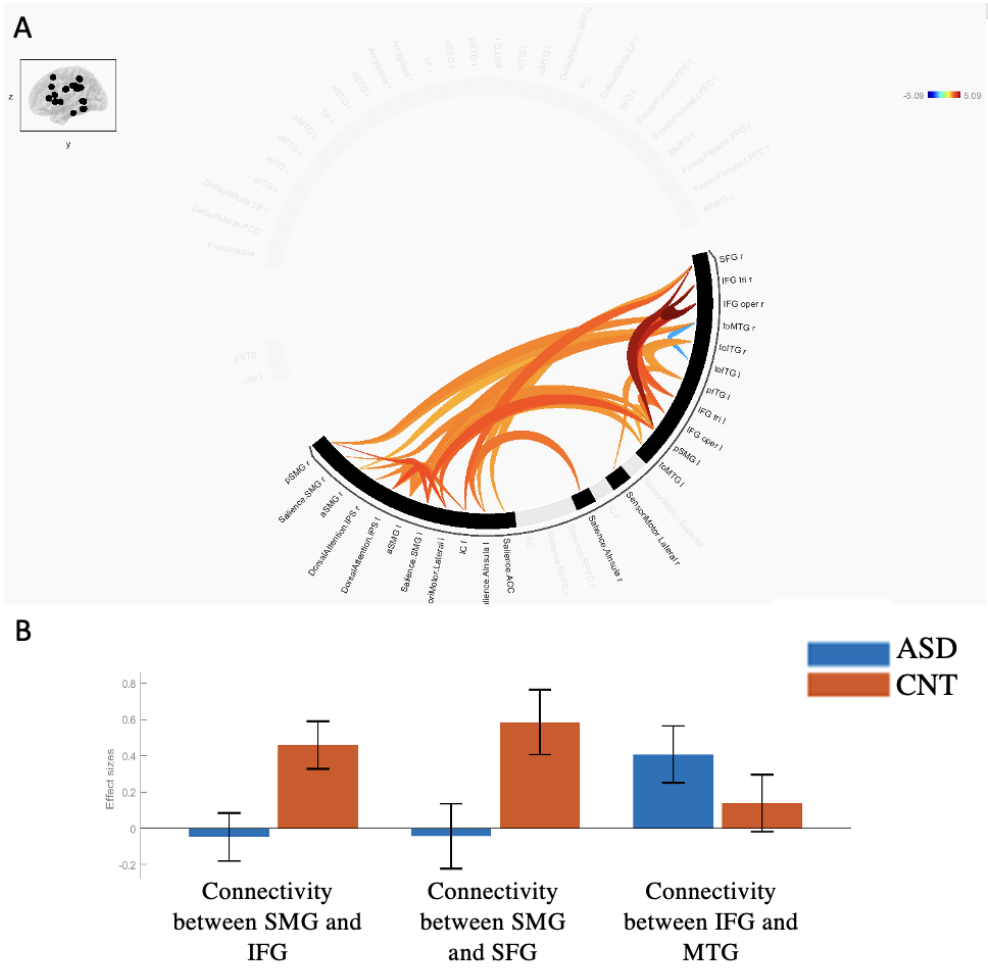

Figure 5.18: Results for the positive social interaction (with a contrast of control group minus ASD group). A: Connectivity map showing where the average connectivity differs between ASD and CNT subjects. The color bar represents t statistics. B: Effect size of the ROIs considered in the connectivity map. Cluster 1/6 (connection between the left SMG and the IFG) showing higher connectivity for the control group. Presented results are shown with a cluster-level *p-uncorrected (MVPA omnibus test); cluster threshold of $p<0.02$ and connection threshold of $p<0.05$. The correction on the cluster-level p-uncorrected (MVPA omnibus test) is made for the number of ROIs being considered.*

ASD connectivity alterations during the identification of social negative interaction

This analysis was performed to evaluate if there were regions that would show higher functional connectivity in the CNT group that would not in the clinical one when a negative interaction was visualized. Results presented in figure: 5.19 translate the higher connectivity between the MTG and the anterior SMG (*T(20)= 4.31; p-FDR: 0.016*), also between the MTG and the insular cortex (*T(20)=3.36 and p-FDR= 0.0299)* and between the SMG and the amygdala (T(20)= 3.48; p-unc: 0.0023), in the control group when compared to the clinical one. However, the connection between the intraparietal sulcus and the STG was higher in the clinical group than in the control one (*T(20)=-2.99; p-unc= 0.0072).*

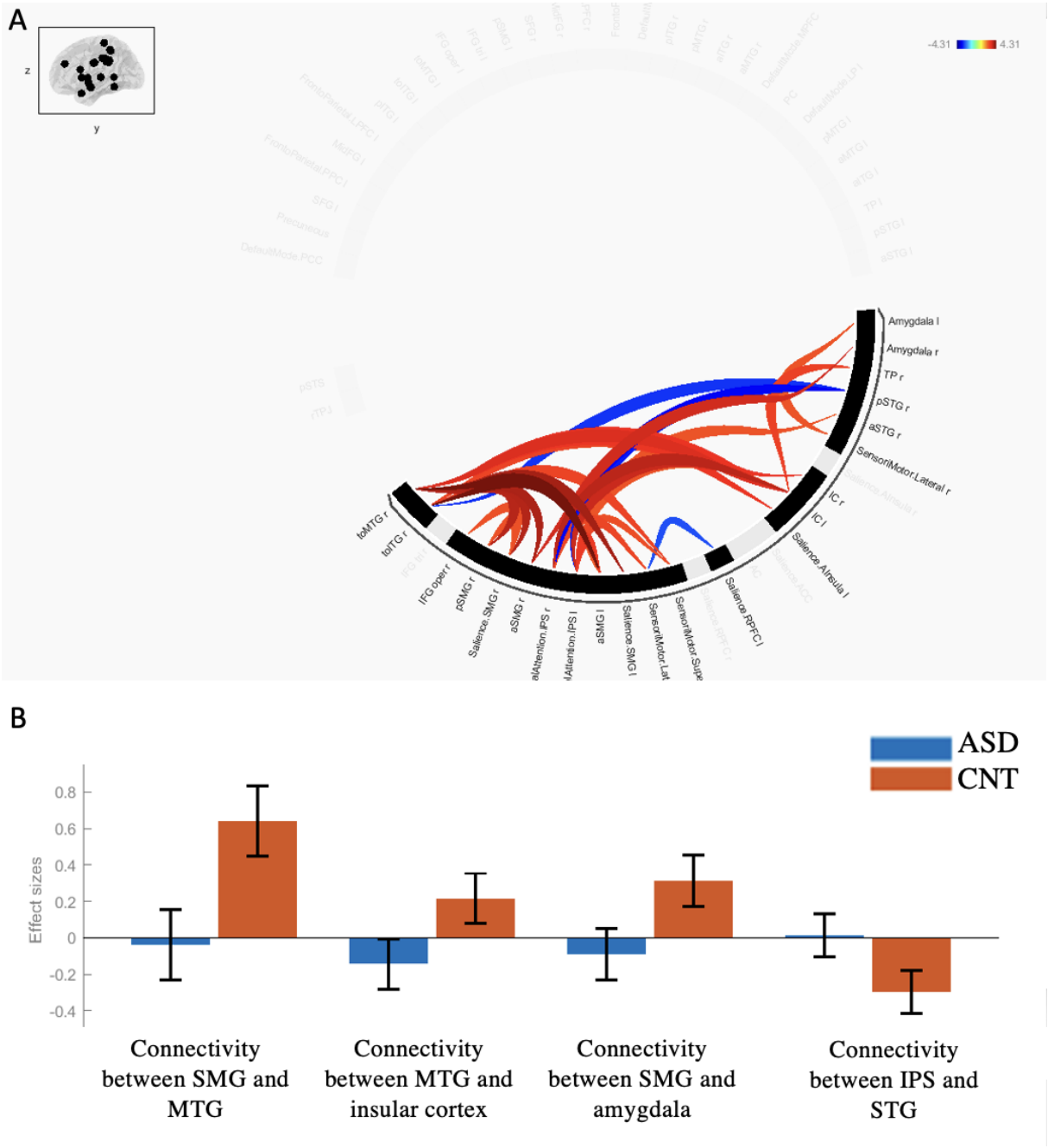

Figure 5.19: Results for the negative social interaction (with a contrast of control minus ASD). A: Connectivity map showing where the average connectivity differs between ASD and CNT subjects; The color bar represents t statistics. B: Effect size of the ROIs considered in the connectivity map. Cluster 1/6 (connection between the MTG and the SMG) showing the higher level of connectivity for the control group. The present results are shown with a cluster-level *p-corrected (MVPA omnibus test); cluster threshold of $p<0.05$ and connection threshold of $p<0.05$. The correction on the cluster-level p-uncorrected (MVPA omnibus test) is made for the number of ROIs being considered.*

The detailed table results can be consulted in appendix: A.37.

For the indifferent interaction, no significant connectivity differences were found between the two groups.

6

Discussion and Conclusion

6.1 ASD alterations on brain activation patterns

The exploratory results evaluating individually both groups from the social interaction versus non-social interaction contrast revealed the activation of the same brain regions, mainly the SMG and the right fusiform. According to the literature, these areas, are important face and/or body processing functional hubs. Also, the connections to the fusiform gyrus are mostly from the inferior occipital gyrus and from the STG, which are regions involved in visual interpretation and moving elements of faces (such as eye gazing and mouth movement), respectively [Kanwisher and Yovel, 2006]. Given the study's social animation task, these results are in agreement.

6.1.1 Involvement of the right SMG and left pSTG in Autism

The right SMG and the left posterior STG activation analysis showed, in our results, higher activation in the control group than in the ASD one. This result showed, as predicted, that these regions belonging to the TPJ, which are normally affected in patients with schizophrenia and bipolar disorder [Madeira et al., 2021], were also affected in people with autism.

A pattern of normal right SMG activation would be useful to avoid biased social interpretations, and several connectivity studies have supported the high connectivity level between the anterior TPJ (where SMG is located), the ACC and the insula, brain areas relevant in social-emotional processes [Silani et al., 2013]. Here, ASD patients tended to have a hypoactivation of these regions when a positive interaction or a negative one was presented rather than an indifferent one. This can be explained given the fact that these two interactions have a higher level of social saliency. The indifferent interaction has a lower level of intensity, becoming harder for our mind to interpret as a social interaction.

Moreover, the left posterior STG activation for the social interaction vs non social interaction contrast, showed significant differences between both groups, having a higher activation in healthy patients. This was due to the negative valence, which shows an abrupt interaction, at a faster pace, with a higher intensity, normally easier to interpret than the others [Tavares et al., 2011].

Therefore, the STG may play a critical role in processing different types of information to give proper meaning to the surrounding world. On contrary to some research that tested this paradigm in other conditions [Madeira et al., 2021], we found that the STG has a higher change

than the right SMG in the condition.

Besides, the STG is highly connected to other key regions of the brain such as the STS, frontal and parietal lobes, and the limbic and associated sensory systems [Jou et al., 2010]. Therefore, STG findings could represent a potential diagnostic biomarker for ASD given the robust discriminative power, especially in the negative animation.

6.1.2 The role of the two mentalizing regions, TPJ and mPFC in Autism

In our study, the mPFC and the TPJ, for many scientists the two most important areas in social cognition [Soares et al., 2016, Ward, 2015], showed, on the contrary, as predicted, a hypoactivation in the control group, during the social interaction vs. nonsocial interaction contrast. However, the consequent hyperactivation in both regions in the ASD group is not significant.

When interpreting each valence separately, during the positive and negative aninations the right TPJ showed higher activation in the group with ASD, and the mPFC showed significantly higher activation in the indifferent animation for the ASD group as well. These different results within the different social interactions can be explained due to the fact that mPFC loses mentalizing specialization as an individual matures while the TPJ gains activation and specialization in mentalizing processes [Kana et al., 2014]. Taking this into account and given the fact that our study subjects are adults, it is reasonable that the positive and negative animations (interactions involving a higher level of social interpretation) might be notably recruting the TPJ when compared to the mPFC. However, and even though it seems to exist a higher activation of TPJ during the positive and negative interactions, our results aren't significant, contrary to the expected since the TPJ is one of the key regions in diagnosing autism [Hao et al., 2022].

Although our results can not be conclusive, the hyperactivation of the TPJ in individuals with autism has already been discussed. Since it is a region involved in joint attention mechanisms, attentional reorienting to salient cues, and visually triggered shifts of attention that have neural underpinnings in common with gaze perception. [Mouga et al., 2022]. Nevertheless, evidence is still limited, and it remains unclear whether this hyperactivity can be explained by, developmental shifts or differences in the methodological approaches.

6.1.3 Effect of the pSTS, a key region in face perception and image network, in Austim

In our results, the posterior STS presented significant differences between the two groups in the social interaction vs. nonsocial interaction contrast and, when evaluating the valences separately, in the positive and negative animations. This suggests a higher level of activity of the posterior STS in the control group, which is in agreement with previous studies [Direito et al., 2019]. Given the importance of the posterior STS in perception of others and handling emotions, as well as evidence of abnormal functionality in social cognition disorders, especially ASD, we can infer that BOLD activity in this region could be tested in clinical trials and potentially be a useful biomarker for the diagnosis of the condition [Direito et al., 2019].

6.2 ASD functional connectivity alterations

6.2.1 Connectivity Analysis when comparing the positive and negative social interactions versus the indifferent one per group

The functional connectivity results for the contrast between indifferent interactions and the positive and negative ones revealed the modulation of two major connections. The connection between IFG and the TPJ and between the IFG and the STS. These three regions have been suggested as key mirror neuron system components [Overwalle, 2009].

The visual input is received by the STS, passes to the IPL, which includes the TPJ, and is just then received by the IFG.

We did not find such functional connections modulation in the ASD group. Although we did not compare directly both groups functional connectivity maps, this might suggest altered network mechanisms in ASD group and be linked to these individual's difficulties in social cognition [Overwalle, 2009].

Also, according to previous investigations, the TPJ and IFG, are quite implicated in the perception of intentional causation [Murdaugh et al., 2014]. The TPJ has substantially high connections within the saliency network [Murdaugh et al., 2014], and this connection is not strongly seen in individuals with ASD. This means that this poor level of connectivity between the two regions can also contribute to a lack of ability to perceive social emotions.

Nevertheless, the higher level of connectivity between these regions in the positive animation was defended by Lewis et al. [Lewis et al., 2007], who affirmed that antagonistic animations (negative interactions) tend to activate medial orbital frontal cortex regions and the affiliative animations (positive interactions) activate an inferior and more lateral orbital frontal cortex region [Tavares et al., 2011]. Since IFG is an inferior region of the frontal cortex [Heather Hsu et al., 2020], our results are consistent.

6.2.2 Connectivity Analysis, when comparing the valences separately, between control and ASD groups

Positive and negative animations were the two interactions illustrated, leading to higher differences in brain connectivity measures between the control and ASD groups. The indifferent one showed no functional connectivity differences between them, indicating that this interaction lacks social saliency, unlike positive and negative ones.

The visualization of both positive and negative interactions, recruited the salience network, specifically the SMG connection with the IFG and the middle temporal gyrus (MTG).

The IFG is known as a monitor of the "emotional state", constituting a big part of the ToM network alongside the TPJ, the STS and the mPFC [Mori and Haruno, 2022] and recent research has reported that the right- SMG, also plays a very important role in distinguishing between one's own emotions and those of others [Madeira et al., 2021]. However, the functional connectivity between these regions, as recruited by the identification of social positive and negative interactions (separately), was lower for the autistic patients. Thus, the salience and

ToM networks are recruited at a higher level in the control group than in the clinical group.

6.3 Conclusions and future work

This study tested the main hypothesis that ASD individuals show altered/different ToM mechanisms, which might be revealed at the brain response level and connectivity. We found that indeed, the pSTS hypoactivation in the clinical group can be tested has a potential biomarker for the condition and that, in individuals with ASD, several regions of the salience network, such as the SMG, AI and MTG, show a poor level of connectivity with regions from the ToM network, such as the STS and the IFG. Our results suggest that functions performed by the SMG and other salience regions, important in interpreting the social environment and perceiving others' social cues might be compromised, due to its poorer communication with TPJ, mPFC, and other ToM regions. These findings support the "disconnection hypotheses" of ASD, which propose that an impairment of a combination of frontotemporal, frontolimbic, frontoparietal, and interhemispheric connections may be at the root of the autistic condition [Hoffmann et al., 2016]. The two analysis performed, show different regions implicated in the ASD condition, which means that both approaches can be useful and provide valuable information.

Nevertheless, this study is based on a small sample size. As such, to increase data accuracy and statistical power, and reduce sensitivity to outliers, the sample size should be increased.

Also, in this study, we are only analyzing the responses to the visualized stimulus without taking into account whether the subject reports that they perceived another type of interaction. The trials were correctly identified at least 80 percent of the time, so the stimulus we were using had a low level of ambiguity. It would be interesting to extend this study to try to study the perceptual differences between groups and, by doing so, take into account the responses of the participants.

Finally, the other important consideration is the difficulty in analyzing this specific condition, ASD. Autism is a spectrum condition, which means it includes a wide range of traits and skills. This may make it more difficult to generalize the findings of certain studies to the entire autistic population.

Even given all these limitations, the obtained results show a good level of consistency. This thesis opens paths for research fronts to improve the identification of more potentially useful candidate biomarkers. The application of different connectivity metrics can also give valuable results and provide more information.

Funding

This work was supported by FCT/UIDB/4950/2020 and FCT/UIDP/4950/2020.

References

[Baron-Cohen et al., 2000] Baron-Cohen, S., Ring, H., Bullmore, E. T., Wheelwright, S. J., Ashwin, C., and Williams, S. (2000). The amygdala theory of autism. *Neuroscience & Biobehavioral Reviews*, 24:355–364.

[Biswal et al., 1995] Biswal, B., Zerrin Yetkin, F., Haughton, V. M., and Hyde, J. S. (1995). Functional connectivity in the motor cortex of resting human brain using echo-planar mri. *Magnetic resonance in medicine*, 34(4):537–541.

[brain networks, nd] brain networks (n.d.). Brain Networks. `https://www.o8t.com/blog/brain-networks`. Acesso em 19 de junho de 2023.

[BrainVoyager, nd] BrainVoyager (nd). The general linear model - brainvoyager user's guide. [Acessado em 12 de Setembro].

[Bullmore and Sporns, 2009] Bullmore, E. T. and Sporns, O. (2009). Complex brain networks: graph theoretical analysis of structural and functional systems. *Nature Reviews Neuroscience*, 10:186–198.

[Buxton and Frank, 1997] Buxton, R. B. and Frank, L. R. (1997). A model for the coupling between cerebral blood flow and oxygen metabolism during neural stimulation. *Journal of Cerebral Blood Flow & Metabolism*, 17:64 – 72.

[Campos et al., 2016] Campos, A. S., Direito, B., Pereira, D. B., and Castelo-Branco, M. (2016). Brain connectivity analysis for real-time fmri neurofeedback experiments. *2017 IEEE 5th Portuguese Meeting on Bioengineering (ENBENG)*, pages 1–4.

[Chen et al., 2019] Chen, J. E., Polimeni, J., Bollmann, S., and Glover, G. H. (2019). On the analysis of rapidly sampled fmri data. *NeuroImage*, 188:807–820.

[CONN Toolbox Developers, SD] CONN Toolbox Developers (S/D). Conn toolbox. Acessado em [data de acesso].

[Dalgleish, 2004] Dalgleish, T. (2004). The emotional brain. *Nature Reviews Neuroscience*, 5(7):583–589.

[Deng et al., 2022] Deng, X., Zhang, J., Liu, R., and Liu, K. (2022). Classifying asd based on time-series fmri using spatial-temporal transformer. *Computers in biology and medicine*, 151 Pt B:106320.

[Di and Biswal, 2023] Di, X. and Biswal, B. B. (2023). A functional mri pre-processing and quality control protocol based on statistical parametric mapping (spm) and matlab. *Frontiers in Neuroimaging*, 1:1070151.

[Direito et al., 2019] Direito, B., Lima, J., Simoes, M., Sayal, A., Sousa, T., Lührs, M., Ferreira, C., and Castelo-Branco, M. (2019). Targeting dynamic facial processing mechanisms in superior temporal sulcus using a novel fmri neurofeedback target. *Neuroscience*, 406:97–108.

[Doan, 2015] Doan, A. (2015). *Andy's Brain Book: Understanding the Anatomy and Function of the Brain*. Wheatmark.

[Faber et al., 2019] Faber, J., Antoneli, P. C., Via, G., Ara'ujo, N. S., Pinheiro, D. J. L. L., and Cavalheiro, E. A. (2019). Critical elements for connectivity analysis of brain networks. *Brain Informatics and Health*.

[Fakhoury, 2015] Fakhoury, M. (2015). Autistic spectrum disorders: A review of clinical features, theories and diagnosis. *International Journal of Developmental Neuroscience*, 43:70–77.

[Farrant and Uddin, 2016] Farrant, K. and Uddin, L. Q. (2016). Atypical developmental of dorsal and ventral attention networks in autism. *Developmental science*, 19(4):550–563.

[Fishman et al., 2019] Fishman, I., Keown, C. L., Lincoln, A. J., Pineda, J. A., and Muller, R.-A. (2019). Brain connectivity in autism: a review of recent studies. *Current psychiatry reports*, 21(12):129.

[Friston, 2011] Friston, K. J. (2011). Functional and effective connectivity: a review. *Brain Connectivity*, 1(1):13–36.

[Friston et al., 2011] Friston, K. J., Ashburner, J. T., Kiebel, S. J., Nichols, T. E., and Penny, W. D. (2011). *Statistical parametric mapping: the analysis of functional brain images*. Academic press.

[Gasquoine, 2014] Gasquoine, P. G. (2014). Contributions of the insula to cognition and emotion. *Neuropsychology Review*, 24:77–87.

[Genovese and Butler, 2020] Genovese, A. and Butler, M. G. (2020). Clinical assessment, genetics, and treatment approaches in autism spectrum disorder (asd). *International Journal of Molecular Sciences*, 21.

[Georgiopoulos, 2019] Georgiopoulos, C. (2019). Imaging studies of olfaction in health and parkinsonism. *Linköping University Medical Dissertations*.

[Glover, 2011] Glover, G. H. (2011). Overview of functional magnetic resonance imaging. *Neurosurgery clinics of North America*, 22 2:133–9, vii.

[Gong et al., 2014] Gong, L., Li, B., Wu, R., Li, A., and Xu, F. (2014). Brain-state dependent uncoupling of bold and local field potentials in laminar olfactory bulb. *Neuroscience Letters*, 580:1–6.

[Hao et al., 2022] Hao, Z., Shi, Y., Huang, L., Sun, J., Li, M., Gao, Y., Li, J., Wang, Q., Zhan, L., Ding, Q., et al. (2022). The atypical effective connectivity of right temporoparietal junction in autism spectrum disorder: a multi-site study. *Frontiers in Neuroscience*, 16:927556.

[Heather Hsu et al., 2020] Heather Hsu, C.-C., Rolls, E. T., Huang, C.-C., Chong, S. T., Zac Lo, C.-Y., Feng, J., and Lin, C.-P. (2020). Connections of the human orbitofrontal cortex and inferior frontal gyrus. *Cerebral Cortex*, 30(11):5830–5843.

[Hoffmann et al., 2016] Hoffmann, F., Koehne, S., Steinbeis, N., Dziobek, I., and Singer, T. (2016). Preserved self-other distinction during empathy in autism is linked to network integrity

of right supramarginal gyrus. *Journal of autism and developmental disorders*, 46:637–648.

[Hughes et al., 2019] Hughes, C., Cassidy, B. S., Faskowitz, J., Avena-Koenigsberger, A., Sporns, O., and Krendl, A. C. (2019). Age differences in specific neural connections within the default mode network underlie theory of mind. *NeuroImage*, 191:269–277.

[Hull et al., 2017a] Hull, J. V., Dokovna, L. B., Jacokes, Z. J., Torgerson, C. M., Irimia, A., and Van Horn, J. D. (2017a). Resting-state functional connectivity in autism spectrum disorders: a review. *Frontiers in psychiatry*, 7:205.

[Hull et al., 2017b] Hull, J. V., Dokovna, L. B., Jacokes, Z. J., Torgerson, C. M., Irimia, A., and Van Horn, J. D. (2017b). Resting-state functional connectivity in autism spectrum disorders: A review. *Frontiers in Psychiatry*, 7.

[Hyatt et al., 2020] Hyatt, C. J., Calhoun, V. D., Pittman, B., Corbera, S., Bell, M. D., Rabany, L., Pelphrey, K., Pearlson, G. D., and Assaf, M. (2020). Default mode network modulation by mentalizing in young adults with autism spectrum disorder or schizophrenia. *NeuroImage: Clinical*, 27:102343.

[intrinsic networks, nd] intrinsic networks (n.d.). intrinsic Networks. `https://how-emotions-are-made.com/notes/Intrinsic_networks`. Acesso em 6 de setembro de 2023.

[Jenkinson et al., 2012] Jenkinson, M., Beckmann, C. F., Behrens, T. E., Woolrich, M. W., and Smith, S. M. (2012). Fsl. *Neuroimage*, 62(2):782–790.

[Jimenez et al., 2019] Jimenez, A. M., Riedel, P., Lee, J., Reavis, E. A., and Green, M. F. (2019). Linking resting-state networks and social cognition in schizophrenia and bipolar disorder. *Human brain mapping*, 40(16):4703–4715.

[Jou et al., 2010] Jou, R. J., Minshew, N. J., Keshavan, M. S., Vitale, M. P., and Hardan, A. Y. (2010). Enlarged right superior temporal gyrus in children and adolescents with autism. *Brain research*, 1360:205–212.

[Kana et al., 2014] Kana, R. K., Libero, L. E., Hu, C. P., Deshpande, H. D., and Colburn, J. S. (2014). Functional brain networks and white matter underlying theory-of-mind in autism. *Social cognitive and affective neuroscience*, 9 1:98–105.

[Kanwisher and Yovel, 2006] Kanwisher, N. and Yovel, G. (2006). The fusiform face area: a cortical region specialized for the perception of faces. *Philosophical Transactions of the Royal Society B: Biological Sciences*, 361(1476):2109–2128.

[Karoğlu et al., 2022] Karoğlu, N., Ferguson, H. J., and Ó Ciardha, C. (2022). Theory of mind in offending: A systematic review. *Trauma, Violence, & Abuse*, 23(5):1610–1628.

[Keehn et al., 2021] Keehn, R. J. J., Pueschel, E. B., Gao, Y., Jahedi, A., Alemu, K., Carper, R., Fishman, I., and Müller, R.-A. (2021). Underconnectivity between visual and salience networks and links with sensory abnormalities in autism spectrum disorders. *Journal of the American Academy of Child & Adolescent Psychiatry*, 60(2):274–285.

[Kwong et al., 1992] Kwong, K. K., Belliveau, J. W., Chesler, D. A., Goldberg, I. E., Weisskoff, R. M., Poncelet, B. P., Kennedy, D. N., Hoppel, B. E., Cohen, M. S., and Turner, R. (1992). Dynamic magnetic resonance imaging of human brain activity during primary sensory stim-

ulation. *Proceedings of the National Academy of Sciences of the United States of America*, 89:5675 – 5679.

[Lewis et al., 2007] Lewis, P. A., Critchley, H. D., Rotshtein, P., and Dolan, R. J. (2007). Neural correlates of processing valence and arousal in affective words. *Cerebral cortex*, 17(3):742–748.

[Lindquist and Wager, 2016] Lindquist, M. A. and Wager, T. D. (2016). Principles of functional magnetic resonance imaging.

[Logothetis, 2008] Logothetis, N. K. (2008). What we can do and what we cannot do with fmri. *Nature*, 453:869–878.

[Madeira et al., 2021] Madeira, N., Martins, R., Duarte, J. V., Costa, G., Macedo, A., and Castelo-Branco, M. (2021). A fundamental distinction in early neural processing of implicit social interpretation in schizophrenia and bipolar disorder. *NeuroImage: Clinical*, 32:102836.

[Masi et al., 2017] Masi, A., DeMayo, M. M., Glozier, N., and Guastella, A. J. (2017). An overview of autism spectrum disorder, heterogeneity and treatment options. *Neuroscience Bulletin*, 33:183 – 193.

[Matsumoto and Tanaka, 2004] Matsumoto, K. and Tanaka, K. (2004). Conflict and cognitive control. *Science*, 303:969 – 970.

[Miani et al., 2021] Miani, A., Imbriani, G., Filippis, G. D., Giorgi, D. D., Peccarisi, L., Colangelo, M., Pulimeno, M., Castellone, M. D., Nicolardi, G., Logroscino, G., and Piscitelli, P. (2021). Autism spectrum disorder and prenatal or early life exposure to pesticides: A short review. *International Journal of Environmental Research and Public Health*, 18.

[Mohammad-Rezazadeh and Frohlich, 2016] Mohammad-Rezazadeh, I. and Frohlich, J. (2016). Brain connectivity in autism spectrum disorder. *Current Opinion in Neurology*, 29(2):137–147.

[Molloy et al., 2014] Molloy, E. K., Meyerand, M. E., and Birn, R. M. (2014). The influence of spatial resolution and smoothing on the detectability of resting-state and task fmri. *NeuroImage*, 86:221–230.

[Mori and Haruno, 2022] Mori, K. and Haruno, M. (2022). Resting functional connectivity of the left inferior frontal gyrus with the dorsomedial prefrontal cortex and temporoparietal junction reflects the social network size for active interactions. *Human Brain Mapping*, 43(9):2869–2879.

[Mouga et al., 2015] Mouga, S., Almeida, J., Café, C., Duque, F., and Oliveira, G. (2015). Adaptive profiles in autism and other neurodevelopmental disorders. *Journal of Autism and Developmental Disorders*, 45:1001–1012.

[Mouga et al., 2022] Mouga, S., Duarte, I. C., Café, C., Sousa, D., Duque, F., Oliveira, G., and Castelo-Branco, M. (2022). Parahippocampal deactivation and hyperactivation of central executive, saliency and social cognition networks in autism spectrum disorder. *Journal of Neurodevelopmental Disorders*, 14(1):1–12.

[Murdaugh et al., 2014] Murdaugh, D. L., Nadendla, K., and Kana, R. K. (2014). Differential role of temporoparietal junction and medial prefrontal cortex in causal inference in autism: An independent component analysis. *Neuroscience Letters*, 568:50–55.

[Newschaffer et al., 2007] Newschaffer, C. J., Croen, L. A., Daniels, J. L., Giarelli, E., Grether,

J. K., Levy, S. E., Mandell, D. S., Miller, L. A., Pinto-Martin, J., Reaven, J., Reynolds, A. M., Rice, C., Schendel, D., and Windham, G. C. (2007). The epidemiology of autism spectrum disorders. *Annual review of public health*, 28:235–58.

[Nieto-Castanon, 2020] Nieto-Castanon, A. (2020). *Handbook of functional connectivity magnetic resonance imaging methods in CONN*. Hilbert Press.

[Ogawa and Lee, 1990] Ogawa, S. and Lee, T. (1990). Magnetic resonance imaging of blood vessels at high fields: In vivo and in vitro measurements and image simulation. *Magnetic Resonance in Medicine*, 16.

[Overwalle, 2009] Overwalle, F. V. (2009). Social cognition and the brain: a meta-analysis. *Human Brain Mapping*, 30:829–858.

[Pamplona, 2014] Pamplona, G. S. P. (2014). Conectividade funcional no cérebro: uma análise das associações com desempenho intelectual e atenção sustentada usando imagens por ressonância magnética.

[Park et al., 2020] Park, K. Y., Lee, J. J., Dierker, D. L., Marple, L. M., Hacker, C. D., Roland, J. L., Marcus, D. S., Milchenko, M., Miller-Thomas, M. M., Benzinger, T. L. S., Shimony, J. S., Snyder, A. Z., and Leuthardt, E. C. (2020). Mapping language function with task-based vs. resting-state functional mri. *PLoS ONE*, 15.

[Phillips and LeDoux, 1992] Phillips, R. and LeDoux, J. (1992). Differential contribution of amygdala and hippocampus to cued and contextual fear conditioning. *Behavioral neuroscience*, 106(2):274.

[Power et al., 2012] Power, J. D., Barnes, K. A., Snyder, A. Z., Schlaggar, B. L., and Petersen, S. E. (2012). Spurious but systematic correlations in functional connectivity mri networks arise from subject motion. *NeuroImage*, 59:2142–2154.

[Randall et al., 2011] Randall, M., Egberts, K. J., Samtani, A., Scholten, R. J. P. M., Hooft, L., Livingstone, N., Sterling-Levis, K., Woolfenden, S., and Williams, K. J. (2011). Diagnostic tests for autism spectrum disorder (asd) in preschool children. *The Cochrane database of systematic reviews*, 7:CD009044.

[Rangaprakash et al., 2020] Rangaprakash, D., Tadayonnejad, R., Deshpande, G., O'Neill, J., and Feusner, J. D. (2020). Fmri hemodynamic response function (hrf) as a novel marker of brain function: applications for understanding obsessive-compulsive disorder pathology and treatment response. *Brain Imaging and Behavior*, 15:1622–1640.

[Rizzolatti and Craighero, 2004] Rizzolatti, G. and Craighero, L. (2004). The mirror-neuron system. *Annual review of neuroscience*, 27:169–92.

[Roca et al., 2011] Roca, M., Torralva, T., Gleichgerrcht, E., Woolgar, A., Thompson, R., Duncan, J., and Manes, F. (2011). The role of area 10 (ba10) in human multitasking and in social cognition: a lesion study. *Neuropsychologia*, 49(13):3525–3531.

[Rujeedawa and Zaman, 2022] Rujeedawa, T. and Zaman, S. H. (2022). The diagnosis and management of autism spectrum disorder (asd) in adult females in the presence or absence of an intellectual disability. *International Journal of Environmental Research and Public Health*, 19.

[Salmón and Leoni, 2019] Salmón, C. E. G. and Leoni, R. F. (2019). Conectividade funcional cerebral utilizando técnicas de imagens por ressonância magnética. *Revista Brasileira de Física Médica*.

[Samsam et al., 2014] Samsam, M., Ahangari, R., and Naser, S. A. (2014). Pathophysiology of autism spectrum disorders: revisiting gastrointestinal involvement and immune imbalance. *World journal of gastroenterology*, 20 29:9942–51.

[Schurz et al., 2020] Schurz, M., Maliske, L., and Kanske, P. (2020). Cross-network interactions in social cognition: A review of findings on task related brain activation and connectivity. *Cortex*, 130:142–157.

[Silani et al., 2013] Silani, G., Lamm, C., Ruff, C. C., and Singer, T. (2013). Right supramarginal gyrus is crucial to overcome emotional egocentricity bias in social judgments. *Journal of neuroscience*, 33(39):15466–15476.

[Smith and Beckmann, 2017] Smith, S. M. and Beckmann, C. F. (2017). Introduction to resting state fmri functional connectivity.

[Soares et al., 2023] Soares, C., Gonzalo, G., Castelhano, J., and Castelo-Branco, M. (2023). The relationship between the default mode network and the theory of mind network as revealed by psychedelics–a meta-analysis. *Neuroscience & Biobehavioral Reviews*, page 105325.

[Soares et al., 2016] Soares, J. M., Magalhães, R., Moreira, P. S., de Sousa, A. V., Ganz, E., Sampaio, A., Alves, V., Marques, P., and Sousa, N. J. (2016). A hitchhiker's guide to functional magnetic resonance imaging. *Frontiers in Neuroscience*, 10.

[Sommer et al., 2007] Sommer, M., Döhnel, K., Sodian, B., Meinhardt, J., Thoermer, C., and Hajak, G. (2007). Neural correlates of true and false belief reasoning. *NeuroImage*, 35:1378–1384.

[Stuss et al., 2001] Stuss, D. T., Floden, D., Alexander, M., Levine, B., and Katz, D. (2001). Stroop performance in focal lesion patients: dissociation of processes and frontal lobe lesion location. *Neuropsychologia*, 39(8):771–786.

[Szamburska-Lewandowska et al., 2021] Szamburska-Lewandowska, K., Konowałek, Ł., and Bryńska, A. (2021). Theory of mind deficits in childhood mental and neurodevelopmental disorders. *Psychiatria polska*, 55(4):801–813.

[Tavares et al., 2011] Tavares, P., Barnard, P. J., and Lawrence, A. D. (2011). Emotional complexity and the neural representation of emotion in motion. *Social Cognitive and Affective Neuroscience*, 6:98 – 108.

[Thomas et al., 2020] Thomas, R. M., Gallo, S., Cerliani, L., Zhutovsky, P., El-Gazzar, A., and van Wingen, G. A. (2020). Classifying autism spectrum disorder using the temporal statistics of resting-state functional mri data with 3d convolutional neural networks. *Frontiers in Psychiatry*, 11.

[Thomas Yeo et al., 2011] Thomas Yeo, B., Krienen, F. M., Sepulcre, J., Sabuncu, M. R., Lashkari, D., Hollinshead, M., Roffman, J. L., Smoller, J. W., Zöllei, L., Polimeni, J. R., et al. (2011). The organization of the human cerebral cortex estimated by intrinsic functional connectivity. *Journal of neurophysiology*, 106(3):1125–1165.

[Uddin and Menon, 2009] Uddin, L. Q. and Menon, V. (2009). The anterior insula in autism: Under-connected and under-examined. *Neuroscience & Biobehavioral Reviews*, 33:1198–1203.

[Ward, 2006] Ward, J. (2006). The student's guide to cognitive neuroscience.

[Ward, 2015] Ward, J. (2015). *The student's guide to cognitive neuroscience*. psychology press.

[Weitlauf et al., 2014] Weitlauf, A. S., Gotham, K. O., Vehorn, A. C., and Warren, Z. (2014). Brief report: Dsm-5 "levels of support:" a comment on discrepant conceptualizations of severity in asd. *Journal of Autism and Developmental Disorders*, 44:471–476.

[Worsley and Friston, 1995] Worsley, K. J. and Friston, K. J. (1995). Analysis of fmri time-series revisited—again. *Neuroimage*, 2(3):173–181.

[yong Park et al., 2019] yong Park, B., Byeon, K., and Park, H. (2019). Funp (fusion of neuroimaging preprocessing) pipelines: A fully automated preprocessing software for functional magnetic resonance imaging. *Frontiers in Neuroinformatics*, 13.

[Zhao et al., 2022] Zhao, Z., Lu, E., Zhao, F., Zeng, Y., and Zhao, Y. (2022). A brain-inspired theory of mind spiking neural network for reducing safety risks of other agents. *Frontiers in neuroscience*, 16:753900.

A

Appendices

Animation movies of the theory-of-mind functional MRI paradigm are available as supplementary videos (1 to 4): https://doi. org/10.1016/j.nicl.2021.102836

A.1 ROIs

A.1.1 Tables listing the brain networks and brain regions used in the functional connectivity analysis.

Network	Coordinates
networks.DefaultMode.mPFC	(1,55,-3)
networks.DefaultMode.LP (L)	(-39,-77,33)
networks.DefaultMode.LP (R)	(47,-67,29)
networks.DefaultMode.posterior cingulate cortex (PCC)	(1,-61,38)
networks.SensoriMotor.Lateral (L)	(-55,-12,29)
networks.SensoriMotor.Lateral (R)	(56,-10,29)
networks.SensoriMotor.Superior	(0,-31,67)
networks.Salience.ACC	(0,22,35)
networks.Salience.Anterior Insula (L)	(-44,13,1)
networks.Salience.Anterior Insula (R)	(47,14,0)
networks.Salience.right prefrontal cortex (RPFC) (L)	(-32,45,27)
networks.Salience.RPFC(R)	(32,46,27)
networks.Salience.SMG (L)	(-60,-39,31)
networks.Salience.SMG (R)	(62,-35,32)
networks.DorsalAttention.intraparietal sulcus (IPS) (L)	(-39,-43,52)
networks.DorsalAttention.IPS (R)	(39,-42,54)
networks.FrontoParietal.LPFC (L)	(-43,33,28)’
networks.FrontoParietal.PPC (L)	(-46,-58,49)
networks.FrontoParietal.LPFC (R)	(41,38,30)
networks.FrontoParietal.PPC (R)	(52,-52,45)

Table A.1: Table with the networks of interest from the Atlas available in the CONN toolbox.

Regions of interest
'atlas.IC r (Insular Cortex Right)'
'atlas.IC l (Insular Cortex Left)'
'atlas.SFG r (Superior Frontal Gyrus Right)'
'atlas.SFG l (Superior Frontal Gyrus Left)'
'atlas.MidFG r (Middle Frontal Gyrus Right)'
'atlas.MidFG l (Middle Frontal Gyrus Left)'
'atlas.IFG tri r (Inferior Frontal Gyrus, pars triangularis Right)'
'atlas.IFG tri l (Inferior Frontal Gyrus, pars triangularis Left)'
'atlas.IFG oper r (Inferior Frontal Gyrus, pars opercularis Right)'
'atlas.IFG oper l (Inferior Frontal Gyrus, pars opercularis Left)'
'atlas.TP r (Temporal Pole Right)'
'atlas.TP l (Temporal Pole Left)'
'atlas.aSTG r (Superior Temporal Gyrus, anterior division Right)'
'atlas.aSTG l (Superior Temporal Gyrus, anterior division Left)'
'atlas.pSTG r (Superior Temporal Gyrus, posterior division Right)'
'atlas.pSTG l (Superior Temporal Gyrus, posterior division Left)'
'atlas.aMTG r (Middle Temporal Gyrus, anterior division Right)'
'atlas.aMTG l (Middle Temporal Gyrus, anterior division Left)'
'atlas.pMTG r (Middle Temporal Gyrus, posterior division Right)'
'atlas.pMTG l (Middle Temporal Gyrus, posterior division Left)'
'atlas.toMTG r (Middle Temporal Gyrus, temporooccipital part Right)'
'atlas.toMTG l (Middle Temporal Gyrus, temporooccipital part Left)'
'atlas.aITG r (Inferior Temporal Gyrus, anterior division Right)'
'atlas.aITG l (Inferior Temporal Gyrus, anterior division Left)'
'atlas.pITG r (Inferior Temporal Gyrus, posterior division Right)'
'atlas.pITG l (Inferior Temporal Gyrus, posterior division Left)'
'atlas.toITG r (Inferior Temporal Gyrus, temporooccipital part Right)'
'atlas.toITG l (Inferior Temporal Gyrus, temporooccipital part Left)'
'atlas.aSMG r (Supramarginal Gyrus, anterior division Right)'
'atlas.aSMG l (Supramarginal Gyrus, anterior division Left)'
'atlas.pSMG r (Supramarginal Gyrus, posterior division Right)'
'atlas.pSMG l (Supramarginal Gyrus, posterior division Left)'
'atlas.AC (Cingulate Gyrus, anterior division)'
'atlas.PC (Cingulate Gyrus, posterior division)'
'atlas.Precuneous (Precuneous Cortex)'
'atlas.Amygdala r'
'atlas.Amygdala l'

Table A.2: Table with the regions of interest from the Atlas available in the CONN toolbox.

A.2 Contrast Estimate Values

A.2.1 SMG

Percentage of Signal (%) Beta Values
Control Group
7.1194
0.9010
8.4529
13.1206
5.3529
18.4465
16.9886
1.5998
4.9094
3.5366
-1.2706

Table A.3: Control Group- SMG

Percentage of Signal (%) Beta Values
ASD Group
-3.2802
1.7210
4.4143
-2.3826
1.4002
-2.1766
2.4253
-0.6089
7.6707
-0.5358
13.4120

Table A.4: ASD Group- SMG

Percentage of Signal (%) Beta Values Control Group		
Positive	Negative	Indifferent
5.4410	6.5210	-4.8425
2.5065	1.4527	-3.0583
5.6236	2.7514	0.0779
11.1529	12.6910	-10.7233
0.9912	5.4780	-1.1164
8.1772	9.9187	0.3506
8.1050	11.4200	-2.5363
0.6729	1.7319	-0.8050
1.7519	2.2953	0.8622
1.1844	6.3619	-4.0096
0.9090	-2.4373	0.2578

Table A.5: Control Group Valences- SMG

Percentage of Signal (%) Beta Values ASD Group		
Positive	Negative	Indifferent
-3.3465	-5.7852	-3.8857
5.0203	7.1821	6.7451
0.4705	0.9533	-0.8032
-1.1461	-5.4577	2.2895
9.5377	7.8058	7.8658
1.1695	3.7941	0.7086
0.6012	4.5573	4.4164
-1.0438	-1.6927	-1.3481
2.1229	2.7056	0.1490
2.2376	3.8219	0.2312
5.2870	4.9462	3.0339

Table A.6: ASD Group Valences- SMG

A.2.2 lpSTG

Percentage of Signal (%) Beta Values
Control Group
7.0424
0.5385
6.1357
6.0794
4.0157
6.6038
2.6076
-3.8997
1.3803
2.8905
1.0304

Table A.7: Control Group- lpSTG

Percentage of Signal (%) Beta Values
ASD Group
1.2265
-9.4471
-3.4871
-4.3735
-0.1673
-1.9536
-2.9788
2.6463
3.5275
0.4764
4.4881

Table A.8: ASD Group- lpSTG

Percentage of Signal (%) Beta Values Control Group		
Positive	Negative	Indifferent
1.6201	9.1924	-3.7701
-2.0770	-1.3395	3.9549
1.4771	6.4701	-1.8115
6.1076	7.0074	-7.0355
0.9145	3.5594	-0.4583
3.2253	5.2433	-1.8648
0.6233	4.8483	-2.8639
0.0132	-5.9429	2.0300
2.7546	-1.2832	-0.0911
-1.5273	4.1879	0.2300
-1.5368	2.7283	-0.1611

Table A.9: Control Group Valences- lpSTG

Percentage of Signal (%) Beta Values ASD Group		
Positive	Negative	Indifferent
2.4289	-1.1199	-0.0825
-10.8072	1.7773	-0.4173
-5.4398	-0.1625	2.1152
3.2872	-12.2650	4.6043
0.8067	0.3968	-1.3708
-4.6056	8.4891	-5.8371
-3.7502	0.7267	0.0446
4.7806	2.1837	-4.3181
4.0218	3.0175	-3.5117
3.3816	1.8713	-4.7765
4.6494	1.3970	-1.5583

Table A.10: ASD Group Valences- lpSTG

A.2.3 pSTS

Percentage of Signal (%) Beta Values
Control Group
9.3754
1.6356
9.3519
7.3707
1.7663
7.9669
5.7592
1.3296
0.2082
5.9878
2.0929

Table A.11: Control Group- STS

Percentage of Signal (%) Beta Values
ASD Group
-0.1567
-5.3675
-5.3855
-2.5533
0.1681
-5.2554
0.8474
-1.4315
4.8877
-6.4831
5.0736

Table A.12: ASD Group- STS

Percentage of Signal (%) Beta Values Control Group		
Positive	Negative	Indifferent
4.3622	8.1906	-3.1775
1.7604	-2.3846	2.2598
6.3520	5.6050	-2.6050
4.9609	6.0005	-3.5907
-0.2010	2.2490	-0.2817
9.0523	3.0911	-4.1764
3.9906	6.9211	-5.1525
1.5098	-0.4187	0.2385
0.0803	1.7178	-1.5899
0.8732	8.3546	-3.2401
4.1573	1.6958	-3.7602

Table A.13: Control Group Valences- STS

Percentage of Signal (%) Beta Values ASD Group		
Positive	Negative	Indifferent
2.6822	-2.4429	-0.3960
-9.2796	0.4012	3.5110
-2.5312	-2.3427	-0.5115
7.4957	-11.8314	1.7823
-0.4094	1.0219	-0.4444
-5.1562	5.6892	-5.7883
-0.1718	0.8414	0.1778
1.8868	-1.0828	-2.2356
2.3076	3.0817	-0.5016
-6.9449	3.9055	-3.4437
1.1381	0.5661	3.3693

Table A.14: ASD Group Valences- STS

A.2.4 TPJ

Percentage of Signal (%) Beta Values
Control Group
0.2051
-0.8853
-2.6015
2.2184
-4.2364
7.3728
-0.9432
-2.9546
-1.6929
-5.1557
-3.4515

Table A.15: Control Group- TPJ

Percentage of Signal (%) Beta Values
ASD Group
0.9401
-4.3167
-2.1119
-8.2391
1.1016
-4.6523
2.6579
1.2955
4.6835
-6.7001
5.8695

Table A.16: ASD Group- TPJ

Percentage of Signal (%) Beta Values Control Group		
Positive	Negative	Indifferent
-0.0255	6.8035	-6.5728
-3.5234	4.5329	-1.8949
-1.5101	-7.7874	6.6961
0.0249	1.5198	0.6737
-4.7749	-1.3826	1.9210
4.1601	3.7273	-0.5146
-1.8636	1.7110	-0.7906
-2.6059	-6.7700	6.4213
-1.6878	-5.8841	5.8790
-9.3150	-0.0654	4.2247
-1.2136	-5.3186	3.0808

Table A.17: Control Group Valences-TPJ

Percentage of Signal (%) Beta Values ASD Group		
Positive	Negative	Indifferent
3.7027	2.2706	3.9378
1.0011	2.1564	4.6141
-0.3267	-0.0042	-0.2967
-2.2640	-4.5746	-2.4199
1.8489	1.0832	1.9144
-3.1886	-1.3062	-4.1348
2.9482	3.3671	6.3935
-1.1507	-2.1062	-2.0313
3.1768	3.2450	3.7685
-0.3509	2.2973	-1.3423
10.4145	10.7025	11.8684

Table A.18: ASD Group Valences- TPJ

A.2.5 mPFC

Percentage of Signal (%) Beta Values
Control Group
1.7953
2.6665
-2.1831
15.3929
0.0414
12.9272
2.8751
-2.4392
0.3334
-5.5549
-0.2446

Table A.19: Control Group- mPFC

Percentage of Signal (%) Beta Values
ASD Group
2.080225
2.024481
0.1542808
-4.2295
9.95874
-4.70095
4.4097
6.4895
4.26146
2.35257
8.9665

Table A.20: ASD Group- mPFC

Percentage of Signal (%) Beta Values Control Group		
Positive	Negative	Indifferent
3.4235	0.1384	-1.7666
3.5888	1.4420	-2.3644
-1.8421	-4.3280	3.9870
10.1734	6.7240	-1.5045
2.9748	-0.7338	-2.1996
7.3204	5.6610	-0.0542
1.8336	1.5019	-0.4603
-0.2545	-4.1926	2.0079
1.4680	0.9293	-2.0639
-3.3868	3.4518	-5.6199
2.6666	2.5759	-5.4871

Table A.21: Control Group Valences- mPFC

Percentage of Signal (%) Beta Values ASD Group		
Positive	Negative	Indifferent
3.4096	-1.1277	-0.2017
-12.9883	1.2497	13.7630
-4.8609	3.8671	1.1481
0.5433	-17.1434	12.3702
3.5797	-0.4675	6.8465
-2.1372	4.7940	-7.3578
-0.4914	2.4231	2.4775
4.7262	0.8876	0.8754
3.2243	-0.7369	1.7740
-2.0617	0.2737	4.1405
0.3596	7.5683	1.0388

Table A.22: ASD Group Valences- mPFC

A.3 Between subject-effects test (TWO-WAY ANOVA)

A.3.1 SMG

Origem	Tipo III Soma dos Quadrados	df	Quadrado Médio	F	Sig.
Modelo corrigido	378.328	5	75.667	4.852	< .001
Intercepto	306.811	1	306.811	19.68	< .001
Group	3.885	1	3.885	0.249	.619
Valence	199.89	2	99.95	6.41	.003
Group*Valence	174.55	2	87.28	5.60	.006
Pattern	935.69	60	15.59		
Total	1620.834	66			
Total corrigido	1314.03	65			

Table A.23: Testing for between-subject effects- SMG

(I) Valence	(J) Valence	Mean (I-J)	Test Statistic Standard Deviation	Sig.	95% C. Interval Lower Limit	Upper Limit
INDIF	NEG	-3.9616*	1.19067	.004	-6.8231	-1.1002
	POS	-3.3439*	1.19067	.018	-6.2054	-.4825
NEG	INDIF	3.9616*	1.19067	.004	1.1002	6.8231
	POS	0.6177	1.19067	.862	-2.2437	3.4791
POS	INDIF	3.3439*	1.19067	.018	0.4825	6.2054
	NEG	-0.6177	1.19067	.862	-3.4791	2.2437

Table A.24: Multiple Comparison - Tukey - SMG

Valence	(I) Group	(J) Group	Mean (I-J)	Statistic	Significance *b*	95% C. Interval	
						Lower Limit	Upper Limit
INDIF	ASD	CNT	4.086*	1.684	.018	0.718	7.454
	CNT	ASD	-4.086*	1.684	.018	-7.454	-0.718
NEG	ASD	CNT	-3.214	1.684	.061	-6.582	0.154
	CNT	ASD	3.214	1.684	.061	-0.154	6.582
POS	ASD	CNT	-2.328	1.684	.172	-5.696	1.040
	CNT	ASD	2.328	1.684	.172	-1.040	5.696

Table A.25: Pairwise Method comparison- SMG

A.3.2 lpSTG

Source	Type III Sum of Squares	df	Mean Square	F	Sig.
Corrected Model	152.187a	5	30.437	1.756	.136
Intercept	28.132	1	28.132	1.623	.208
Group	68.704	1	68.704	3.963	.051
Valence	54.762	2	27.381	1.579	.215
Group * Valence	28.721	2	14.360	0.828	.442
Pattern	1040.231	60	17.337		
Total	1220.550	66			
Corrected Total	1192.419	65			

Table A.26: Testing for Between-Subject Effects - lpSTG

A.3.3 STS

Origem	Tipo III Soma dos Quadrados	df	Quadrado Médio	F	Sig.
Modelo corrigido	322.559a	5	64.512	4.977	< .001
Intercepto	20.954	1	20.954	1.617	.208
Group	71.096	1	71.096	5.485	.023
Valence	122.708	2	61.354	4.734	.012
Group * Valence	128.755	2	64.378	4.967	.010
Padrão	777.669	60	12.961		
Total	1121.182	66			
Total corrigido	1100.228	65			

Table A.27: Testing for between-subject effects- STS

a. $R^2 = 0.293$ (R^2 Ajustado = 0.234)

(I) valence	(J) valence	Mean (I-J)	Statistic	Sig.	95% C. Int Lower Limit	Upper Limit
INDIF	NEG	-6.0089*	1.24583	<.001	-9.0802	-2.9376
	POS	-5.6340*	1.24583	<.001	-8.7053	-2.5627
NEG	INDIF	6.0089*	1.24583	<.001	2.9376	9.0802
	POS	0.3749	1.24583	0.951	-2.6964	3.4462
POS	INDIF	5.6340*	1.24583	<.001	2.5627	8.7053
	NEG	-0.3749	1.24583	0.951	-3.4462	2.6964

Table A.28: Multiple comparisons- Tuckey- STS

Valence	(I) Group	(J) Group	Mean (I-J)	Statistic	Significance *b*	95% C. Interval	
						Lower Limit	Upper Limit
INDIF	ASD	CNT	1.872	1.535	.227	-1.198	4.943
	CNT	ASD	-1.872	1.535	.227	-4.943	1.198
NEG	ASD	CNT	-3.929*	1.535	.013	-6.999	-.858
	CNT	ASD	3.929*	1.535	.013	.858	6.999
POS	ASD	CNT	-4.171*	1.535	.009	-7.242	-1.100
	CNT	ASD	4.171*	1.535	.009	1.100	7.242

Table A.29: Pairwise Method comparisson

A.3.4 TPJ

Source	Type III Sum of Squares	df	Mean Square	F	Sig.
Corrected Model	152.187a	5	30.437	1.756	.136
Intercept	28.132	1	28.132	1.623	.208
Group	68.704	1	68.704	3.963	.051
Valence	54.762	2	27.381	1.579	.215
Group * Valence	28.721	2	14.360	0.828	.442
Pattern	1040.231	60	17.337		
Total	1220.550	66			
Corrected Total	1192.419	65			

Table A.30: Testing for between-subject effects - TPJ

A.3.5 mPFC

Source	Type III Sum of Squares	df	Mean Square	F	Sig.
Corrected Model	186.819a	5	37.364	1.657	.159
Intercept	49.878	1	49.878	2.212	.142
Group	0.574	1	0.574	0.025	.874
Valence	1.301	2	0.650	0.029	.972
Group * Valence	184.944	2	92.472	4.102	.021
Pattern	1352.686	60	22.545		
Total	1589.383	66			
Corrected Total	1539.505	65			

Table A.31: Testing for between-subject effects - mPFC

Valence	(I) Group	(J) Group	Mean (I-J)	Statistic	Significance *b*	95% C. Interval	
						Lower Limit	Upper Limit
INDIF	ASD	CNT	4.764*	2.025	.022	0.714	8.813
	CNT	ASD	-4.764*	2.025	.022	-8.813	-0.714
NEG	ASD	CNT	-1.053	2.025	.605	-5.103	2.997
	CNT	ASD	1.053	2.025	.605	-2.997	5.103
POS	ASD	CNT	-3.151	2.025	.125	-7.201	0.899
	CNT	ASD	3.151	2.025	.125	-0.899	7.201

Table A.32: Pairwise Method Comparison- mPFC

Analysis Unit	Statistic	p-unc	p-FDR
Cluster 1/406	F(8,13) = 10.24	0.000169	0.068696
Connection networks.Salience.SMG (R) (62,-35,32)-networks.Language.pSTG (R) (59,-42,13)	F(4,17) = 8.21	0.000708	0.085051
Connection atlas.aSMG r -networks.Language.pSTG (R) (59,-42,13)	F(4,17) = 6.74	0.001933	0.281658
Connection atlas.aSMG r (Supramarginal Gyrus, anterior division Right)-atlas.toMTG r	F(4,17) = 5.96	0.003461	0.281658
Cluster 2/406	F(8,13) = 6.15	0.002118	0.228521
Cluster 3/406	F(8,13) = 5.98	0.002405	0.228521
Connection atlas.pITG l (Inferior Temporal Gyrus-networks.Language.IFG (R) (54,28,1)	F(4,17) = 6.91	0.001711	0.139468
Cluster 4/406	F(8,13) = 5.79	0.002783	0.228521
Connection atlas.TOFusC l -networks.Salience.SMG (L) (-60,-39,31)	F(4,17) = 11.86	0.000087	0.014229
Connection atlas.TOFusC l-networks.Salience.SMG (R) (62,-35,32)	F(4,17) = 5.65	0.004408	0.359254
Cluster 5/406	F(8,13) = 5.78	0.002814	0.228521
Connection atlas.LG l (Lingual Gyrus Left) -atlas.SFG r	F(4,17) = 7.10	0.001491	0.242997
Cluster 6/406	F(8,13) = 5.45	0.003654	0.247259
Cluster 7/406	F(8,13) = 5.25	0.004304	0.249634

Table A.33: Connectivity values of entire task- Exploratory

Analysis Unit	Statistic	p-unc	p-FDR
Cluster 1/595	F(2,19) = 23.39	0.000008	0.004469
Connection networks.Salience.SMG (R) (62,-35,32)-networks.Language.pSTG (R) (59,-42,13)	T(20) = 6.10	0.000006	0.000945
Connection networks.Salience.SMG (R) (62,-35,32)-atlas.toMTG r	T(20) = 4.47	0.000232	0.018927
Connection atlas.aSMG r (Supramarginal Gyrus)-atlas.toMTG r	T(20) = 3.89	0.000903	0.073587
Connection atlas.aSMG r (Supramarginal Gyrus)-networks.Language.pSTG (R) (59,-42,13)	T(20) = 3.70	0.001406	0.076366
Connection networks.Salience.SMG (R) (62,-35,32)-atlas.IFG oper r (Inferior Frontal Gyrus)	T(20) = 2.98	0.007342	0.149587
Connection networks.Salience.SMG (R) (62,-35,32)-atlas.pSMG r (Supramarginal Gyrus)	T(20) = 2.83	0.010410	0.188544
Connection networks.Salience.SMG (R) (62,-35,32)-atlas.SFG r (Superior Frontal Gyrus Right)	T(20) = 2.16	0.043419	0.252761
Connection networks.Salience.SMG (R) (62,-35,32)-atlas.FOrb r (Frontal Orbital Cortex Right)	T(20) = 2.09	0.049260	0.267647

Table A.34: Connectivity values of negative interaction- Exploratory

Analysis Unit	Statistic	p-unc	p-FDR
atlas.Ver7 (Vermis 7) - atlas.Cereb2 l (Cerebellum Crus2 Left)	T(20) = 2.69	0.014102	0.229870
atlas.Cereb7 l (Cerebellum 7b Left) - networks.Visual.Occipital (0,-93,-4)	T(20) = 3.11	0.005524	0.256509
atlas.Ver7 (Vermis 7) - atlas.Cereb1 l (Cerebellum Crus1 Left)	T(20) = 2.58	0.017844	0.264421
atlas.Ver7 (Vermis 7) - networks.Visual.Occipital (0,-93,-4)	T(20) = 2.38	0.027653	0.271047
atlas.Ver7 (Vermis 7) - networks.Cerebellar.Anterior (0,-63,-30)	T(20) = 2.29	0.033257	0.271047
atlas.Cereb7 l (Cerebellum 7b Left) - networks.Cerebellar.Posterior (0,-79,-32)	T(20) = 2.79	0.011293	0.284382
atlas.Cereb7 l (Cerebellum 7b Left) - atlas.OP r (Occipital Pole Right)	T(20) = 2.56	0.018769	0.302975
atlas.Cereb7 l (Cerebellum 7b Left) - atlas.Cereb1 r (Cerebellum Crus1 Right)	T(20) = 2.52	0.020446	0.302975
atlas.Cereb7 l (Cerebellum 7b Left) - atlas.Cereb2 l (Cerebellum Crus2 Left)	T(20) = 2.31	0.031564	0.395759
atlas.Cereb7 l (Cerebellum 7b Left) - atlas.OP l (Occipital Pole Left)	T(20) = 2.23	0.037642	0.415646
atlas.toITG l - networks.Cerebellar.Anterior (0,-63,-30)	T(20) = 2.52	0.020284	0.521709
atlas.Cereb2 r (Cerebellum Crus2 Right) - atlas.Cereb2 l (Cerebellum Crus2 Left)	T(20) = 2.57	0.018258	0.548376
atlas.Cereb2 r (Cerebellum Crus2 Right) - atlas.Cereb1 l (Cerebellum Crus1 Left)	T(20) = 2.57	0.018453	0.548376
atlas.Cereb3 l (Cerebellum 3 Left) - atlas.pITG l	T(20) = -2.78	0.011551	0.337530
atlas.Cereb3 l (Cerebellum 3 Left) - atlas.Ver9 (Vermis 9)	T(20) = -2.69	0.013950	0.337530
atlas.Cereb3 l (Cerebellum 3 Left) - atlas.Ver7 (Vermis 7)	T(20) = -2.34	0.029893	0.337530
atlas.Cereb9 r (Cerebellum 9 Right) - networks.DefaultMode.LP (R) (47,-67,29)	T(20) = 3.55	0.002023	0.109893
atlas.Cereb7 r (Cerebellum 7b Right) - atlas.Cereb9 l (Cerebellum 9 Left)	T(20) = 2.97	0.007631	0.248922
atlas.Cereb7 r (Cerebellum 7b Right) - atlas.Cereb9 r (Cerebellum 9 Right)	T(20) = 2.82	0.010518	0.248922
atlas.Cereb7 r (Cerebellum 7b Right) - networks.DefaultMode.LP (L) (-39,-77,33)	T(20) = 2.61	0.016767	0.273304
atlas.pITG l (Inferior Temporal Gyrus, posterior division Left) - atlas.toITG l	T(20) = 3.12	0.005449	0.286650
atlas.pITG l (Inferior Temporal Gyrus, posterior division Left) - atlas.pITG r)	T(20) = 2.49	0.021650	0.317695

Table A.35: Connectivity values of indifferent interaction- Exploratory

Analysis Unit	Statistic	p-unc	p-FDR	p-FWE
Cluster 1/6	F(2,19) = 4.93	0.018890	0.094450	
Connection atlas.IFG oper r - atlas.IFG tri r	T(20) = 5.09	0.000056	0.003242	
Connection atlas.pSMG l - atlas.SFG r	T(20) = 4.68	0.000143	0.008323	
Connection atlas.pSMG l - atlas.IFG oper r	T(20) = 4.29	0.000360	0.010428	
Connection atlas.pSMG l - atlas.IFG tri r	T(20) = 3.13	0.005274	0.082457	
Connection atlas.IFG oper l - atlas.IFG tri r	T(20) = 2.97	0.007595	0.120416	
Connection atlas.IFG oper l - atlas.IFG oper r	T(20) = 2.93	0.008305	0.120416	
Connection atlas.pSMG l - atlas.IFG oper l	T(20) = 2.74	0.012617	0.121962	
Connection networks.SensoriMotor.Lateral - atlas.pSMG l	T(20) = 2.96	0.007730	0.149574	
Connection networks.Salience.SMG - atlas.pSMG l	T(20) = 3.10	0.005687	0.164913	
Connection networks.DorsalAttention.IPS - networks.SensoriMotor.Lateral	T(20) = 3.26	0.003915	0.227042	
Connection atlas.pSMG r - networks.Salience.SMG	T(20) = 3.17	0.004780	0.277218	
Connection atlas.IC l - atlas.SFG r	T(20) = 2.95	0.007925	0.278839	
Connection networks.DorsalAttention.IPS - atlas.IC l	T(20) = 2.86	0.009615	0.278839	
Connection atlas.aSMG l - atlas.toMTG r	T(20) = 2.59	0.017630	0.296326	
Connection atlas.aSMG l - atlas.pSMG l	T(20) = 2.54	0.019506	0.296326	
Connection atlas.IFG tri l - atlas.IFG oper r	T(20) = 3.07	0.006038	0.339270	
Connection atlas.IFG tri l - atlas.SFG r	T(20) = 2.77	0.011699	0.339270	
Connection atlas.pSMG r - atlas.IFG tri r	T(20) = 2.54	0.019555	0.378066	
Connection networks.DorsalAttention.IPS - atlas.aSMG l	T(20) = 2.56	0.018753	0.465477	
Connection atlas.aSMG r - networks.DorsalAttention.IPS	T(20) = 2.59	0.017596	0.510298	
Connection networks.Salience.AInsula - networks.Salience.AInsula	T(20) = 2.74	0.012506	0.725363	

Table A.36: Connectivity values of positive interaction- ROI analysis- CNT(+1)ASD(-1)

Analysis Unit	Statistic	p-unc	p-FDR	p-FWE
Cluster 1/6	F(2,19) = 6.46	0.007241	0.043446	
Connection atlas.toMTG r - atlas.aSMG l	T(20) = 4.31	0.000343	0.016309	
Connection atlas.toMTG r - networks.Salience.SMG (L)	T(20) = 3.87	0.000946	0.016309	
Connection atlas.toMTG r - atlas.aSMG r	T(20) = 3.79	0.001145	0.016309	
Connection atlas.toMTG r - networks.Salience.SMG (R)	T(20) = 3.73	0.001311	0.016309	
Connection atlas.toMTG r - atlas.pSMG r	T(20) = 3.70	0.001406	0.016309	
Connection atlas.toITG r - atlas.aSMG l	T(20) = 4.31	0.000343	0.019892	
Connection atlas.toMTG r - atlas.IC l	T(20) = 3.36	0.003103	0.029996	
Connection atlas.toITG r - networks.Salience.SMG (L)	T(20) = 3.74	0.001282	0.037180	
Connection atlas.toMTG r - atlas.IC r	T(20) = 3.19	0.004572	0.037879	
Connection atlas.toMTG r - networks.Salience.AInsula (L)	T(20) = 3.12	0.005450	0.039512	
Connection atlas.aSMG r - atlas.Amygdala r	T(20) = 3.48	0.002354	0.068266	
Connection networks.DorsalAttention.IPS (L) - atlas.IC l	T(20) = 3.53	0.002094	0.082659	
Connection networks.DorsalAttention.IPS (R) - atlas.IC l	T(20) = 3.65	0.001576	0.091404	
Connection atlas.IC l - atlas.TP r	T(20) = 2.88	0.009225	0.099003	
Connection networks.DorsalAttention.IPS (L) - atlas.aSMG l	T(20) = 3.03	0.006611	0.105346	
Connection networks.DorsalAttention.IPS (L) - atlas.pSTG r	T(20) = -2.99	0.007265	0.105346	
Connection atlas.toITG r - networks.Salience.AInsula (L)	T(20) = 2.87	0.009427	0.109058	
Connection atlas.toITG r - networks.SensoriMotor.Superior (0,-31,67)	T(20) = 2.85	0.009880	0.109058	
Connection atlas.toITG r - atlas.pSTG r	T(20) = -2.81	0.010917	0.109058	
Connection atlas.toITG r - atlas.IC l	T(20) = 2.66	0.014879	0.109058	
Connection networks.DorsalAttention.IPS (L) - networks.SensoriMotor.Lateral (L) (-55,-12,29)	T(20) = 2.84	0.010065	0.116758	
Connection networks.DorsalAttention.IPS (L) - networks.SensoriMotor.Superior (0,-31,67)	T(20) = 2.72	0.013120	0.126829	
Connection networks.DorsalAttention.IPS (R) - atlas.pSTG r	T(20) = -3.20	0.004543	0.131734	
Connection atlas.aSMG l - atlas.aSTG r	T(20) = 2.66	0.014922	0.141676	
Connection atlas.aSMG l - atlas.IC l	T(20) = 2.66	0.014942	0.141676	

Table A.37: Connectivity values of negative interaction- ROI analysis- CNT(+1)ASD(-1)